

# EXCEPTIONAL NEW REAGENTS FOR BIOCONJUGATION

by

Corey Blaine Garmon

A thesis submitted to the faculty of  
The University of North Carolina at Charlotte  
in partial fulfillment of the requirements  
for the degree of Master of Science in  
Chemistry

Charlotte

2016

Approved by:

---

Dr. Craig Ogle

---

Dr. Markus Etzkorn

---

Dr. Jerry Troutman

---

Dr. Didier Dréau

©2016  
Corey Blaine Garmon  
ALL RIGHTS RESERVED

## ABSTRACT

COREY BLAINE GARMON. Exceptional new reagents for bioconjugation. (Under the direction of Dr. CRAIG OGLE)

At about the turn of this century the term “click” chemistry came into the common vernacular amongst chemists. “Click” is used to describe reactions that are “spring-loaded” and proceed well in a predictable manner, with no offensive byproduct and are soluble in innocuous solvents. In the chemical world it draws to mind the biosynthesis of a peptide or DNA. The prototypical example of this for the synthetic chemist is the 1,3-dipolar cycloaddition reaction of an azide with an alkyne.

This project has entailed the synthesis of a new platform for bioconjugation reagents based upon isatoic anhydride. These new reagents meet the criteria originally suggested for click reagents: They react quickly and predictably with amines, such as those found on lysine residues, to form amides. They have an inoffensive byproduct (CO<sub>2</sub>) upon conjugation. They are soluble in innocuous solvents including water. They also have an additional very desirable property; they add a chromophore and a fluorophore to the conjugate and therefore are traceable.

Click reactions have become a principle tool in bioconjugation, the process of introducing chemical functionality into biomolecules through a covalent bond. Click reactions offer a way of selectively incorporating functionality into biomolecules despite the presence of a large number of functional groups. These new reagents allow for conjugation via lysine residues. The applicability of this platform has been demonstrated through the construction of new antibody-drug conjugates, a growing class therapeutics used in the treatment of multiple types of cancer that allow for targeted drug delivery.

## TABLE OF CONTENTS

LIST OF ABBREVIATIONS	vi
CHAPTER 1: INTRODUCTION	1
1.1 Bioconjugation Background	1
1.2 The Bioconjugation Reagent	3
1.3 Click Chemistry	5
1.4 Bioorthogonal Techniques	7
1.5 Common Bioconjugation Techniques and Reagents for Proteins	10
1.6 Antibody-Drug Conjugates	15
1.7 Isatoic Anhydride	18
CHAPTER 2: PROJECT OVERVIEW AND OBJECTIVES	22
2.1 Project Overview	22
2.2 Synthetic Scheme Development	22
2.3 Reactivity of Platform	23
2.4 Development of Antibody-Drug Conjugates	23
CHAPTER 3: SYNTHESIS	25
3.1 Derivation of Isatoic Anhydride	25
3.2 Water-Soluble Derivation	29
3.3 Limitations of Water-Soluble Synthesis	35
CHAPTER 4: STABILITY AND REACTIVITY OF ANHYDRIDE MOIETY	39
4.1 Hydrolytic Stability	39
4.2 Reactivity with Primary Amines	41

	v
CHAPTER 5: BIOCONJUGATION WITH ISATOIC ANHYDRIDE REAGENTS	43
5.1 Determining the Degree of Labeling	43
5.2 Determination of $\epsilon_{330}$ and $C_{280}$	44
5.3 Bioconjugation Parameters	49
5.4 Further Functionalization after Conjugation	57
CHAPTER 6: DEVELOPMENT OF ANTIBODY-DRUG CONJUGATES	59
6.1 Antibody-Drug Conjugate Overview	59
6.2 Prodrug Synthesis	61
6.2.1 Gemcitabine and 5-Fluorouracil	62
6.2.2 Colchicine Overview	67
6.2.3 Colchicine Derivation	68
6.2.4 Computation Analysis of Colchicine Derivatives	75
6.3 Antibody-Drug Conjugate Synthesis	79
6.4 Biological Evaluation	82
CHAPTER 7: CONCLUSIONS	86
CHAPTER 8: EXPERIMENTAL	89
REFERENCES	139

## LIST OF ABBREVIATIONS

1M7	1-methyl-7-nitroisatoic anhydride
5-FU	5-fluorouracil
Ab	antibody
ACN	acetonitrile
ADC	antibody-drug conjugate
BSA	bovine serum albumin
CDI	carbonyldiimidazole
CES2	carboxylesterase 2
CuAAC	copper-catalyzed azide-alkyne cycloaddition
DCM	dichloromethane
DI	deionized
DMF	dimethylformamide
DMSO	dimethyl sulfoxide
DNA	deoxyribonucleic acid
DOL	degree of labeling
EDC	1-ethyl-3-(3-dimethylaminopropyl)carbodiimide
ELISA	enzyme-linked immunosorbent assay
ESI	electrospray ionization
EtOAc	ethyl acetate
FDA	Food and Drug Administration
GPC	gel permeation chromatography
HPLC	high-performance liquid chromatography

HRP	horseradish peroxidase
IA	isatoic anhydride
IPA	isopropyl alcohol
LC	liquid chromatography
LC-MS	liquid chromatography–mass spectrometry
mAb	monoclonal antibody
MeOH	methanol
MS	mass spectrometry
MUC1	mucin 1
NHS	N-hydroxysuccinimide
NMIA	N-methylisatoic anhydride
NMR	nuclear magnetic resonance
PEG	polyethylene glycol
PET	positron emission tomography
RNA	ribonucleic acid
RT	room temperature
SHAPE	selective 2-hydroxyl acylation analyzed by primer extension
TEA	triethylamine
TFA	trifluoroacetic acid
THF	tetrahydrofuran
THPTA	tris(3-hydroxypropyltriazolylmethyl)amine
UV-vis	ultraviolet-visible

## CHAPTER 1: INTRODUCTION

### 1.1 Bioconjugation Background

Bioconjugation is the process of introducing functionality into a biomolecule through a covalent bond. This allows for the derivation of biomolecules with selected functionalities, giving them useful and desirable properties. The development of new bioconjugates has given researchers the ability to perform tasks that had not been previously possible and has had a huge impact in many fields, especially within biology, biochemistry, and therapeutics.

Many modern techniques require the use of specially designed bioconjugates. Enzyme-linked immunosorbent assay (ELISA) is an example of one such technique that utilizes an antibody conjugated to a detector functionality. The use of this bioconjugate allows for the qualitative and quantitative analysis of complex protein samples. The general ELISA protocol involves immobilizing the sample on a surface, usually in a well, followed by incubation with the antibody-detector bioconjugate. The antibody is chosen such that it selectively binds the analyte of interest. Incubation is followed by washing to remove any unbound bioconjugate. The detector functionality can now be used to quantify the amount of analyte present in the sample. The most commonly utilized detector functionality in ELISA is the enzyme horseradish peroxidase (HRP). HRP catalyzes the oxidation of 3,3',5,5'-tetramethylbenzidine to produce a colored product which can be measured spectrophotometrically to quantify to amount of analyte present.<sup>1</sup>



There are multiple variations of ELISA (Figure 1-1). The use of these antibody-HRP bioconjugates as detection molecules has found use in other analytical techniques, most notably in western blot analysis, a widely used biochemical technique.<sup>2</sup>

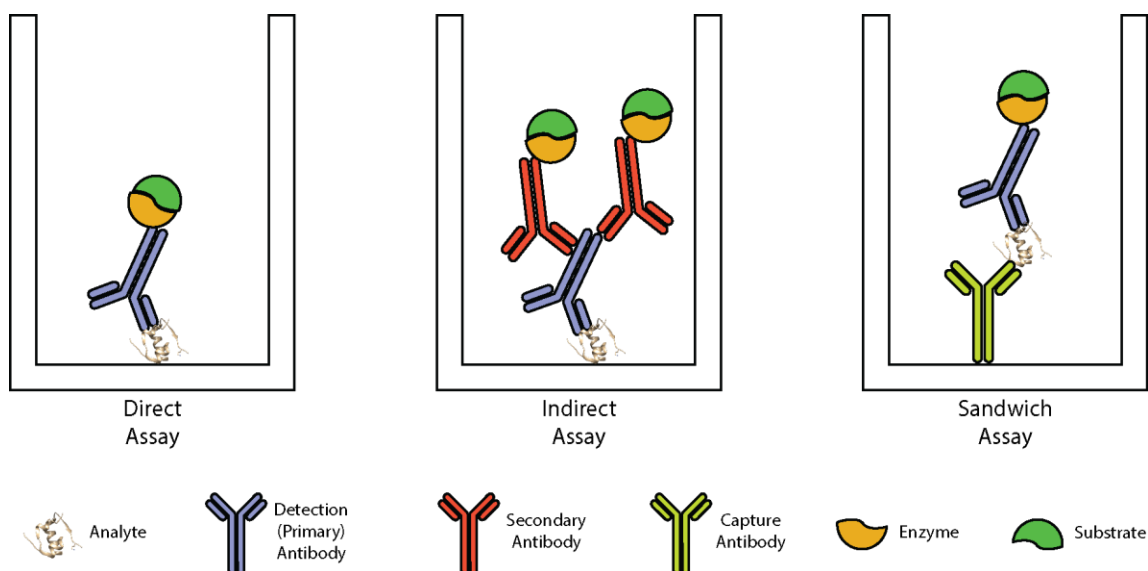


Figure 1-1: Different types of ELISA utilizing antibody bioconjugates

Bioconjugates are commonly used in assays and quantification techniques but have also found use in other applications including detection and imaging, purification, diagnostics, and therapeutics. Fluorescence microscopy utilizes a fluorophore conjugated a highly specific targeting functionality such as an antibody, allowing for the imaging of specific analytes within cells. This and other imaging functionalities, such as quantum dots and PET sensitive molecules, can be conjugated to biomolecules to track their biodistribution and localization within the body. Ligands can be conjugated to solid supports such as silica particles in a column. Proteins that specifically bind to this ligand can then be purified from a complex mixture of proteins by passing it through this

column. Finally bioconjugates are starting to gain more use in therapeutics, particularly antibody-drug conjugates (ADCs) which allow for site-specific drug delivery. ADCs are discussed in more detail later. A more complete discussion of the use of bioconjugates in modern applications can be found in *Bioconjugate Techniques*.<sup>3</sup>

## 1.2 The Bioconjugation Reagent

Bioconjugates are used in many applications but how is bioconjugation effectively carried out? Bioconjugation requires the use of bioconjugation reagents; heterobifunctional cross linkers that can be used to conjugate to biomolecules. These reagents must contain a functional group that can react with and conjugate to a biomolecule. This allows for the introduction of a functionality into the biomolecule, such as a fluorophore, or for the introduction of a functional group that can be conjugated in a second step. Conjugation to the biomolecule needs to take place under mild conditions which does not perturb the activity of the biomolecule. In most cases loss of bioactivity defeats the purpose of bioconjugation and renders the bioconjugate useless for its intended application. Conjugation often requires the utilization of a functional group that can undergo conjugation at physiological pH and without heat, which can cause proteins to denature. It is also often desirable for the bioconjugation reagent to be water soluble allowing for conjugation to take place under a protein's native environment.

Bioconjugation techniques generally result in biomolecules that have been labeled multiple times at multiple sites. It is desirable to be able to control both the sites of modification and the degree of modification. Poor control over these parameters can result in bioconjugates that contain little to no activity. For example if an enzyme becomes conjugated at its active site then it will lose much to all of its activity. Complete

loss of activity results in bioconjugates that cannot be used for their intended purpose. Loss of biomolecule activity can also result from poor control over the degree of modification.

The properties of the linker introduced into the bioconjugate also need to be taken into account and can vary depending on the application. One very important aspect of the linker is its stability. For many applications, such as visualization and immobilization, the bioconjugation reagent needs to form a linkage that is strong and stable. Examples of this are reagents that result in the formation of amides, thioethers, and triazoles. For other applications such as drug delivery the linker should be labile and cleaved under specific conditions. A disulfide bond is an example of a linkage that can be cleaved in a reductive environment. Other types of bonds are pH sensitive and can be selectively cleaved at specific pHs. Examples of these include imines, hydrazones, oximes (Figure 1-2). Each of these have different hydrolytic stabilities at certain pHs, giving more control over the properties of the bioconjugation reagent.<sup>4</sup>

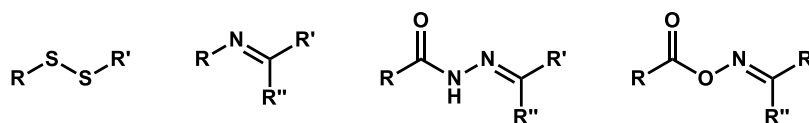


Figure 1-2: Examples of cleavable linkages that are reducible, such as disulfides, or pH sensitive, such as imines, hydrazones, and oximes

The length of the linker should also be chosen with the application in mind. Having a linker that is too small or big can impact the bioconjugation process and can affect how the final bioconjugate will perform. For example it can be difficult to

conjugate biomolecules to quantum dots or nanoparticles because these usually contain polymer surface coatings giving them a steric barrier to conjugation. It has been shown that the use of longer linkers improves quantum dot conjugation and the overall performance of the final bioconjugate.<sup>5</sup> Polyethylene glycol (PEG) is commonly used as a spacer because it improves water solubility, helps prevent non-specific interactions, and gives improved circulation half-lives.<sup>6</sup>

### 1.3 Click Chemistry

Bioconjugation requires at least three different components; the biomolecule, the functionality being incorporated into the biomolecule (the cargo), and the bioconjugation reagent. The bioconjugation reagent must selectively react with the biomolecule to allow for the incorporation of a unique functional group or chemical handle into the biomolecule. This chemical handle can now be used to conjugate the cargo to the biomolecule giving the final bioconjugate (Figure 1-3A). However it is not always possible or desirable to incorporate a chemical handle into the biomolecule that can directly react with a functional group present in the cargo. In these situations a functional group that is highly selective for the chemical handle on the biomolecule is incorporated into the cargo (Figure 1-3B).

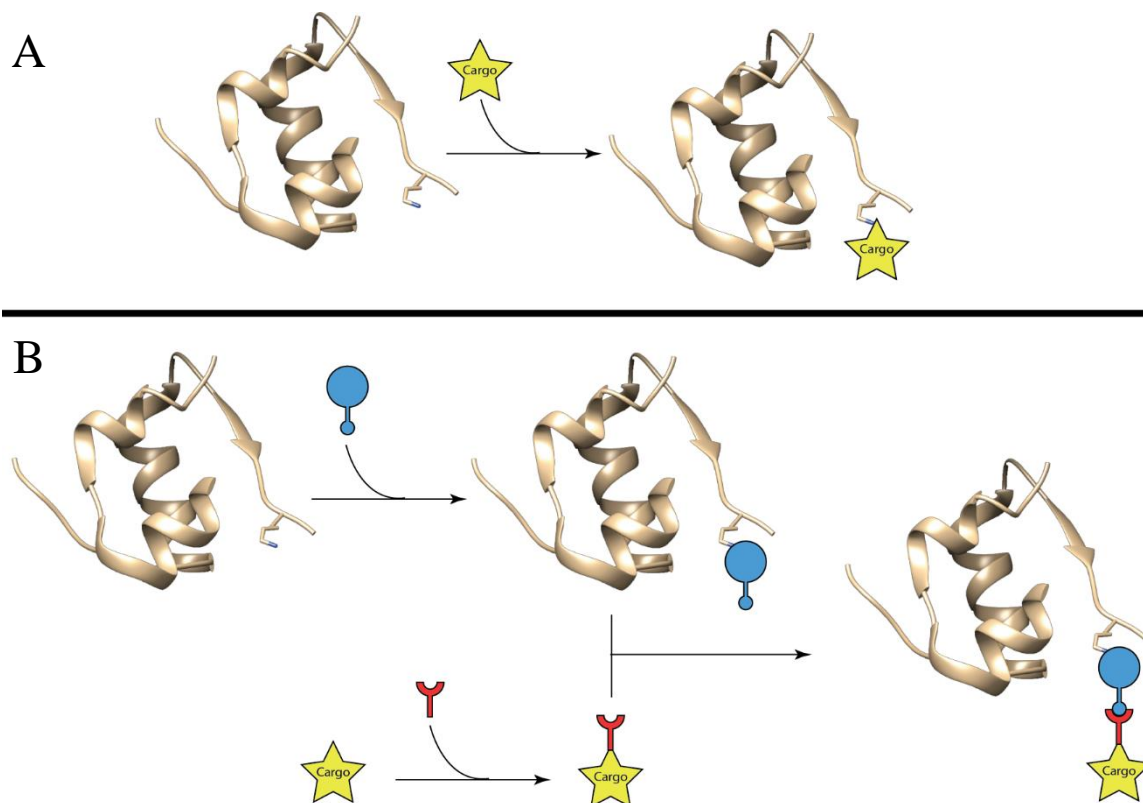


Figure 1-3: Two general strategies used for bioconjugation; direct incorporation of the cargo (A) and incorporation of complementary functional groups into the biomolecule and cargo that can then be conjugated together

These strategies require the stepwise conjugation of smaller building blocks to form the final bioconjugate. Ideally each reaction in these pathways would utilize “click” chemistry. Click chemistry was a term coined by Sharpless in 2001 in which he put forth a set of criteria to define a nearly ideal reaction.<sup>7</sup> To name a few, these reactions must be modular, utilize chemical functional groups that are highly selective for each other, have high reaction rates and give very high yields, generate only inoffensive byproducts, and utilize no solvent or benign solvents such as water. Not only does the use of click chemistry allow for the effective construction of bioconjugates but it also allows for the

incorporation of chemical groups into the linkage to give the bioconjugate enhanced chemical properties, such as PEG groups.

The prototypical example of a click reaction is the copper(I) catalyzed 1,3-dipolar cycloaddition between azides and alkynes. This reaction gives very high yields, up to 99.8%, has high reaction rates of 10 to 200 M<sup>-1</sup>s<sup>-1</sup>, and proceeds in water over a wide range of temperatures and pH's.<sup>8</sup> Although these cycloaddition can be carried out with other 1,3-dipoles, azides are the most common groups utilized. They are stable towards hydrolysis and dimerization and are inert in the presence of many standard organic reaction conditions.<sup>7</sup> All of these qualities makes the cycloaddition between azides and alkynes one of the most useful and widely utilized click reactions in organic synthesis.

#### 1.4 Bioorthogonal Techniques

Click chemistry is a powerful tool for organic synthesis however the conditions for certain click reactions may not be compatible with biomolecules or in biological systems. This brings us to another class of reactions that are useful for bioconjugation, bioorthogonal reactions. These are reactions that utilize functional groups that selectively and rapidly react with each other under physiological conditions while only reluctantly undergoing reactions with functional groups naturally found in proteins.<sup>9</sup> These reactions require the use of functional groups that are not present in biological systems, that are inert in the complex chemical environments found in biological systems, and that selectively react with each other to form a linkage. These reactions should also take place in aqueous environments and utilize reaction conditions that are compatible with biological systems.

There has been much effort to turn the azide alkyne cycloaddition reaction into a bioorthogonal reaction. Both the azide and alkyne are inert to functional groups not found in biological systems and have excellent stability under physiological conditions. However for this reaction to take place with useful rates requires the use of significant heat or a catalyst. Heat cannot be used as it causes proteins to become denatured and metal catalysts such as copper and ruthenium are often incompatible with biological systems. For example the copper catalyzed azide alkyne cycloaddition cannot be used *in vivo* because of copper's toxicity in living systems. Copper also limits its applications *in vitro* because it can cause protein precipitation upon complexation with the protein.<sup>10</sup>

Alternative methods have been explored to activate the alkyne towards cycloaddition which would improve biocompatibility. It was found that cyclooctyne reacts rapidly with azides under mild conditions (Figure 1-4). Cyclooctyne, the smallest stable cycloalkyne, contains a considerable amount of ring strain due to its large deviation from the ideal 180° bond angle at the triple bond. This ring strain promotes cycloaddition and eliminates the need for copper(I).<sup>11</sup>

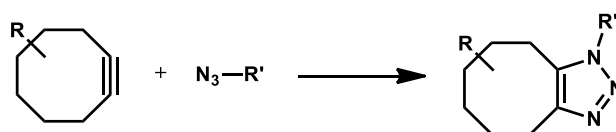


Figure 1-4: Strain promoted [3 +2] azide-alkyne cycloaddition

The Staudinger ligation is another commonly used bioorthogonal reaction (Figure 1-5).<sup>12</sup> This is a chemoselective method that involves the reduction of an azide with triphenylphosphine. These two species are bioorthogonal to almost all functionalities

found in biological systems and can undergo conjugation at room temperature in aqueous environments. This reaction is based off of the Staudinger reduction in which an azide is reduced to an amine by reacting with triphenylphosphine. The key difference in the Staudinger ligation is that the triphenylphosphine is placed in proximity to an acyl donor, most commonly a methyl ester. This allows the ylide intermediate to undergo intramolecular nucleophilic acyl substitution resulting in a stable amide bond.<sup>12</sup>

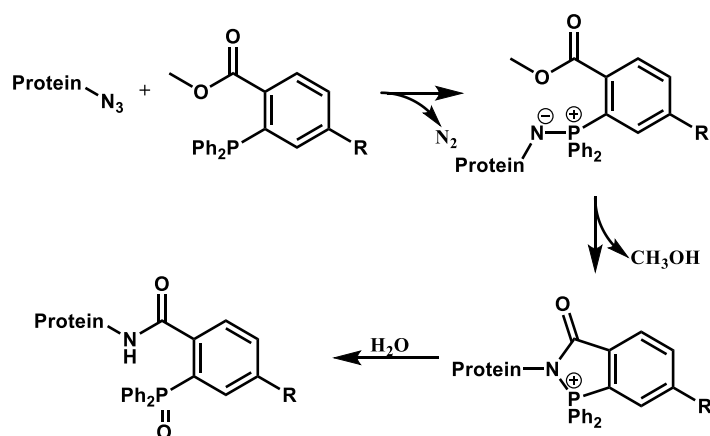


Figure 1-5: The Staudinger ligation between an azide and a triphenylphosphine



A modification of the Staudinger ligation utilizes a phosphinothioester which results in an amide bond that does not contain the phosphine oxide (Figure 1-6). This is known as the traceless Staudinger ligation. Any bioconjugation reagent that forms a linkage that contains no part of the bioconjugation reagent or any other residual atoms is considered traceless.<sup>13</sup>

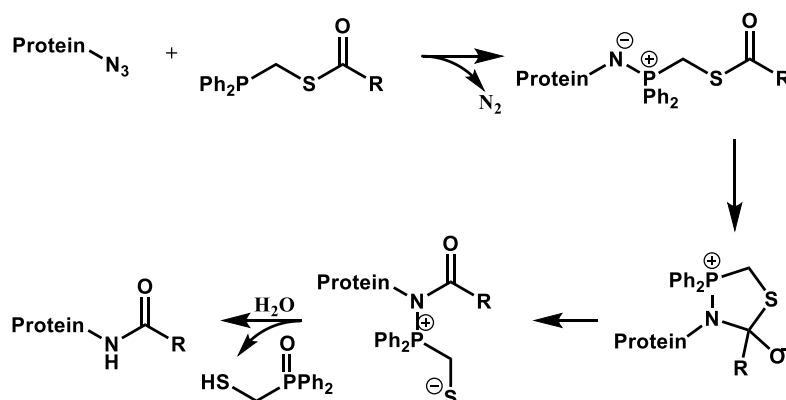


Figure 1-6: The traceless Staudinger ligation, which results in no residue atoms being incorporated into the linkage

### 1.5 Common Bioconjugation Techniques and Reagents for Proteins

Many techniques have been developed for the bioconjugation of proteins, each with different site selectivity and functional group compatibility.<sup>14</sup> Proteins are made up of amino acids containing various side groups which offer unique chemical handles. Researchers can exploit the varying chemical properties and reactivities of these groups for conjugation at specific residues. A majority of the techniques developed target either lysine or cysteine residues.<sup>15</sup>

Lysine is an attractive target for bioconjugation because it contains a nucleophilic amine and is one of the most solvent exposed amino acids.<sup>3</sup> Many strategies involve the

coupling of the lysine with a carboxylic acid via nucleophilic acyl substitution resulting in the formation of an amide. However these reactions do not occur under mild conditions. For this reason the carboxylic acid is commonly converted into an activated ester, making it more susceptible to nucleophilic attack.

One of the most commonly utilized strategies is to form an activated N-hydroxysuccinimide (NHS) or sulfo-NHS ester (Figure 1-7). The carboxylic acid is first reacted with a carbodiimide, most commonly EDC, to give o-acylisourea. This intermediate can be used for bioconjugation however it is not very stable and is susceptible to hydrolysis leading to decreased yields. Reaction with NHS leads to the formation of an activated NHS ester that is considerably more stable towards hydrolysis allowing for more efficient conjugation. These NHS esters can be used for bioconjugation of lysine under physiological pH.<sup>16</sup> Bioconjugation reagents of this type are zero-length crosslinkers because they result in the formation of a bond containing no additional atoms.<sup>3</sup>

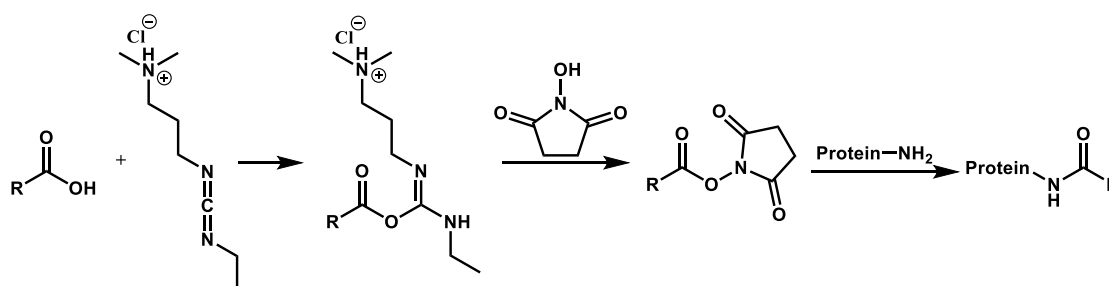


Figure 1-7: Lysine modification via an activated NHS ester resulting in the formation of an amide bond

Squarates have also been utilized for the bioconjugation of lysine. Squarates are heterobifunctional reagents which allows for the conjugation of two separate groups (Figure 1-8). Reaction of the first amine results in the formation of an intermediate that reacts with other amines at a greatly reduced rate.<sup>17</sup> Squarates result in conjugates with a small spacer, which may be an advantage depending on the application of the conjugate.

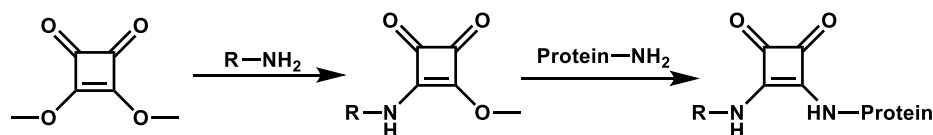


Figure 1-8: Lysine modification via heterobifunctional squarates

Many other reagents have been used for the conjugation of lysine including isocyanates, isothiocyanates, imidoesters, and fluorophenyl esters.<sup>18</sup>

Cysteine offers another unique chemical handle for bioconjugation through its nucleophilic thiol. One reliable strategy used for the conjugation of cysteine is through 1,4-addition to Michael acceptors such substituted maleimides (Figure 1-9).<sup>19</sup>

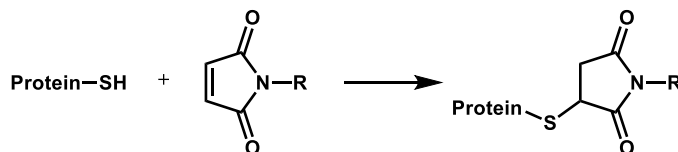


Figure 1-9: Cysteine modification via maleimides

Pyridyl disulfides are also commonly used for cysteine modification (Figure 1-10). These undergo disulfide exchange with cysteine at physiological pH. This results in

the formation of bioconjugate with a disulfide linkage. This is an example of a reversible linkage that can be cleaved under reductive conditions resulting in the release of the functional group. A notable advantage of this strategy is that pyridine-2-thione is also a product of this reaction. This can be measured spectrophotometrically at 343 nm allowing one to measure the progress of the reaction.<sup>20</sup>

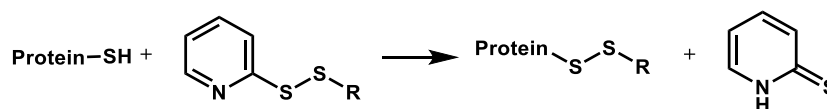


Figure 1-10: Cysteine modification via pyridyl disulfide resulting in the formation of a disulfide

The techniques mentioned so far are not site-specific. For example, a reagent that targets lysine residues will react with any available lysine on the protein. Developing methods that only target a specific site offers many advantages but is much more challenging. Poor control over the sites of conjugation can have negative effects such as loss of protein function. It has been shown, in the design of protein microarrays, that controlling the orientation of proteins is essential if these microarrays are to be used as quantitative tools. Proteins selectively immobilized on one site reflect the activities of proteins in solution while randomly oriented proteins showed lowered and varying degrees of activity.<sup>21</sup>

One method for site-specific conjugation is native chemical ligation which selectively targets N-terminal cysteine (Figure 1-11). The cysteine undergoes nucleophilic acyl substitution with a thioester containing the functionality being conjugated to the protein. This is followed by a quick internal S→N acyl shift resulting in

the formation of an amide bond. This results in conjugation to the backbone of proteins through a peptide bond. This method has been used for the direct synthesis of moderate sized proteins such as cytokines.<sup>22</sup>

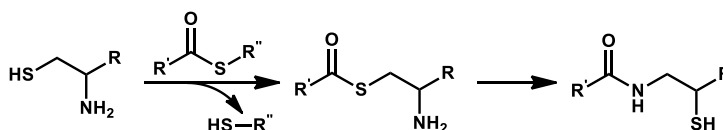


Figure 1-11: Site-specific conjugation via native chemical ligation that selectively occurs at N-terminal cysteine residues

An extension of this method is expressed protein ligation (Figure 1-12). Here target proteins are expressed as a fusion protein containing an intein. Inteins catalyze the formation of thioester at the C-terminus of the target protein. These can be treated with proteins containing an N-terminal cysteine which results in chemical ligation. Alternatively these can be reacted with a nucleophile to install other functionalities at the N-terminus of proteins.<sup>17</sup>

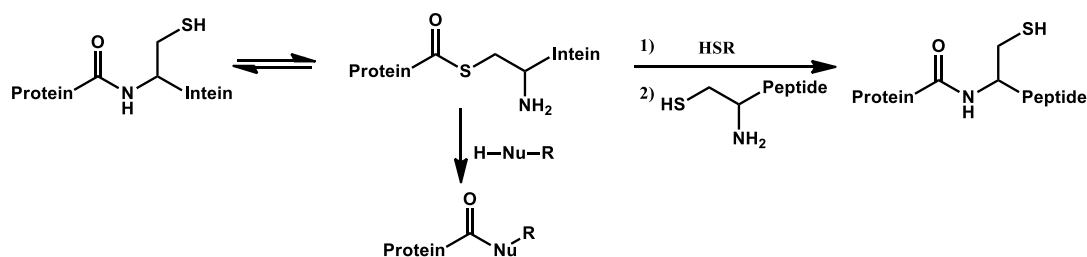


Figure 1-12: Site-specific conjugation via expressed chemical ligation utilizing an intein to form a reactive thioester

## 1.6 Antibody-Drug Conjugates

In the early 1900's Paul Ehrlich conceived the idea of the "magic bullet", a molecule capable of selectively delivering a drug to a diseased site. He came up with this idea after his observations that dyes of different chemical structure were selectively absorbed by different tissues. His ideas laid out the foundation for antibody-drug conjugates (ADCs) for targeted therapy. These are composed of a cytotoxic drug bound to a monoclonal antibodies (mAbs), which selectively bind receptors on target cells. These are connected with a stable, labile linkage which allows the drug to stay on the antibody until it reaches its target.<sup>23</sup>

It would be nearly 80 years after Ehrlich idea of the magic bullet before significant progress was made in ADCs. This was largely due to the difficulty associated with producing and purifying antibodies. This changed in 1975 with the first successful production of mAbs.<sup>24</sup> For the first time researchers had easy access to antibodies, allowing for more thorough studies to be carried out on ADCs. In 2000 gemtuzumab ozogamicin (Mylotarg®) became the first FDA approved ADC, used for the treatment of acute myeloid leukemia.<sup>25</sup> This was a landmark achievement in the field of ADCs, despite it being withdrawn from the market in 2010.<sup>25</sup> Today there are over 20 FDA approved monoclonal antibodies and only two FDA approved ADCs; brentuximab vedotin and trastuzumab emtansin.<sup>26</sup>

ADCs contain three key components; a mAb, a linker, and a cytotoxic drug. Each of these parts must be carefully chosen or designed to obtain an effective product. When introduced into the body, ADCs circulate in the bloodstream until the antibody binds a receptor at the diseased site. Upon binding the ADC is brought into the cell via

endocytosis. Once internalized the ADC linkage is designed to be cleaved, releasing the drug and killing the cell. This whole process results in site-specific drug delivery (Figure 1-13).

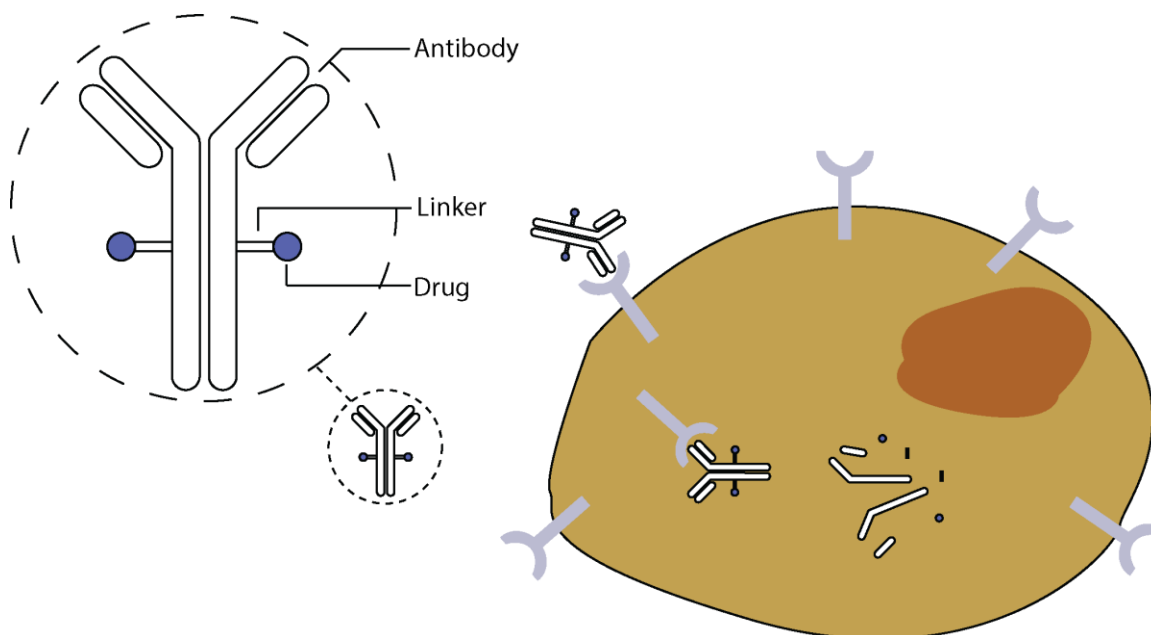


Figure 1-13: Antibody-drug conjugates selectively bind to antigens at the target site, at which point they are internalized through receptor-mediated endocytosis. In the cell, the conjugate is broken down causing the release of the drug

Antibodies are large proteins that are used by the immune system to destroy pathogens. Antibodies target these pathogens by binding to specific receptors on their surface known as antigens. Specifically, monoclonal antibodies are only used in ADCs.<sup>25</sup> These are identical antibodies that exhibit monovalent affinity and only bind one particular antigen, making them excellent targeting components in ADCs. Effective ADCs take advantage of antigens that are overexpressed at the diseased site.

There are currently three main classes of potent toxins that are being studied as anticancer drugs; maytansinoids, auristatins, and calicheamicins.<sup>26</sup> Maytansinoids and auristatins target tubulin while calicheamicins target DNA. Since tubulin and DNA are present in both normal cells and malignant cells it is important that these toxins are only delivered to the tumor cells. Localization at the diseased site is made possible by the antibody and allows for the use of these highly potent cytotoxic drugs. These toxins cannot be used in traditional, non-targeted treatment. Brentuximab vedotin and trastuzumab emtansin utilize a derivative of auristatin and maytansinoid respectively.

Probably the most important component that determines the success of the final ADC is the linker. The linker must be conditionally stable; it needs to be stable during circulation while ADC reaches its target but it must also be cleaved allowing for the release of the drug once it reaches the target.<sup>23</sup> Failure to release the drug typically results in greatly reduced or no activity. Examples of linkages that have been used include dipeptides, hydrazones, and disulfides. Dipeptide linkers take advantage of proteases in cells allowing them to be cleaved once internalized into the cell. This type of linker has been used to develop ADCs that are significantly stable in circulation with half-lives upwards of six days.<sup>27</sup> Hydrazones (pH sensitive) and disulfide linkages typically take advantage of the acidic and reductive conditions present in lysosomes.

Finally, the method used to conjugate the drug to the antibody must be considered. The loading stoichiometry and conjugation heterogeneity are factors that determine how effective the ADC is.<sup>23</sup> Antibodies typically contain many lysine residues (upwards of a 100) and a few interchain cysteines. Conjugation to either one of these residues results in a heterogeneous mixture although cysteine conjugation gives greater



uniformity. However more complex methods, such as recombinant methods, are required for complete control over the sites of conjugation.<sup>23</sup> The stoichiometry of drug conjugation can also have drastic effects on the properties of the ADC. Heavily loaded antibodies should be more potent drugs and require a smaller dose. However it has been shown that two to four drugs is typically optimal as heavily loaded antibodies tend to be rapidly cleared from circulation.<sup>28</sup>

There is still much research and work that is needed on the effective design and synthesis of ADCs. For example it has been shown that the localization of ADCs in tumors upon injection to be less than 0.05%, showing that these do not have good targeting capabilities.<sup>29</sup> It is desirable to be able to control the degree of labeling of the antibodies and to also control where the labeling is taking place. Antibodies generally have 40 to 86 lysine residues that are modified to a variable degree. Strategies that target lysine typically result in antibodies that have been labeled 0 to 8 times. ADCs made using these strategies result in a heterogeneous mixture of ADCs containing various degrees of labeling at different lysine residues and can contain up to 45 million different molecules.<sup>29</sup> It is desirable to have a much better defined and homogenous sample especially if the ADCs are to be used in therapeutics.

### 1.7 Isatoic Anhydride

Isatoic anhydride (Figure 1-14) has a history of being used in biochemical studies. It's derivative, N-carboxymethylisatoic anhydride, was first used in 1969 where it was found to react with the enzyme DNA polymerase from *E. coli*.<sup>30</sup> This study showed that isatoic anhydride derivatives could be used to conjugate to proteins. Following this it was also found that these derivatives could be reacted with DNA and RNA where it was

found to conjugate onto the nucleosides adenine and guanine. Most recently isatoic anhydride derivatives have been used for selective 2-hydroxyl acylation analyzed by primer extension (SHAPE) analysis. It was found that N-methylisatoic anhydride (NMIA) would selectively react with the 2-hydroxyl groups located in flexible regions of the RNA and that it showed the same reactivity for all four nucleotides. SHAPE analysis gives information on the secondary and tertiary structure of RNA segments and on the internal base pairing.<sup>31</sup> Later it was found that 1-methyl-7-nitroisatoic anhydride (1M7) was a more reactive and more useful reagent for SHAPE analysis.<sup>32</sup>

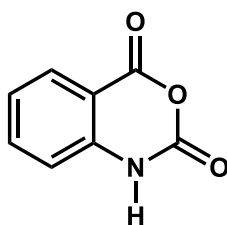


Figure 1-14: Structure of isatoic anhydride

Although isatoic anhydride and its derivatives have been used in biochemical studies, its potential for bioconjugation has largely gone unnoticed. Isatoic anhydride contains three different functional groups, each with unique reactivity's. The anhydride allows for conjugation to biomolecules as this undergoes nucleophilic acyl substitution with primary amines such as those found on lysine sidechains. The amide can be deprotonated allow it to undergo  $S_N2$  reactions with electrophiles. Finally the aromatic ring can undergo electrophilic aromatic substitution. While the anhydride must be reserved for bioconjugation, the amide and aromatic ring can be used to introduce a wide

variety of functionalities into the molecule. My research is focused around the development of new reagents for bioconjugation based off of isatoic anhydride.

A desirable property of bioconjugation reagents is high water solubility. Two synthetic schemes are currently used to render the isatoic anhydride derivatives water soluble. One incorporates an N,N-dimethyl group onto isatoic anhydride while the other incorporates a primary iodo. Both of these are easily made water soluble by the formation of a quaternary ammonium salt. Additionally, these two intermediates are complementary to each other in that one is electrophilic while the other is nucleophilic. This gives us a large substrate scope for formation of the quaternary ammonium and allows for the incorporation of a larger variety of functionalities.

These isatoic anhydride reagents exhibit many properties that define a “click” reagent. They are water-soluble, wide in scope, require simple reaction conditions, generate inoffensive byproducts, and are “spring-loaded” towards the formation of a single product. The bioconjugation step simply requires mixing the isatoic anhydride reagent with the biomolecule in an aqueous solution. These reagents have been shown to have excellent stability in the presence of water but react rapidly with primary amines such as those on lysine. So the anhydride is spring-loaded towards the formation of an amide. Additionally, the only other product formed is carbon dioxide, an inoffensive byproduct that bubbles out of solution. The production of carbon dioxide has the effect of lowering the pH of the solution, however this can be mitigated through the use of an appropriate buffer. Finally they have an additional characteristic that is not needed to be defined as a click reagent, they are self-reporting. Upon conjugation and decarboxylation the isatoic anhydride moiety undergoes a shift in both absorbance (to region not

characteristic of most biomolecules) and fluorescence. Both of these properties allow for the degree of bioconjugation to be tracked and quantified.

## CHAPTER 2: PROJECT OVERVIEW AND OBJECTIVES

### 2.1 Project Overview

The purpose of this project is to develop a highly adaptable, UV-traceable platform for the bioconjugation of proteins that is based off of isatoic anhydride. This scaffold is designed to selectively conjugate to solvent-exposed lysine residues, through nucleophilic acyl substitution. This project can be divided into three separate parts. First, a synthetic method for the incorporation of a variety of functional groups into isatoic anhydride must be developed. Second, the hydrolytic stability and the reactivity with amines and proteins will be examined. Finally, this new platform will be used to develop a series of antibody-drug conjugates.

### 2.2 Synthetic Scheme Development

First a synthetic scheme will be developed for the derivation of isatoic anhydride. The functionality will be incorporated into isatoic anhydride by substitution at the nitrogen. This scheme needs to be wide in scope, allowing for the incorporation of a wide variety of different functional groups. Additionally, another general scheme needs to be developed that allows for the introduction of a group to help impart water-solubility into this platform. This will be accomplished through the formation of a quaternary ammonium salt. Water-solubility is a desired property in bioconjugation reagents as it allows the conjugation to take place in a proteins native environment.

### 2.3 Reactivity of Platform

Once an effective method has been developed for producing the isatoic anhydride derivatives the next step is to examine the stability and reactivity of these derivatives. The anhydride in this platform is designed to react with nucleophiles in proteins, particularly amines present on lysine residues. Because these reagents are designed to be used under aqueous conditions the anhydride must be relatively stable towards hydrolysis but also react quickly with primary amines. In particular the anhydride must be stable under the basic conditions required to keep lysine residues unprotonated and reactive. The hydrolytic stability of these reagents will be determined and compared against the reaction rate with butylamine, which is used as a model for lysine.

The built-in UV properties of these reagents give an easy way to determine the degree of labeling (DOL) on a protein. Parameters affecting the DOL will be examined using the protein BSA. Ideally this platform could achieve a variety of DOLs by changing simple parameters such as reaction time, pH, and concentration. In particular pH is an important parameter for this platform. If the pH is too high, the reagent may hydrolyze before conjugation takes place. However if it is too low the lysine residues may become protonated and unreactive.

### 2.4 Development of Antibody-Drug Conjugates

The last goal of this project is to develop antibody-drug conjugates utilizing these new reagents. A key step in the development of these conjugates is the incorporation of this platform into the prodrugs. This not only allows for conjugation of the drug to the antibody, but also allows for the amount of drug-loading onto the antibody to be easily characterized through the spectroscopic properties of the platform. Additionally the

platform will be incorporated into the prodrugs through a labile linkage, allowing for cleavage of the drug once at the target. The antibody used in this project selectively binds to the MUC1 antigen which is overexpressed in multiple types of cancer. The cytotoxins that will be used are gemcitabine, 5-fluorouracil, and colchicine.

## CHAPTER 3: SYNTHESIS

### 3.1 Derivation of Isatoic Anhydride

Isatoic anhydride contains three functional groups with unique reactivities, two of which are exploited in this research (Figure 3-1). The first is the amide which is used to introduce functionality into isatoic anhydride through the nucleophilic substitution reaction. The second is the anhydride which undergoes nucleophilic acyl substitution. This functional group is utilized to react with nucleophilic groups on proteins such as lysine residues, allowing for the conjugation of a functionality onto the protein. The anhydride must be reserved during the derivation of isatoic anhydride to allow for bioconjugation to take place. For this reason it is important to keep the reaction conditions anhydrous during the derivation of isatoic anhydride.

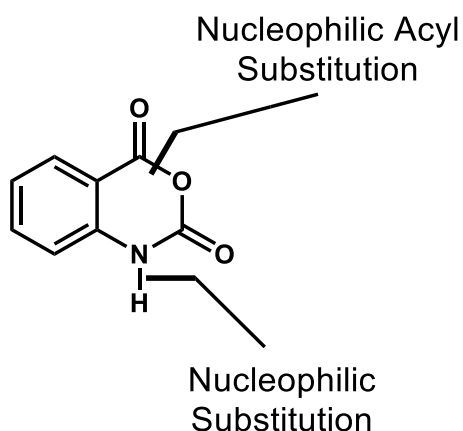


Figure 3-1: Isatoic anhydrides functional groups that are exploited in this platform



To introduce functionality into isatoic anhydride first the amide is deprotonated followed by an  $S_N2$  reaction with a primary halide. This is a two-step, one pot synthesis that is carried out under anhydrous conditions to prevent the hydrolysis of the anhydride functionality. This reaction is performed in anhydrous DMF under an inert atmosphere of nitrogen (Figure 3-2).

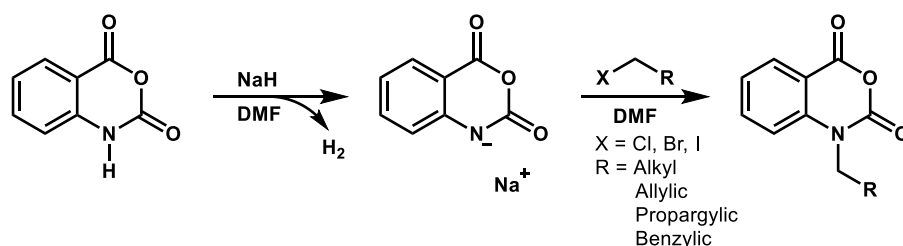


Figure 3-2: Synthetic scheme for incorporation of functionality into isatoic anhydride involving deprotonation of the nitrogen followed by substitution with a primary halide

The first step is the deprotonation of the amide functional group resulting in a nucleophilic nitrogen that can now undergo  $S_N2$  reactions with electrophiles. Currently this is done by using sodium hydride as the base. Sodium hydride is a strong non-nucleophilic base which allows for deprotonation of the nitrogen with no reaction with the anhydride. Further, upon deprotonation hydrogen gas is formed which bubbles out of solution, driving the reaction to completion. A small excess of sodium hydride is used to ensure complete deprotonation.

Sodium hydride is however a less than ideal base. It readily reacts with ambient water to give off highly flammable hydrogen gas. We have shown that other bases can be used in this step, such as sodium hydroxide and sodium carbonate, however these reagents do not have a strong driving force to push the reaction to completion and they

are more nucleophilic causing the reaction with anhydride to become a competing reaction. This results in reduced yields of the final product.

After deprotonation of the nitrogen a wide variety of functional groups can be introduced onto isatoic anhydride by a  $S_N2$  reaction with electrophilic halides. We have shown that this reaction can be carried out using chloride, bromide, and iodide reactants and that these can be primary, allylic, benzylic, or propargylic. However we have found that this reaction cannot be carried with acid chlorides as this results in a rearrangement in which the anhydride functionality is lost (Figure 3-3).

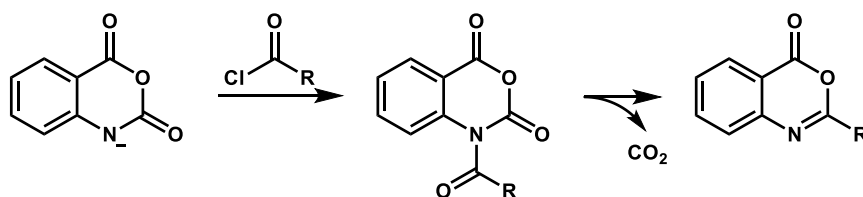
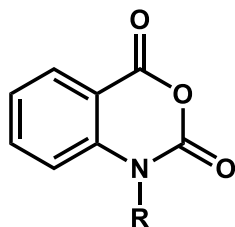


Figure 3-3: Rearrangement observed upon reaction with acid chlorides

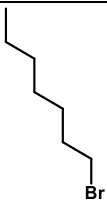
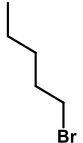
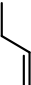
The product was purified and isolated by first removing the DMF under vacuum and with heat. Next the product is extracted into DCM by washing with ice cold saturated sodium bicarbonate. The DCM is then removed under vacuum resulting in a crude solid which is generally recrystallized in IPA and in some cases t-butyl alcohol. Using this strategy a variety of isatoic anhydride derivatives have been synthesized with varying yields (Table 3-1).

Table 3-1: Neutral isatoic anhydride derivatives



Entry	R	% yield
3a		28
3b		62
3c		53
3d		31*
3e		19*
3f		47*
3g		58
3h		36*
3i		37*
3j		50*
3k		46

Table 3-1 continued

<b>3l</b>		57*
<b>3m</b>		28*
<b>3n</b>		76*

\*Reagent only synthesized once, highest yield obtained reported otherwise

This synthetic method has not been optimized but instead demonstrates a general method for the incorporation of functionality into isatoic anhydride. This method generally gives moderate yields (30-70%), however some have been shown to give low yields. For example, **3a** has been synthesized multiple times but generally gives low yields. This reagent seems to be more susceptible to nucleophilic acyl substitution which could be due to the inherent basicity present in the tertiary amine. Additionally, **3a** is recrystallized in tert-butanol, as IPA will react with it. tert-Butanol freezes at 26 °C, making it difficult for the complete precipitation of product.

### 3.2 Water-Soluble Derivation

The above strategy can be used to incorporate a diverse range of functional groups into our bioconjugation platform, however these reagents lack one important property in that they are generally not soluble in water. These reagents are designed to be used in biological and biochemical studies where the vast majority of reactions are carried in aqueous systems. Additionally, it is ideal to perform bioconjugation of proteins in aqueous environments. The use of organic solvents could cause proteins to become

denatured and can also change the nucleophilicities of the amines in lysine. For these reasons it is important that these reagents are water-soluble to make a viable bioconjugation platform.

Two of the reagents from table 3-1, the dimethylamine product **3a** and the alkyl iodo product **3b**, can be used to easily synthesize water-soluble derivatives. Both of these reagents can be further conjugated by the formation of quaternary ammonium salt (Figure 3-4). The introduction of this charged group into the platform helps render these isotopic anhydride derivatives water-soluble. Additionally these two reagents utilize complementary chemistries to form the ammonium salt, **3a** through a nucleophilic tertiary amine and **3b** through an electrophilic primary iodide. The use of these complementary chemistries increases the scope of functionalities that can be introduced into the water-soluble platform.

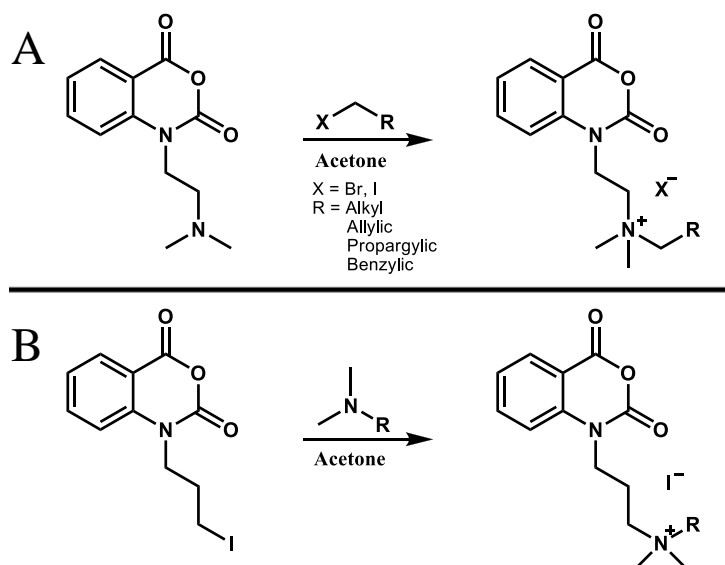
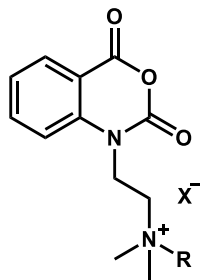


Figure 3-4: Synthesis of water-soluble derivatives using **3a** (A) and **3b** (B)

**3a** results in the formation of an ammonium salt by an  $\text{S}_{\text{N}}2$  reaction with primary or activated halides (Figure 3-4A). In these reactions the functionality being incorporated into the platform is brought in through the halides. These reactions are carried out in anhydrous acetone or anhydrous THF. The use of these solvents generally results in the product precipitating out of solution upon the formation of the salt. This not only provides a driving force for the reaction but it also generally gives pure product that can easily be collected by filtration. A number of functionalities have been incorporated into the water-soluble platform using this strategy for **3a** (Table 3-2).

Table 3-2: Water-soluble derivatives made from **3a**

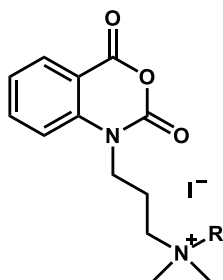
Entry	R	X	% yield
<b>3o</b>		$\text{Br}^-$	89
<b>3p</b>		$\text{I}^-$	64
<b>3q</b>		$\text{Br}^-$	84*
<b>3r</b>		$\text{Br}^-$	53*
<b>3s</b>	Me	$\text{I}^-$	69*
<b>3t</b>			-,**
<b>3u</b>		$\text{I}^-$	26*
<b>3v</b>		$\text{Br}^-$	76*

\*Reagent only synthesized once, highest yield obtained reported otherwise

\*\*Product not isolated, product formation was determined by ESI analysis of reaction mixture

The synthesis of the water-soluble derivatives using **3b** is carried out in much the same way, with the functionality now being brought in through a tertiary amine (Figure 3-4B). These reactions are also carried out in anhydrous acetone or THF generally resulting in the precipitation of the product, allowing for easy synthesis and clean-up of the final products. Water-soluble derivatives made using this method are shown in table 3-3.

Table 3-3: Water-soluble derivatives made from **3b**



Entry	R	% yield
<b>3w</b>		64
<b>3x</b>		~*,**



Table 3-3 continued

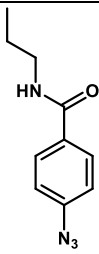
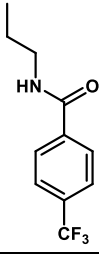
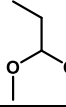
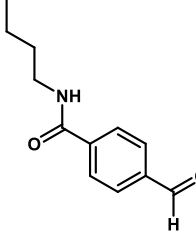
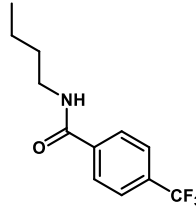
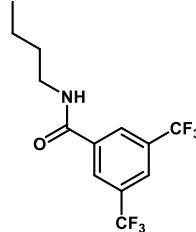
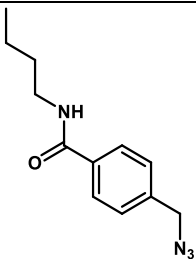
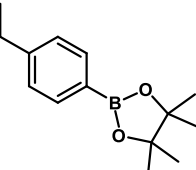
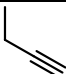
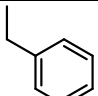
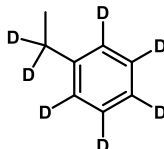
<b>3y</b>		66
<b>3z</b>		33 <sup>*</sup>
<b>3a'</b>		69 <sup>*</sup>
<b>3b'</b>		74
<b>3c'</b>		69
<b>3d'</b>		52

Table 3-3 continued

<b>3e'</b>		59
<b>3f'</b>		43*
<b>3g'</b>		78*
<b>3h'</b>		68*
<b>3i'</b>		41*

\*Reagent only synthesized once, highest yield obtained reported otherwise

\*\*Product not isolated, product formation was determined by ESI analysis of reaction mixture

The synthesis of water-soluble derivatives utilizing **3a** and **3b** has been demonstrated but not optimized. These reactions generally give moderate to high yields (50-89%). In general the product precipitates from solution as it is formed, however this is not universal. Some products, such as **3u**, had to be precipitated through the addition of ethyl ether, leading to reduced yields. Others, such as **3t** and **3x**, were confirmed by ESI but were unable to be precipitated.

### 3.3 Limitations of Water-Soluble Synthesis

Quaternization of **3a** requires the use of a halide that is electrophilic enough to react with its tertiary amine group. To determine the rates at which **3a** reacts with various

halides kinetic experiments were carried out in which the amount of unreacted **3a** remaining in solution was monitored by NMR. We have found that **3a** reacts with halide substrates to form ammonium salts at widely different rates. Reactions with primary chlorides and bromides give no appreciable product after 24 hours, even with heating to 50 °C, showing that these are not very suitable reagents for use with **3a**. However **3a** reacts with primary iodides, although these reactions are fairly slow. It was found that a reaction of 150 mM **3a** with an equimolar amount of iodobutane was ten percent complete in five hours at 25 °C.

The reaction rates of activated halides such as allylic, propargylic, and benzylic halides were also examined. When 50 mM **3a** was mixed with ten equivalents of allyl chloride no reaction was observed by NMR at 25 °C. When the temperature is increased to 45 °C the reaction did take place but at a slow rate, with a half-life of 43 hours. Moving to the more reactive activated bromides we found that these reactions occur appreciably faster than the corresponding chlorides, so fast that it is not necessary to monitor them by NMR. For example, when a small excess of propargyl bromide is added to a solution of **3a** salts can be seen precipitating immediately and collection of these salts after 15 minutes results in a yield of between 80 and 90%. All of this shows that the reactant chosen for reaction with **3a** needs to be about as reactive as allyl bromide. Activated bromides and iodides are the most ideal reagents as these reactions occur at reasonably fast rates. Activated chlorides and primary iodides can also be used however heat is usually required for the reactions to take place at reasonable rates.

The formation of ammonium salts with **3b** requires the use of tertiary amines. Various spacers can be put between the isatoic anhydride and a primary iodide, however

two in particular, the ethylene and the propylene spacers, would seem to give enhanced quaternization rates due to anchimeric assistance. The anchimeric assistance results from the oxygen present on carbonyl donating electron density to the alpha carbon, resulting in the formation of a five or six membered ring, making the iodide a better leaving group. It is known that the formation of five membered rings is more favorable in anchimeric assistance leading us to believe that the ethylene spacer would give the largest rate enhancement.<sup>33</sup>

Competition assays were performed to determine the reaction rates compared to iodobutane. In these assays the reagent of interest was mixed with iodobutane in equimolar amounts followed by the addition of N,N-dimethyloctylamine. If there is rate enhancements due to anchimeric assistance it is expected that our reagents would outcompete iodobutane in the formation of the ammonium salt. The disappearance of the reagents was monitored by NMR (Figure 3-5). Both reactions were carried out at a concentration of 30 mM. Upon running this experiment with the isatoic anhydride derivative containing the ethylene spacer, the unexpected result that this reagent was deactivated relative to primary iodides was obtained, with very little reacting during the course of the experiment. However the reagent with the propylene spacer, **3b**, did show the expected rate enhancement. In light of this data **3b**, along with **3a**, became the primary reagents for synthesis of water-soluble isatoic anhydride derivatives.

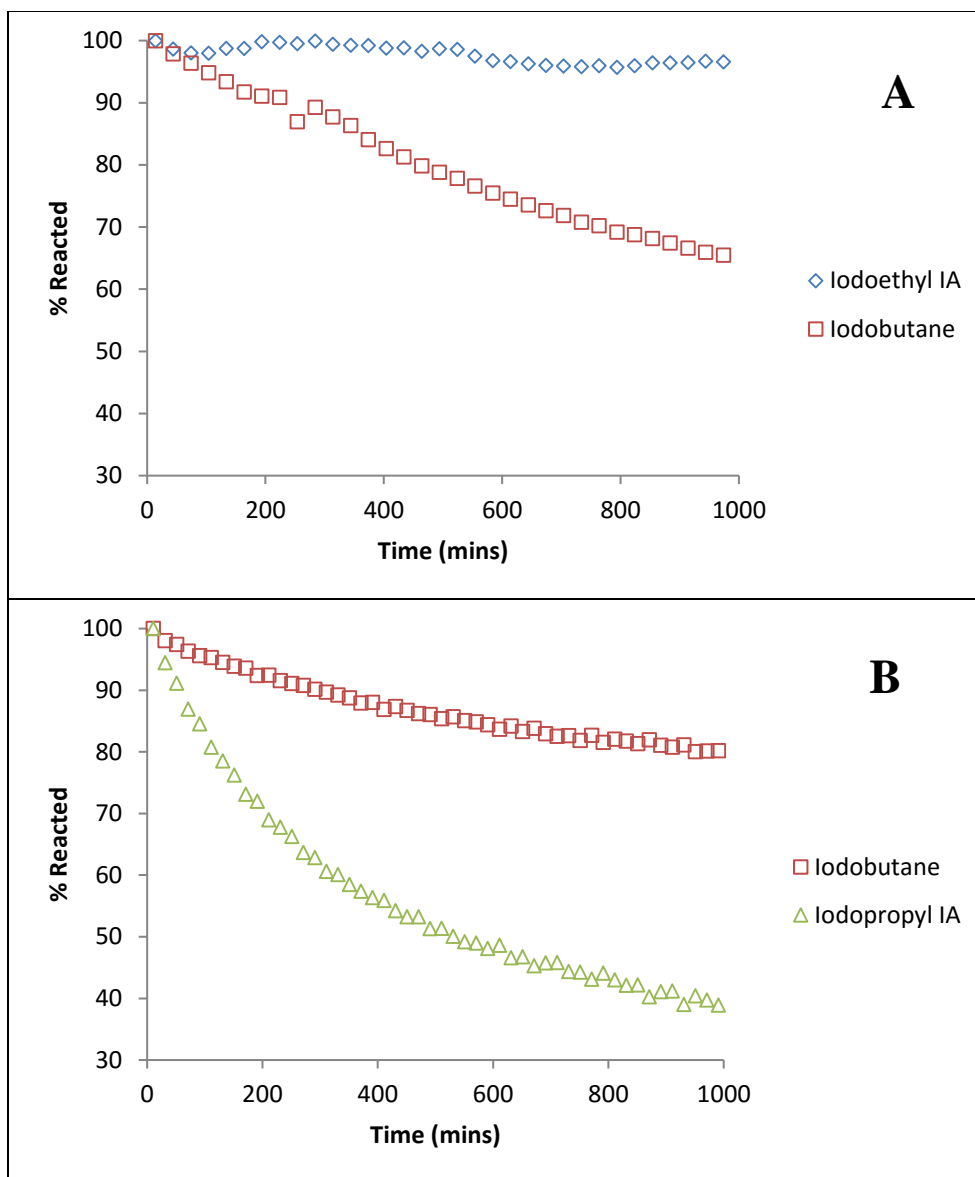


Figure 3-5: Competition assays of iodoethyl IA (A) and iodopropyl IA (B). Both reactions were carried out at a concentration of 30 mM with each competing with one equivalent of iodobutane for one equivalent of tertiary amine N,N-dimethyloctylamine

## CHAPTER 4: STABILITY AND REACTIVITY OF ANHYDRIDE MOIETY

### 4.1 Hydrolytic Stability

For effective conjugation of proteins bioconjugation reagents must selectively react with them. Reagents designed to react with nucleophilic lysine residues are also susceptible to hydrolysis. However once hydrolyzed these reagents lose their ability for conjugation. Almost all bioconjugation reactions are carried out under aqueous conditions in which the concentration of water is much greater than the concentration of protein. For this reason it is imperative that these new reagents undergo amidization with primary amines much faster than they undergo hydrolysis. Anhydrides are not known for their stability towards hydrolysis however we have been able to show that the anhydride present in isatoic anhydride derivatives have remarkable hydrolytic stability.

The half-lives of our reagents in the presence of water were determined by monitoring the hydrolysis of the water-soluble propargyl derivative **3o** by  $^1\text{H}$  NMR at 25 °C. These experiments were carried out with varying concentrations of sodium bicarbonate buffer at pD 8.4 in  $\text{D}_2\text{O}$ . It is important to determine the hydrolytic stability under basic conditions because the bioconjugation reactions must be carried out in basic conditions. These conditions are required to keep the lysine residues unprotonated and therefore nucleophilic. The progress of the hydrolysis reaction can be easily tracked by monitoring the signals present in the aromatic region. Both the reagent and the hydrolyzed product give sharp, well resolved peaks in this region (Figure 4-1). The

percent hydrolyzed at any given time was determined by the ratio between the reagent peak at 8.1 ppm and the product peak at 7.7 ppm.

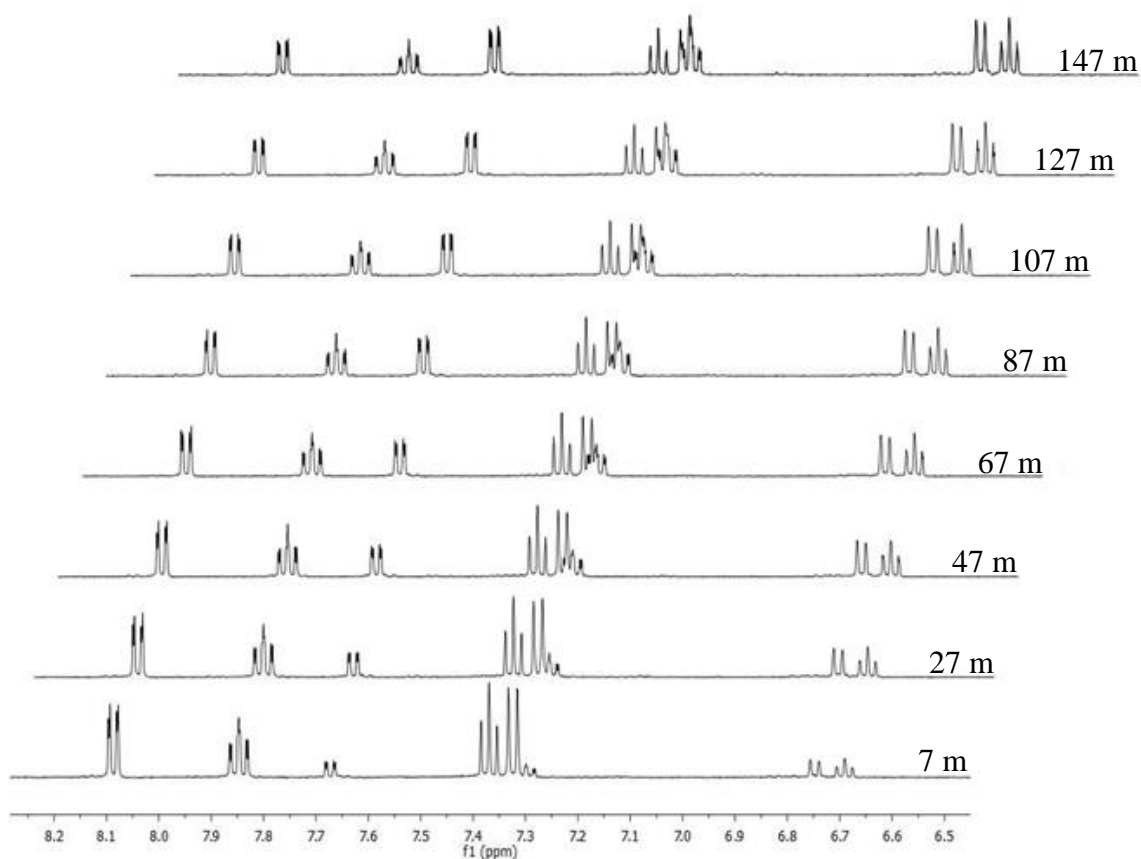


Figure 4-1: Kinetics trace of the hydrolysis of **3o** at 25 °C in 25 mM bicarbonate buffer at pH 8.4 tracked by <sup>1</sup>H NMR

Under these basic conditions, in which hydrolysis is promoted, these reagents have been shown to have excellent hydrolytic stability at a variety of buffer concentrations (Table 4-1). It was found to have a half-life of 16 hours in DI water with increasing hydrolysis rates as the buffer concentration is increased, as expected. It was also determined that that when dissolved in DI water and stored in a refrigerator at 4 °C

that the half-life increased to greater than 48 hours, showing that, when dissolved in neutral water, these reagents do not need to be used immediately .

Table 4-1: Half-life of **3o** at various bicarbonate concentrations at 25 °C

Bicarbonate Concentration (mM)	Half-life (min)
0	982
5	693
10	187
15	139
25	67
50	37
100	13

#### 4.2 Reactivity with Primary Amines

The target of these new reagents are the primary amines found on lysine residues, therefore it is important to determine how these react with primary amines in the presence of water. These experiments were carried out at 25 °C by reacting **3o** with varying equivalents of n-butylamine (0.25, 1, 10 eqs) in varying concentrations of sodium bicarbonate buffer (0, 10, 100 mM) at pD 8.4. These reactions were very fast, so fast in fact that attempts to monitor the reaction by rapid injection <sup>1</sup>H NMR in which the reagents are mixed together inside the spectrometer failed to capture any kinetic data. The first scan was collected at five seconds after injection. It was found that in every case that reaction was complete in under five seconds which can be seen by the complete disappearance of the reagent peak at 8.1 ppm (Figure 4-2).



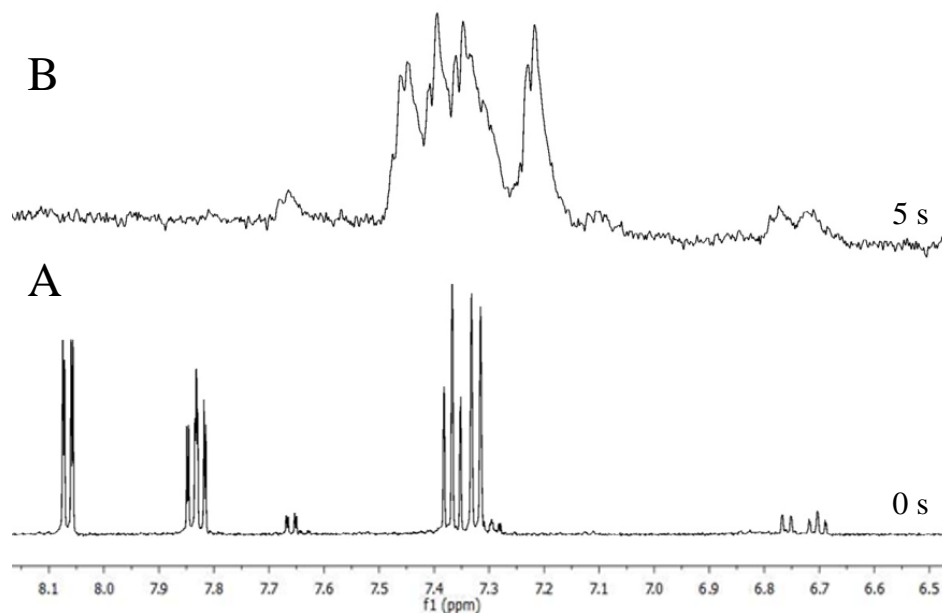


Figure 4-2: **3o** reaction with 10 equivalents of butylamine in DI water at 25 °C showing <sup>1</sup>H NMR of aromatics before injection (A) and five seconds after injection (B)

It should however be noted that the concentrations of butylamine (up to 5.5 mM) used in these experiments is much higher than the concentration of lysine residues used in most bioconjugation procedures. It was necessary to use these high concentrations so that the reaction could be seen by NMR. However, even with these relatively large concentrations of butylamine, water is ten thousand times more concentrated and there is very little increase in the amount of hydrolyzed product during the reaction. This data shows that our platform contains a carbonyl that is reasonably hydrolytically stable but also activated enough to rapidly undergo reactions with primary amines. Because of this our platform should be able to effectively conjugate to lysine residues under basic aqueous conditions.

## CHAPTER 5: BIOCONJUGATION WITH ISATOIC ANHYDRIDE REAGENTS

### 5.1 Determining the Degree of Labeling

The degree of labeling (DOL) is a measure of the average number of groups that have been coupled to a protein. The DOL is generally determined by measuring the absorption spectrum of the labeled protein. The concentration of the protein and the label can be independently determined by measuring the absorbance spectrum and exploiting Beer-Lambert's law. The DOL can then be calculated from the following equation:<sup>34</sup>

$$\text{DOL} = \frac{A_{\text{label}}\epsilon_{\text{prot}}}{A_{\text{prot}}\epsilon_{\text{label}}}$$

Equation 5-1

where  $A_{\text{label}}$  and  $A_{\text{prot}}$  are the absorbances from the label and protein respectively, and  $\epsilon_{\text{label}}$  and  $\epsilon_{\text{prot}}$  are the molar extinction coefficients of the label and protein respectively.

The protein concentration is generally determined by measuring its absorption at 280 nm, the wavelength at which the aromatic residues tryptophan and tyrosine most strongly absorb. Equation 5-1 works best when the label has little to no absorbance at 280 nm. However, most labels do have some contribution to absorbance at 280 nm. To obtain a more accurate measurement of the DOL a correction factor,  $C_{280}$ , must be introduced into the equation. This variable is a ratio of the molar extinction coefficients of the label

at 280 nm to its max absorbance. Introduction of this variable gives the modified DOL equation.<sup>34</sup>

$$\text{DOL} = \frac{A_{\text{max}}\epsilon_{\text{prot}}}{(A_{280}-A_{\text{max}}C_{280})\epsilon_{\text{max}}}$$

Equation 5-2

where  $A_{\text{max}}$  is the max absorbance of the label,  $A_{280}$  is the absorbance of the conjugate at 280 nm, and  $\epsilon_{\text{max}}$  is the molar extinction coefficient at the labels max absorbance.

To use equation 5-1 or 5-2, most bioconjugation reagents require conjugation of a group that has a unique and significantly strong absorbance separated from 280 nm to the protein. Whenever this is not the case other, more complicated methods must be used to determine the DOL, such as analysis of fragments of the bioconjugate by MS/MS. However, with the platform presented here, the DOL can always be determined using the above formulas by utilizing the platforms unique absorbance at 330 nm after conjugation has taken place, thus eliminating the need for more complicated analysis techniques.

## 5.2 Determination of $\epsilon_{330}$ and $C_{280}$

It was first shown that this platform gives a unique absorbance after conjugation using bovine serum albumin (BSA) and the water-soluble propargyl derivative **3o**. **3o** contains an alkyne functionality which can undergo the copper catalyzed 1,3-dipolar cycloaddition click reaction with azides. This introduces a unique chemical handle onto the protein that can be further built onto, allowing for the construction of more complex groups. BSA is the most abundant protein found in bovine blood. It is one of the most well studied proteins, has a high water-solubility of about 40 mg/mL, and is very

inexpensive making it a great protein for studying our platform. BSA weighs roughly 66.5 kDa and consists of a single peptide chain with 583 amino acid residues.<sup>35</sup> 59 of these amino acids are lysine residues and about 30-35 of these are solvent exposed and able to react with isatoic anhydride derivatives.

To conjugate to BSA, a solution of BSA is made up in the desired reaction buffer. **3o** is then dissolved in DI water and immediately added to the BSA solution. This is allowed to sit at room temperature for the desired amount of time at which point 5  $\mu$ L of ammonium hydroxide is added. Ammonium hydroxide contains ammonia which immediately reacts with any remaining bioconjugation reagent, stopping the reaction. Two general methods are used to analyze the reaction. In the first method the bioconjugate is isolated by passing the reaction mixture through a gel permeation chromatography (GPC) column. Passing the reaction through a GPC column purifies the conjugate by removing the small molecules. The bioconjugates' absorption and fluorescence profile can then be measured. In the second method the crude reaction mixture is analyzed by HPLC in-line with a diode array detector and a mass spectrometer. HPLC separates the components of the reaction, which means that purification of the bioconjugate is not necessary.

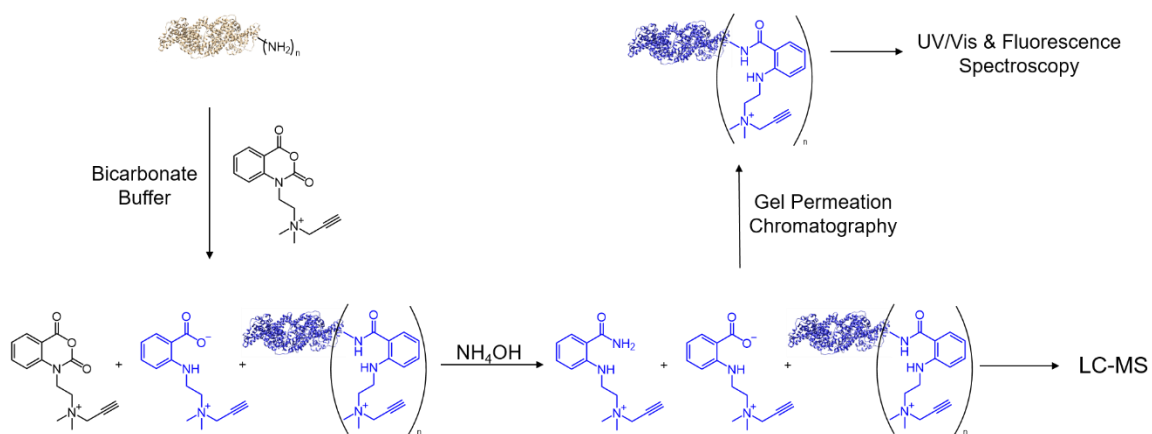


Figure 5-1: Reaction scheme and cleanup for conjugation of **3o** to BSA

The conjugation reaction was carried out in a 10 mM bicarbonate buffer at a pH of 8.4. BSA was at a concentration of 0.54 mM with five equivalents of **3o**. This was allowed to sit for one hour, at which point the conjugate was isolated by GPC. LC traces show the increase in absorbance at 330 nm after conjugation.

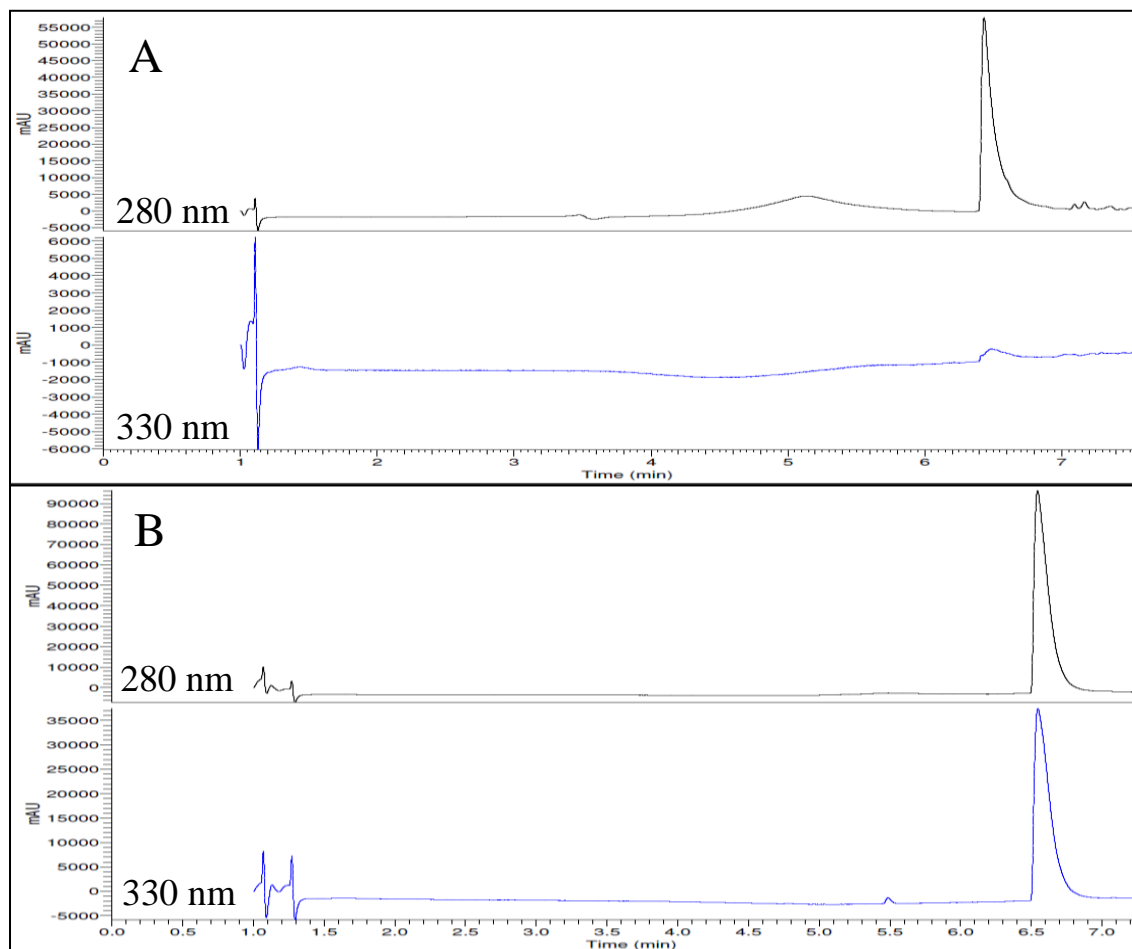


Figure 5-2: LC traces of BSA before conjugation (A) and after conjugation (B) with **3o**, showing the change in absorbance at 330 nm

The absorbance of the conjugate was also measured on a plate reader and compared to native BSA (Figure 5-3A). It can be seen that labeling with **3o** gives the conjugate an absorption from about 300 to 380 nm with a maximum absorbance at 330 nm. The fluorescence of the conjugate was also measured by exciting at 330 nm (Figure 5-3B). There is now a strong fluorescence at 420 nm. This shows that labeling with this platform gives the bioconjugates a unique spectroscopic profile that can be used to characterize the conjugate and easily determine the DOL.

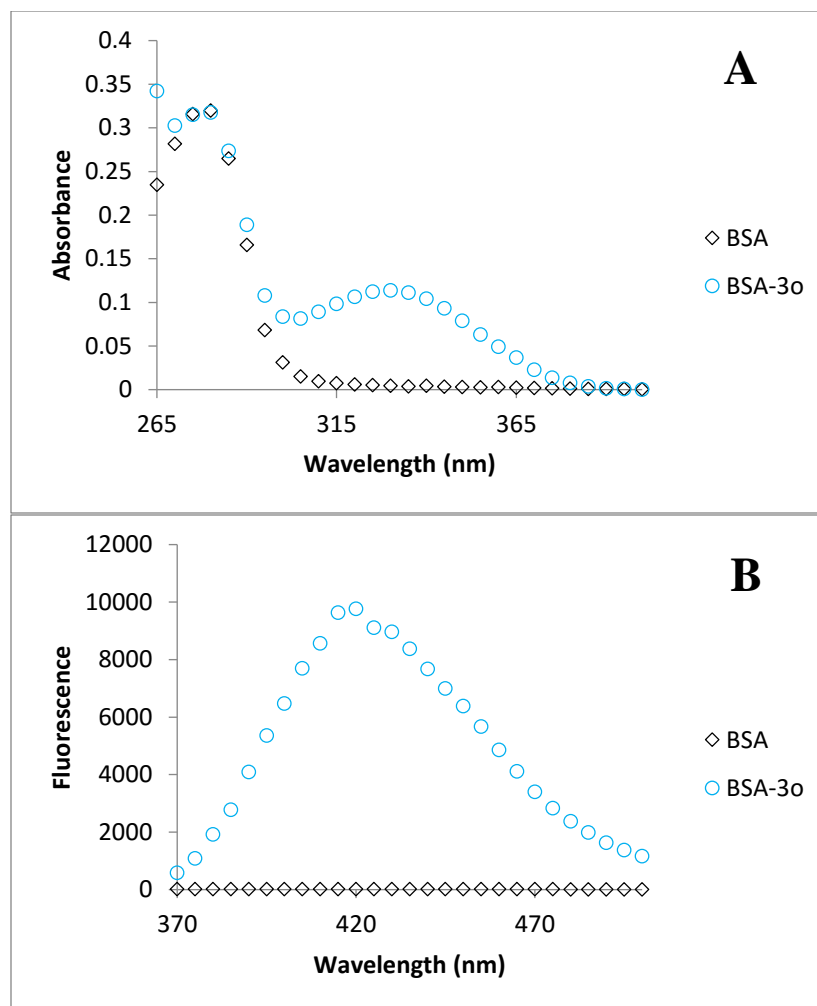


Figure 5-3: Absorbance (A) and fluorescence (B) of BSA before and after conjugation with **3o**

To use equation 5-2 with this new platform the molar extinction coefficient and correction factor of the isatoic anhydride reagents after conjugation must first be determined. Conjugating through lysine residues in proteins results in ring-opening of the anhydride reagent which is what gives the absorbance at 330 nm. To determine the molar extinction coefficient and correction factor, the reagents were ring-opened using butylamine as a model for lysine. To get clean conversion to ring-opened product **5a** (Figure 5-4), ten molar equivalents of butylamine were added to **3o** immediately followed

by an equal volume of anhydrous DMSO. The suspension was sonicated until all the solids had completely dissolved, followed by dilution to a known concentration with 25 mM bicarbonate buffer at pH 8.4. Each reaction was analyzed by LC with a UV-vis detector to confirm complete conversion to product. After confirming clean product, the absorbance of each solution was measured from 250 to 450 nm. **5a** was found to have a molar extinction coefficient of  $2942 \text{ M}^{-1}\text{cm}^{-1}$  at 330 nm, with a correction factor of 0.2. The same experiment was carried out with the water-soluble alkyl azide derivative **3p** to give ring-opened product **5b** (Figure 5-4), which was found to have a molar extinction coefficient of  $3009 \text{ M}^{-1}\text{cm}^{-1}$  at 330 nm, with a correction factor of 0.2.

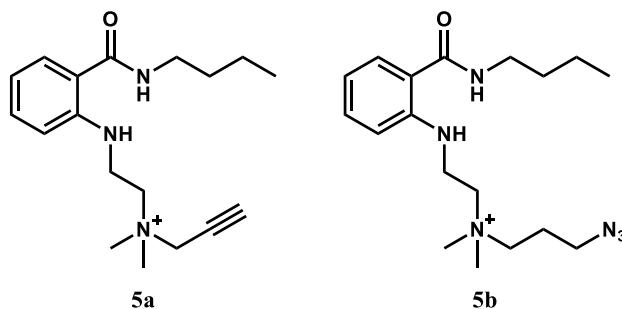


Figure 5-4: Products **5a** and **5b** formed by the reaction of reagents **3o** and **3p**, respectively, with butylamine

### 5.3 Bioconjugation Parameters

A variety of variables influence the DOL such as reaction time, stoichiometry, and pH. These variables can be exploited to give better control over the DOL of a bioconjugate and therefore its properties. For example, in the production of ADCs, a lower DOL of around two to four has been shown to be most effective. Higher DOLs result in a sample in which a larger portion of the antibodies have been conjugated to in



their antigen binding region, reducing their targeting ability. Additionally ADCs with higher DOLs are cleared from circulation more rapidly than those with lower DOLs.<sup>28</sup>

All of the parameters explored here were performed using BSA and **3o**. However it was first shown that our platform gives reproducible results. This was done by reacting a 1 mg/mL solution of BSA (15  $\mu$ M) with a 1 mg/mL solution of **3o** (2.8 mM) in a 10 mM bicarbonate solution at pH 8.4. The reaction was stopped after one hour and cleaned up by GPC. The fluorescence profile was then measured on a plate reader (Figure 5-5). It can be seen that all three reactions give nearly identical profiles showing that conjugating with these reagents is very reproducible.

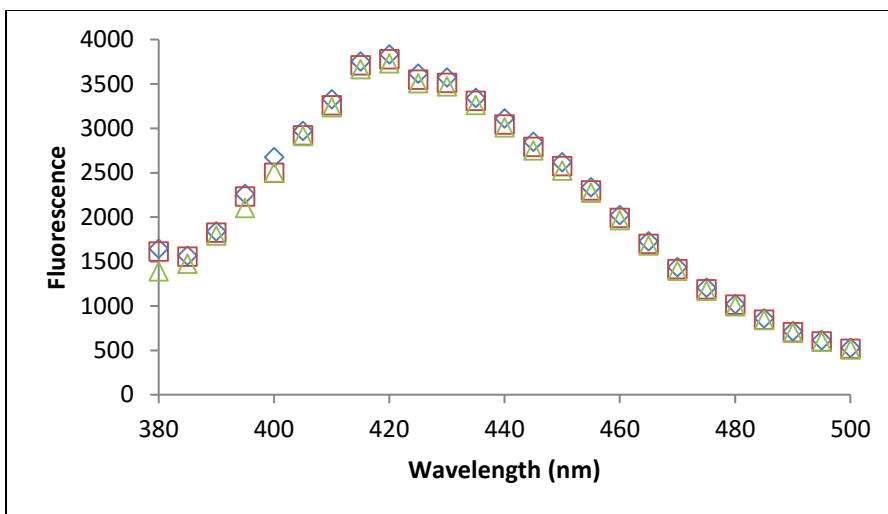


Figure 5-5: Fluorescence profile in triplicate of BSA at 1 mg/mL labeled with 187 equivalents of **3o** in 10 mM bicarbonate at pH 8.4

The first parameter that was examined was pH. pH plays an important role when using this platform; a basic solution is required to keep the lysine residues unprotonated and nucleophilic. However, as the pH increases the rate of hydrolysis of these reagents

also increases. To determine the effect of pH on the DOL, five reactions were carried out using BSA and **3o**, both at a concentration of 1 mg/mL. These were performed using buffers at a concentrations of 10 mM with a range of pHs from 6.4 to 10.6 (Figure 5-6). The DOL increases from 6.4 to 8.4 at which point it starts to decrease. This shows that reaction rate increases with increasing basicity but at about pH 8.4 the hydrolysis reaction starts to outcompete the bioconjugation reaction, suggesting that this is the optimum pH for this platform.

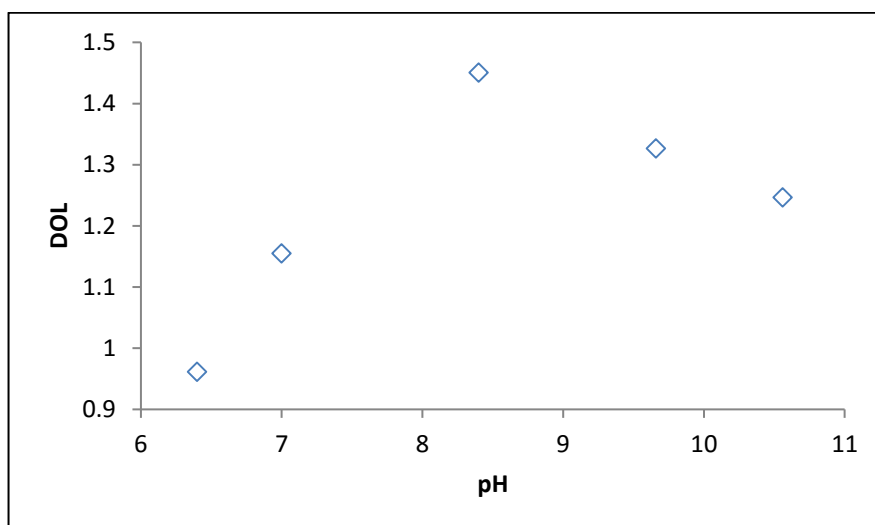


Figure 5-6: BSA at 1 mg/mL labeled with 187 equivalents of **3o** with 10 mM buffers at various pHs, showing that pH 8.4 gives the highest DOL

Next the effect of the buffer concentration at pH 8.4 on the reaction was examined using a bicarbonate buffer. BSA and **3o** were reacted at a concentration of 1 mg/mL each with buffer concentrations of 5, 15, 25, 50, and 100 mM (Figure 5-7). It can be seen that a buffer concentration of around 15 to 25 mM gives the highest DOL, with the DOL decreasing as the buffer concentration increases past 25 mM. This is to be expected as we have already shown that an increase in buffer concentration results in an increase in the rates of hydrolysis of the reagent (Table 4-1).

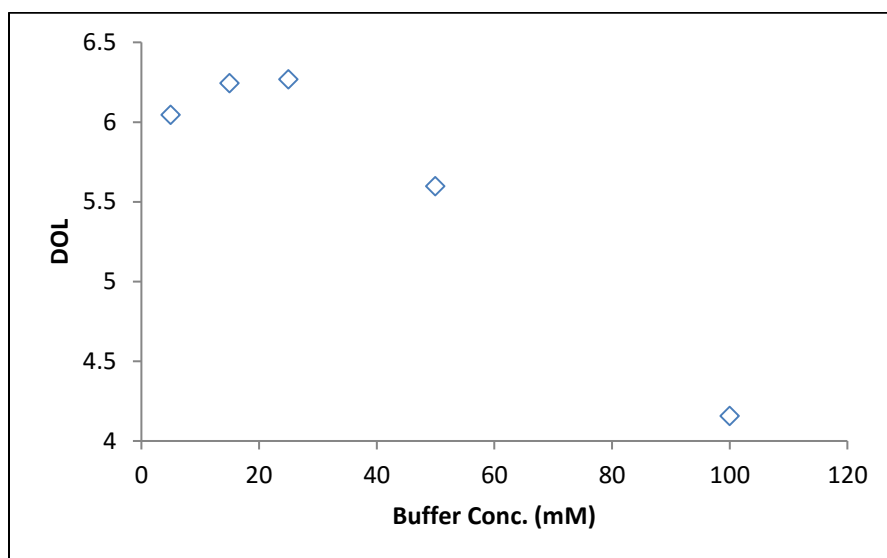


Figure 5-7: BSA at 1 mg/mL labeled with 187 equivalents of **3o** in various concentrations of bicarbonate buffer at pH 8.4

The effect of reaction time on the DOL was also examined. For this experiment, BSA at a concentration of 0.54 mM was reacted with five equivalents of **3o** in a 10 mM bicarbonate buffer at pH 8.4. At each time point an aliquot was taken and ammonium hydroxide was added. The reaction was then cleaned up by a GPC column and the absorbance at 330 nm was measured on a plate reader (Figure 5-8). The reaction is

complete after about an hour at which point the DOL has reached 4.5. It can be seen that the reaction proceeds rapidly at first, reaching a DOL of 3.6 after 2 minutes, and then slowly increases to the final DOL at an hour. Additionally, it shown that 90% of **3o** reacts with BSA. This high reaction efficiency is due to the concentration of the reagents being relatively high, which is possible due to the high solubility of BSA in water. The effect of reagent concentration on the DOL is discussed later in this chapter.

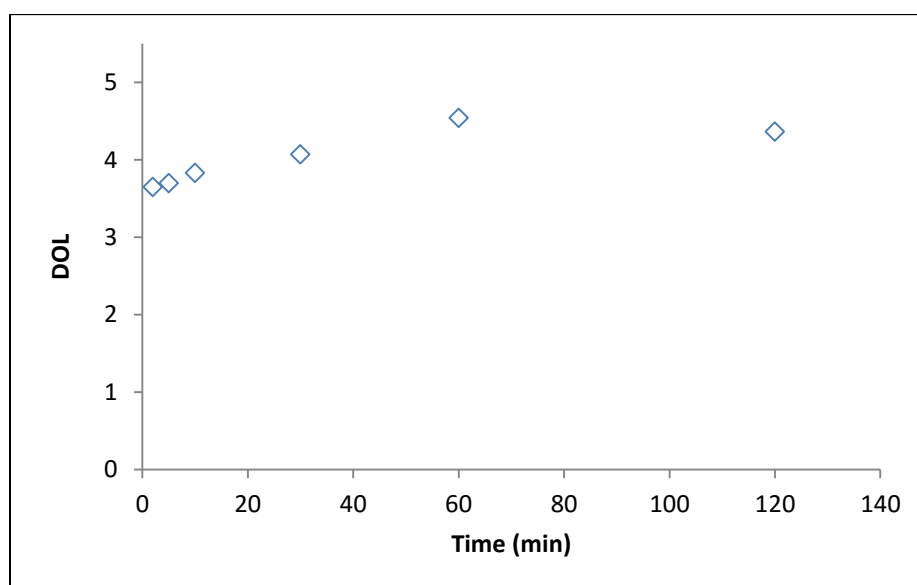


Figure 5-8: DOL at various time points of BSA, at 36 mg/mL, labeled with 5 equivalents of **3o** in 10 mM bicarbonate at pH 8.4

The last parameter that was explored was the reagent concentration. The effect on DOL of each reagent was measured individually. For **3o**, BSA at a concentration of 15  $\mu$ M was reacted with 1, 10, and 100 equivalents of **3o** in a 10 mM bicarbonate buffer at pH 8.4. The DOL was measured at various time points (Figure 5-9). With 1 and 10 equivalents the reaction is complete within five minutes with a DOL of 0.4 and 1.5 respectively. When reacted with 100 equivalents, the DOL reaches about 8.6 after just five minutes and is still rising after 2 hours, at a much slower rate than initially.

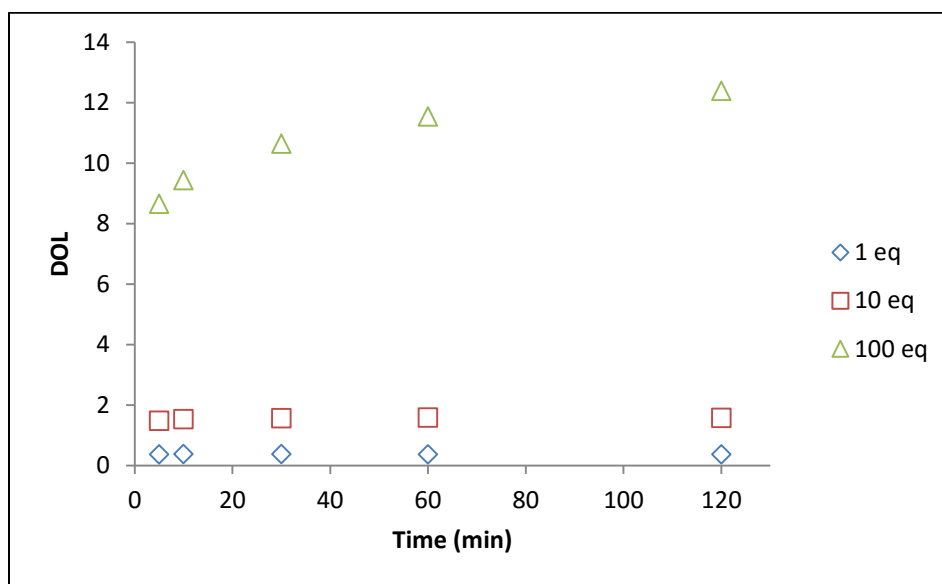


Figure 5-9: BSA at 1 mg/mL labeled with various equivalents of **3o** in 10 mM bicarbonate at pH 8.4

To examine the effect of the BSA concentration various concentrations of BSA were reacted with **3o**, held at a constant concentration, for one hour in a 100 mM bicarbonate buffer at pH 8.4. For the lowest BSA concentration, BSA at 15  $\mu$ M was reacted with 100 equivalents of **3o**. The BSA concentration was increased to a 150  $\mu$ M, at

which point it was reacting with only 10 equivalents of **3o** (Figure 5-10). The DOL decreases from 6.4 at the lowest concentration of BSA to 4.0 at the highest concentration. This is expected because with a higher concentration of BSA, **3o** will on average conjugate fewer times to each molecule.

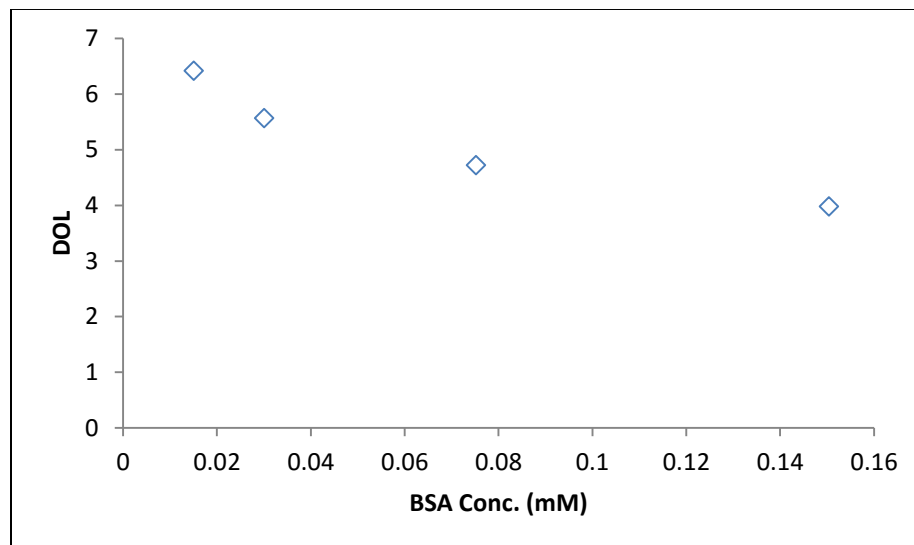


Figure 5-10: BSA at various concentrations labeled with **3o** at a concentration of 1.5 mM in 100 mM bicarbonate buffer at pH 8.4

When examining at the effect of BSA concentration, the reaction mixture was separated by HPLC and analyzed with a UV-vis detector. This is so that the amount of hydrolyzed **3o** in the sample could be measured. In any reaction, ideally there would be no waste and all reagents would be incorporated into the product. However, when conjugating to a protein under aqueous conditions, some of the isatoic anhydride reagent is going to be lost due to hydrolysis. By measuring the amount of hydrolyzed **3o** in the reaction, it can be determined how the concentration of the reagents effects the **3o** reaction efficiency (Figure 5-11). It can be seen that there is almost a linear increase in **3o**

reaction efficiency with BSA concentration, with almost 40% efficiency when BSA, at a concentration of 150  $\mu\text{M}$ , is reacted with 10 equivalents of **3o**.

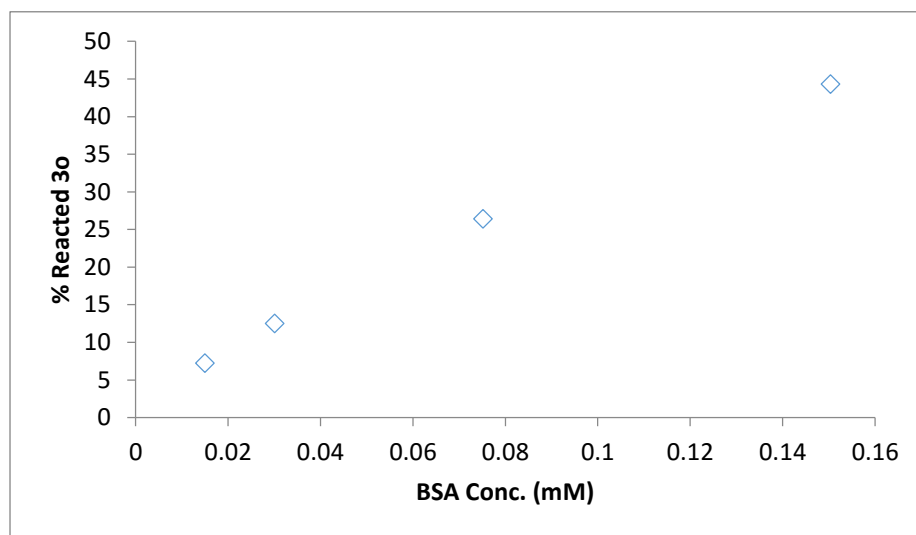


Figure 5-11: Increasing the BSA concentration with holding the concentration of **3o** constant, showing that there is an increase in the reaction efficiency of **3o** as BSA concentration is increased.

This data shows that the DOL can be determined by utilizing the platforms unique absorbance at 330 nm and that the DOL can easily be controlled by adjusting various parameters of the reaction. It should be noted that the experiments carried in figures 5-6 through 5-11 were only carried out a single time each. However each experiment produced the expected trend. It was shown, through triplicate data, that the reagents give highly reproducible results (Figure 5-5). It is reasonable that the optimal pH for this platform is close to 8.4, due to the conjugation reaction competing with hydrolysis. Additionally, the trends were the same across the experiments. For example, both figure 5-8 and 5-9 show the DOL increasing with time. Figure 5-8, in which a high

concentration of BSA (36 mg/mL) was utilized, shows a reaction efficiency of about 90%. This high efficiency agrees with the trend shown in figure 5-11.

#### 5.4 Further Functionalization after Conjugation

Conjugation of **3o** to a protein inserts an alkyne functional group onto the protein, a group that is generally not found in proteins. This gives a chemical handle that can be further conjugated to through the copper-catalyzed azide-alkyne cycloaddition (CuAAC) click reaction, allowing for the incorporation of more complex functionalities into the protein. This reaction is known to proceed at room temperature to give quantitative yields. However, the alkyne being present on the surface of a protein could present problems. The protein acts as a steric barrier, which may prevent the alkyne from being able to associate with the copper catalyst or the azide reagent. Additionally it is known that groups present in proteins, specifically histidine residues, are capable of chelating to copper ions.<sup>36</sup> This poses two problems to the reaction. First, chelating of the copper removes the catalyst from the solution, stopping the reaction. Second, copper complexing with the protein may result in the precipitation of the protein.

To determine if **3o** was able to undergo the click reaction after conjugation to a protein, the bioconjugate was reacted with the azide reagent **5b**. The reaction was set up using a protocol developed by M. G. Finn, which is designed for use in bioconjugation.<sup>37</sup> Briefly, a 7.5  $\mu$ M solution of BSA with a DOL of 1 was made up in 100 mM bicarbonate buffer at a pH of 7.9. Two equivalents of the ring-opened **5b** reagent were then added. Copper sulfate and tris(3-hydroxypropyltriazolylmethyl)amine (THPTA) were added to give a concentration of 0.1 mM and 0.5 mM respectively. Finally aminoguanidine was added followed by sodium ascorbate, both to a concentration of 5 mM. Two reactions



were set up, one was kept at 25 °C and the other at 35 °C. These were reacted for a total of 24 hours with aliquots taken at various time point to measure the reaction progress (Figure 5-12). Each time point was spun through a GPC column to purify the conjugate.

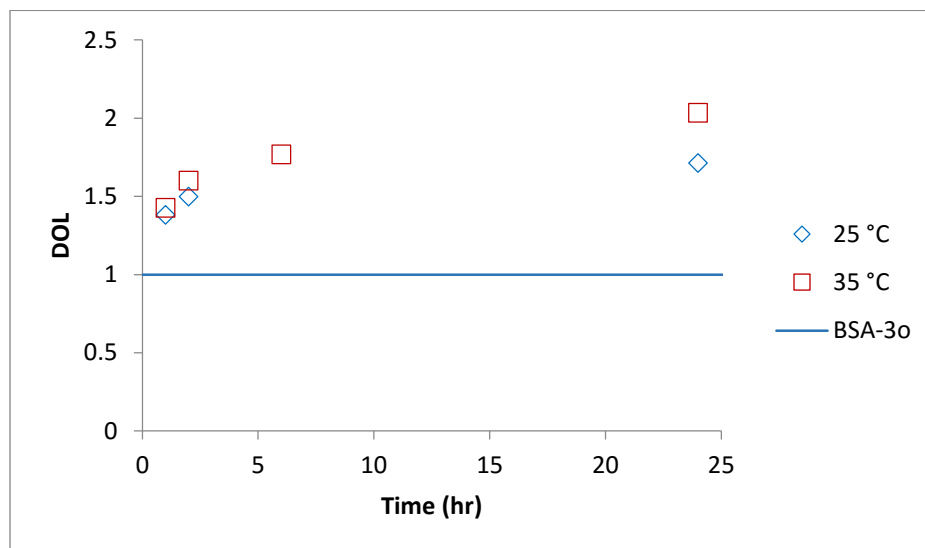


Figure 5-12: Azide-alkyne click reaction progress using BSA labeled with **3o** with a DOL of 1

The DOL is expected to double if the reaction goes to completion because another group containing the ring-opened isatoic anhydride is being added. It is seen that at 25 °C the reaction only goes to about 70% completion in 24 hours. This could be due to the steric hindrance caused by the BSA or from the BSA sequestering the copper ions. However, when reacted at 35 °C the reaction now goes to completion in 24 hours, showing that when an alkyne is conjugated to a protein using an isatoic anhydride reagent that it can still effectively undergo the CuAAC reaction.

## CHAPTER 6: DEVELOPMENT OF ANTIBODY-DRUG CONJUGATES

### 6.1 Antibody-Drug Conjugate Overview

Development of an antibody-drug conjugate (ADC) utilizing this new platform was a final goal of this project. ADCs utilize the high selectivity and specificity of the antibody (Ab) to deliver a cytotoxic payload to diseased tissues. This targeting ability make ADCs highly attractive therapeutics platforms for the treatment of cancer, wherein the chosen cytotoxin would ideally be delivered to only tumor sites. Accordingly, the localization of the cytotoxic payload serves to mitigate side effects associated with traditional therapeutic paradigms, while concurrently increasing the local concentration of the cytotoxin. Additionally, this platform can facilitate the application of compounds otherwise hampered by inherently low therapeutic indices.

Several important design parameters must be considered in the development of an effective ADC. Parameters such as: choice of cytotoxin, linker length and associated chemistry governing the connection of the cytotoxin to the Ab, amount of drug attached to the Ab, and the site of attachment on the Ab. ADCs with a low amount of drug-loading, typically between two and four, have been shown to be the most effective.<sup>28</sup> One result of a higher loading is that a greater proportion of the ADCs will be conjugated through their binding region, reducing or eliminating their targeting ability. Despite low drug-loading, ADCs must deliver an effective dose to the target. For this reason it is important to use a highly cytotoxic compound which is still effective at small doses. For

this project three FDA approved drugs were chosen for incorporation into an ADC; gemcitabine, 5-fluorouracil (5-FU), and colchicine (Figure 6-1), each of which will be discussed in more detail in the following sections.

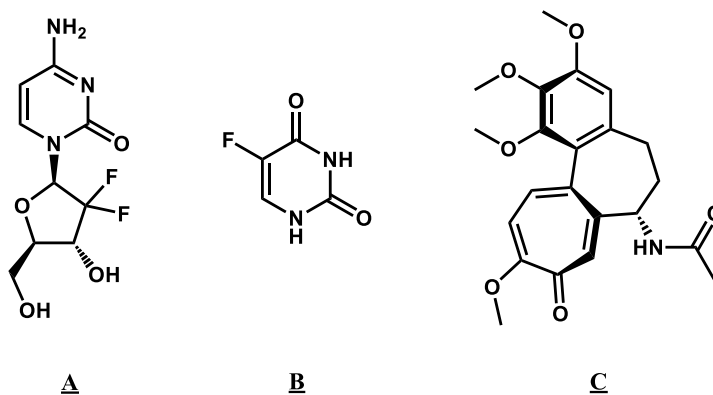


Figure 6-1: FDA approved drugs; A. Gemcitabine, B. 5-Fluorouracil, C. Colchicine

ADCs utilize monoclonal antibodies that selectively bind with cellular markers that are overexpressed at the target. The Ab used in the development of ADCs for this project is the monoclonal Ab TAB004 provided by the Mukherjee group at UNCC. TAB004 has been specifically engineered to bind the peptide backbone of the glycoprotein mucin 1 (MUC1).<sup>38</sup> Mucins are a family of proteins that are overexpressed in several types of cancer including breast, prostate, lung, and pancreatic cancer.<sup>39</sup> MUC1 is the most comprehensively studied of the mucin proteins and plays a crucial role in the progression of cancer. This protein has been found to be overexpressed in over 90% of breast cancers.<sup>40</sup> In healthy cells MUC1 is heavily glycosylated, shielding its peptide core. However, tumor-associated MUC1 is hypoglycosylated, exposing its peptide core. This core is composed of tandem repeats of 20 amino acids, which is the presumptive

target of TAB004. MUC1 is an excellent target for a variety of cancers<sup>40</sup>. The utilization of an Ab that targets hypoglycosylated MUC1 allows for the effective development of ADCs.

## 6.2 Prodrug Synthesis

The first step in development of an ADC is the incorporation of a linker that allows the desired payload to be conjugated to the Ab. This linker serves several distinct purposes that govern the pharmacokinetics of the resulting ADC. Structurally, the linker serves to connect the payload to the Ab in a distant dependent manner (Figure 6-2). This parameter is an important design parameter which can be used to modulate the performance of the ADC. Additionally, the linker must contain a functional group (Figure 6-2) that is stable during circulation but selectively cleaved upon cellular internalization or localization. Without being cleaved once at the target, the cytotoxin will presumably remain inactive. ADCs are internalized into the cell through receptor-mediated endocytosis, at which point they undergo intracellular trafficking through an array of pathways.<sup>41</sup> When designed correctly, ADCs can take advantage of specific trafficking routes. For example, the ADC gemtuzumab incorporates an acid-labile hydrazone linkage, which is designed to be cleaved within the lysosome where it experiences a drop in pH.<sup>42</sup> Other ADCs have been designed with peptide linkers that are selectively cleaved by intracellular enzymes.<sup>43</sup>

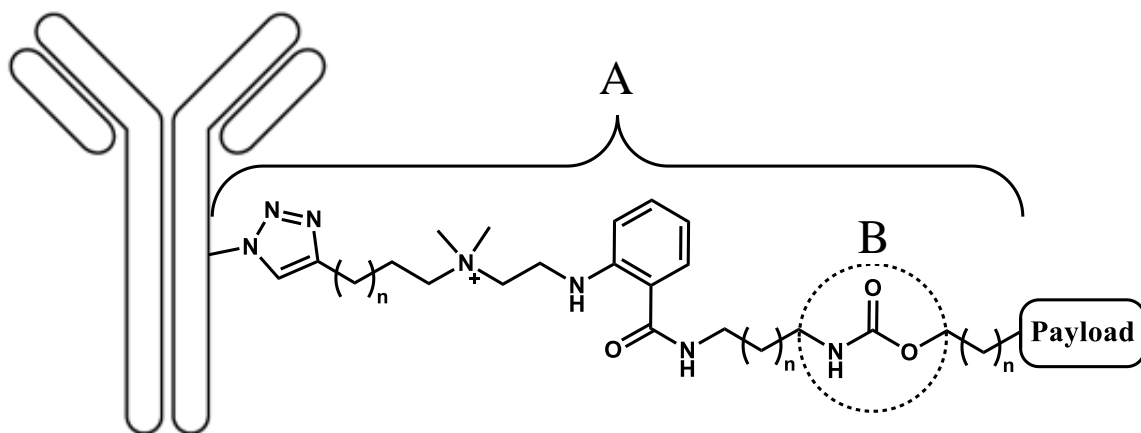


Figure 6-2: Linker serves the purpose of creating distance between the payload and the Ab (A) and contains a labile functional group (B)

The ADCs designed in this project will utilize linkages that are enzymatically cleavable once in the cell. In particular, the prodrugs will be designed with linkages that contain functional groups, known to be substrates for the enzyme carboxylesterase 2 (CES2). CES2 enzymes are responsible for the hydrolysis of amides, esters, and carbamates in many drugs and pharmaceuticals, including orlistat, irinotecan, and doxazolidine.<sup>44</sup> Prodrugs designed here will incorporate either carbamate or carbonate linkages, which are putative substrates for CES2. CES2 has been shown to be overexpressed in many types of cancer, including pancreatic, thyroid, renal, stomach, and ovarian cancer.<sup>45</sup>

### 6.2.1 Gemcitabine and 5-Fluorouracil

Gemcitabine and 5-FU are cytotoxins that are listed as some of the most important medications in the World Health Organization's list of essential medicines.<sup>46</sup> They are commonly used in the treatment of various types of cancer including breast, bladder, ovarian, lung, and pancreatic cancer.<sup>47</sup> In particular, pancreatic cancer is one of

the deadliest and most difficult to treat forms of cancer, with a median survival rate of less than five months after diagnosis.<sup>48</sup> Both of these drugs have mechanisms that interfere with DNA synthesis and repair. When gemcitabine is internalized it becomes triphosphorylated by a series of enzymes forming gemcitabine triphosphate (Figure 6-3). In this triphosphate form, it can be incorporated into a growing DNA strand by replacing cytidine. After incorporation, only one more nucleotide is incorporated into the strand. Gemcitabine being in a non-terminal position prevents DNA polymerases from proceeding and also blocks its removal by DNA repair enzymes. By preventing the synthesis of DNA, gemcitabine causes cellular apoptosis.<sup>47</sup>

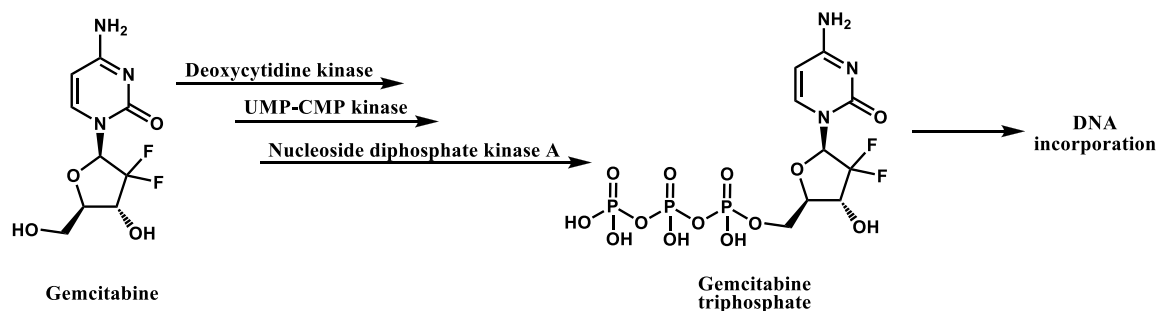


Figure 6-3: Phosphorylation of gemcitabine to gemcitabine triphosphate by a series of enzymes

5-FU is quickly converted into a variety of active metabolites upon internalization, which have different effects on the cell. The most important of these is fluorodeoxyuridine monophosphate (Figure 6-4B) which binds to and inhibits the activity of thymidylate synthase. Thymidylate synthase is the only source of thymidylate in cells, a molecule that is necessary for DNA replication and repair.<sup>49</sup> Capecitabine (Figure 6-5A) is a prodrug of 5-FU that was designed to be less toxic and a more effective

alternative to 5-FU. Capecitabine is used to mimic continuous infusion of 5-FU.<sup>50</sup> Once capecitabine is brought into the cell it is rapidly converted into 5-FU through a series of enzymes (Figure 6-4A). Capecitabine is synthetically produced and during its production a number of impurities are formed. Capecitabine impurity A (Figure 6-5B) is one such impurity that will be utilized here. This is an impurity in which there is no carbamate present, leaving a nucleophilic amine open for functionalization.

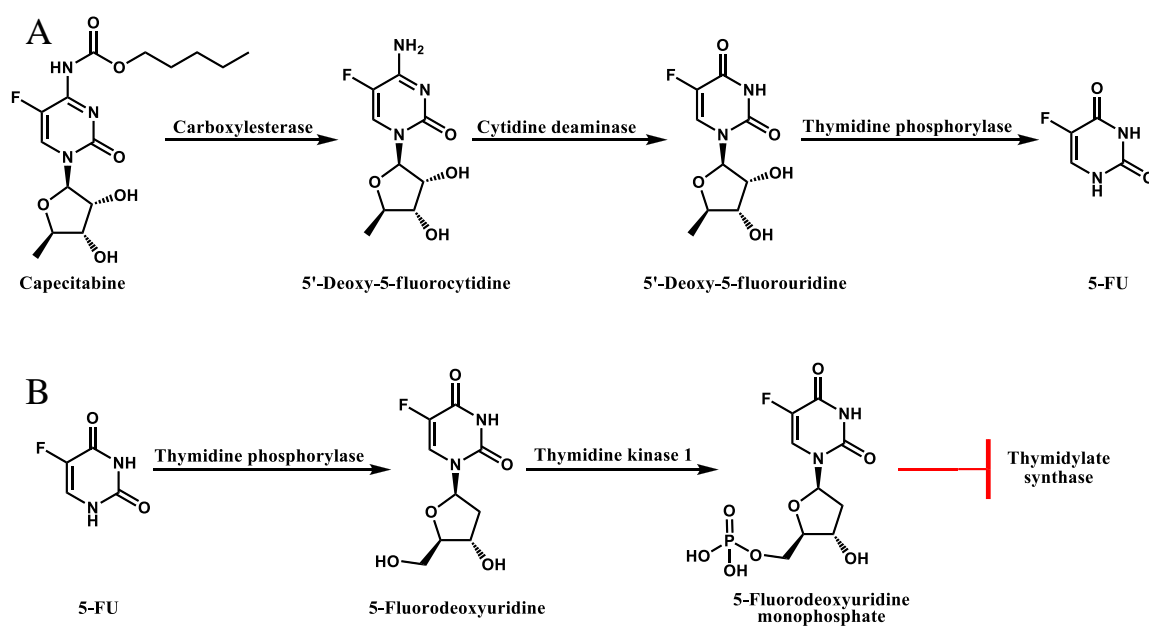


Figure 6-4: Enzymatic breakdown of prodrug capecitabine to 5-FU (A) and conversion of 5-FU to the active metabolite fluorodeoxyuridine monophosphate which inhibits thymidylate synthase (B)

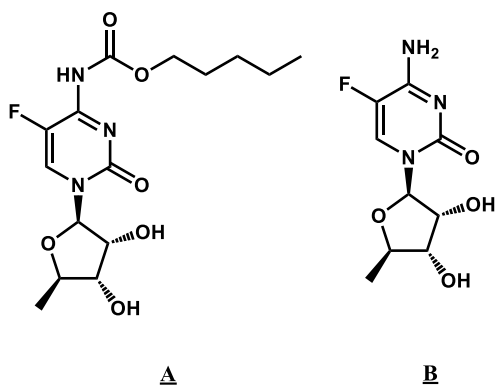


Figure 6-5: Structures of capecitabine (A) and capecitabine impurity A (B)

Gemcitabine and capecitabine impurity A contain nucleophilic hydroxyl groups and amine groups which can be used as chemical handles for functionalization. **6a** was used to incorporate alkynes into these cytotoxins. The hydroxyl of 4-pentyn-1-ol was treated with carbonyldiimidazole (CDI) to form the corresponding *O*-alkyl carbamoylimidazole **6b** (Figure 6-6), followed by methylation with iodomethane to form the *O*-alkyl carbamoylimidazolium salt **6c**.

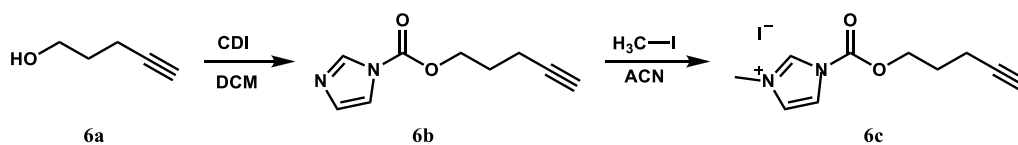


Figure 6-6: Activation of the hydroxyl group in 4-pentyn-1-ol through the reaction with CDI followed by methylation with iodomethane

Gemcitabine contains three nucleophilic groups, two hydroxyls and one amine (Figure 6-1A). It is expected that each of these functional groups will react with the activated carbonyl group in a kinetically controlled process (Figure 6-7). All three of



these products were seen by LC-MS, each of which could potentially be used to form an ADC. However, only two of the three products were able to be purified. Compounds **6d** and the **6e** were isolated in 7% and 8% respectively.

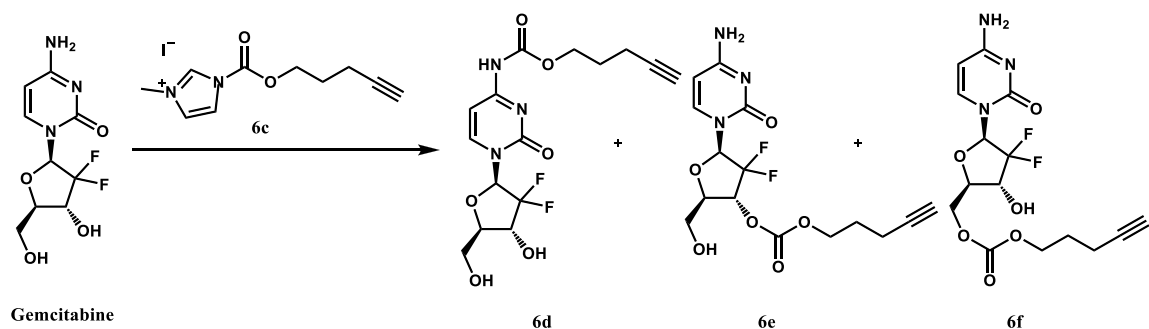


Figure 6-7: Reaction of gemcitabine with **6c** resulting in the incorporation of an alkyne at multiple sites through a carbamate linkage

Capecitabine impurity A was derivatized with **6c** in a fashion similar to that used for derivatizing gemcitabine. The two major products seen by LC-MS were the cyclic carbonate derivative and the amine functionalized derivate **6g**.

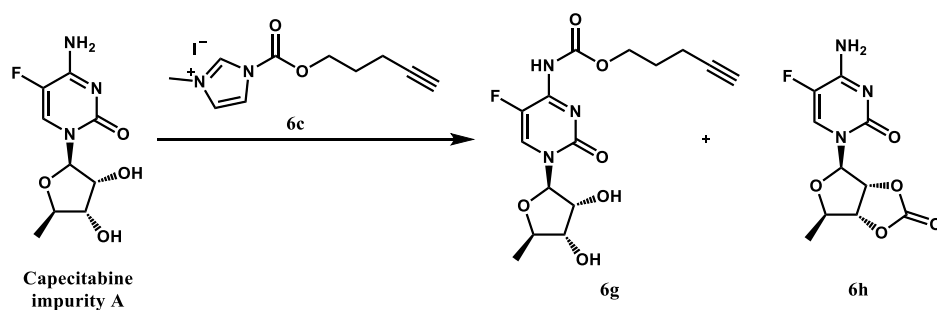


Figure 6-8: Reaction of capecitabine with **6c** resulting in the incorporation of an alkyne in product **6g** and the formation of a cyclic carbonate in **6h**

Three prodrugs have been synthesized that contain alkyne functional groups, two gemcitabine derivatives and one capecitabine derivative. These can be incorporated into an Ab by first functionalizing the Ab with one of the water-soluble azide derivatives in our platform and then by using the copper catalyzed azide-alkyne cycloaddition (CuAAC) reaction. Each of these derivatives contains either a carbonate (**6e**) or carbamate (**6d**, **6g**) linkage which has the potential of being enzymatically cleaved inside the cell to give off the native drug. However, when using these derivatives, the extent of drug loading onto the Ab platform cannot be easily determined due to the lack of the isatoic anhydride moiety. They can give information about how the carbonate and carbamate linkages effect the potency of the cytotoxins through biological studies.

#### 6.2.2 Colchicine Overview

Colchicine is a cornerstone molecule in both synthetic organic chemistry and biological sciences alike. Colchicine first appears in the pharmacopeia almost 2000 years ago when medicinal preparations of the meadow saffron colchicinum autumnale<sup>51</sup> were described in *De Materia Medica*. Modern therapeutic applications of colchicine includes its sole application in the treatment of gout.<sup>52</sup> Colchicine is an antimitotic drug that inhibits the linear polymerization of tubulin during mitosis. During prometaphase colchicine binds to tubulin as it polymerizes, causing a bend in the polymer at each binding site. As a result the tubulin curls back in on itself, preventing it from reaching the chromosomes and resulting in cellular apoptosis.<sup>53</sup>

Colchicine is not used in cancer treatments due to its very narrow therapeutic index. There is no clear distinction between therapeutic and lethal doses, with the reported lethal doses being as low as 7 and 26 mg.<sup>52</sup> Conversely, however, this toxicity

also makes colchicine a salient candidate as a cytotoxin for the development of a unique ADC platform. ADCs are generally only capable of delivering a small amount of drug per unit to the respective targets, but with colchicine's high toxicity, only a small amount needs to be delivered to be effective. Further, the unique mechanism of colchicines action classifies it as a substoichiometric antimetabolic, in that small mole ratios of colchicine to tubulin still strongly inhibits linear polymerization.<sup>54</sup>

### 6.2.3 Colchicine Derivation

There are two general methods that can be utilized so that the amount of drug incorporated in the ADC platform can be quantified using the chromatic properties of this platform (Figure 6-9). The first route will be the construction of a prodrug that contains the anhydride (Figure 6-9A). This will enable direct quantification of the drug content utilizing the chromophore of the new bioconjugation platform via a simple UV scan. In the second method complementary functional groups, such as azides and alkynes, are introduced onto the prodrug and Ab separately (Figure 6-9B). These are introduced using the anhydride in the platform, so that the ring-opened isatoic anhydride moiety is introduced into both the drug and the Ab. When these are then conjugated together the absorbance of the linkers can be used to determine the amount of drug loading. Both of these methods will be demonstrated using colchicine.

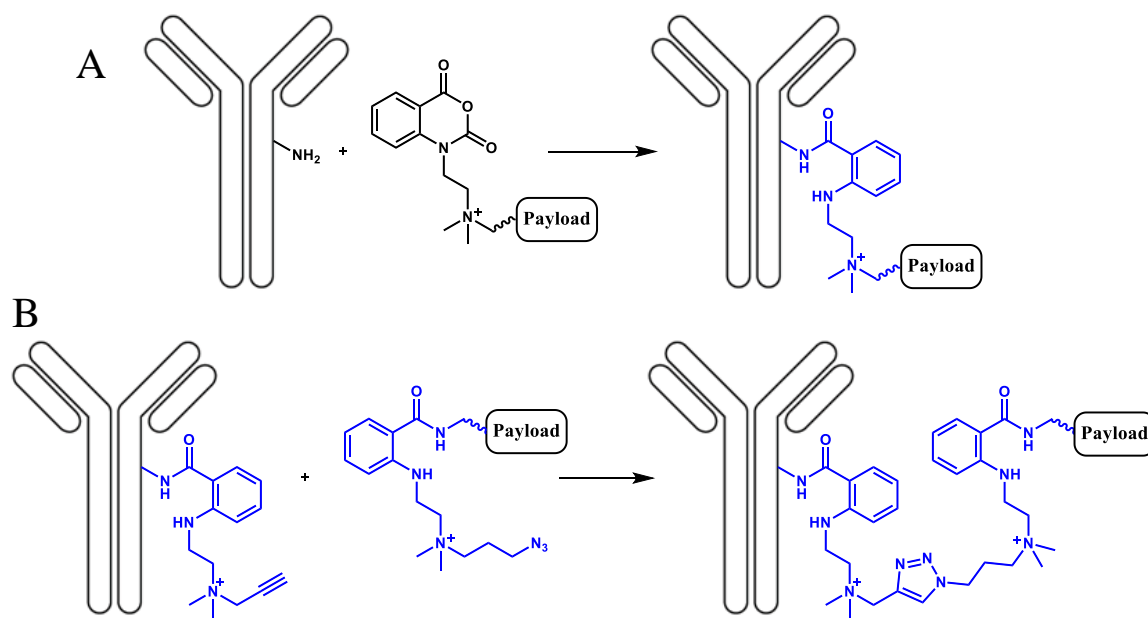


Figure 6-9: Two general methods for forming ADCs utilizing either one (A) or two (B) isatoic anhydride moieties

The first step for derivation of colchicine is the substitution of the methoxy group present on the seven-membered ring with a primary or secondary amine, using previously described procedure (Figure 6-10).<sup>55</sup>

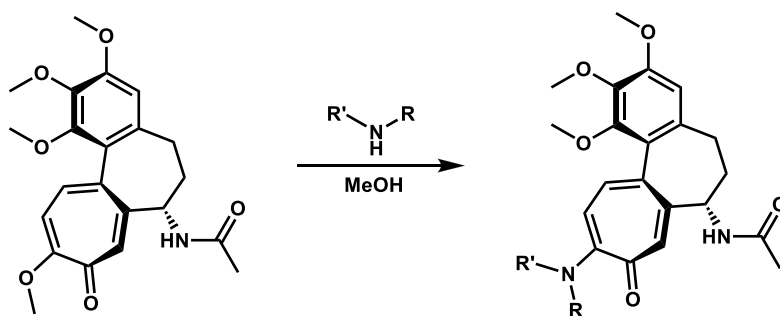


Figure 6-10: Substitution of methoxy in colchicine with a primary or secondary amine

This procedure was carried out with 3 different amines; N-boc-1,3-propanediamine, N-methylethanolamine, and piperazine-1-ethanol (Figure 6-11). The procedure that was followed calls for colchicine to be stirred with four equivalents of the amine in methanol. This gave clean conversion to the mono-protected diamine when it stirred at 40 °C overnight. This was then deprotected with trifluoroacetic acid to give the free amine. However, for the secondary amines, the rate of reaction was much slower and there was less than 10% product conversion after sitting overnight at 55 °C. To get a significant rate enhancement, we tried using the amine as the solvent. Colchicine was able to be dissolved in the N-methylethanolamine, and after 2 hours at 40 °C there was complete conversion to product. For the piperazine-1-ethanol, 10% methanol was used as a co-solvent to dissolve colchicine and the reaction was complete after 6 hours at 40 °C.

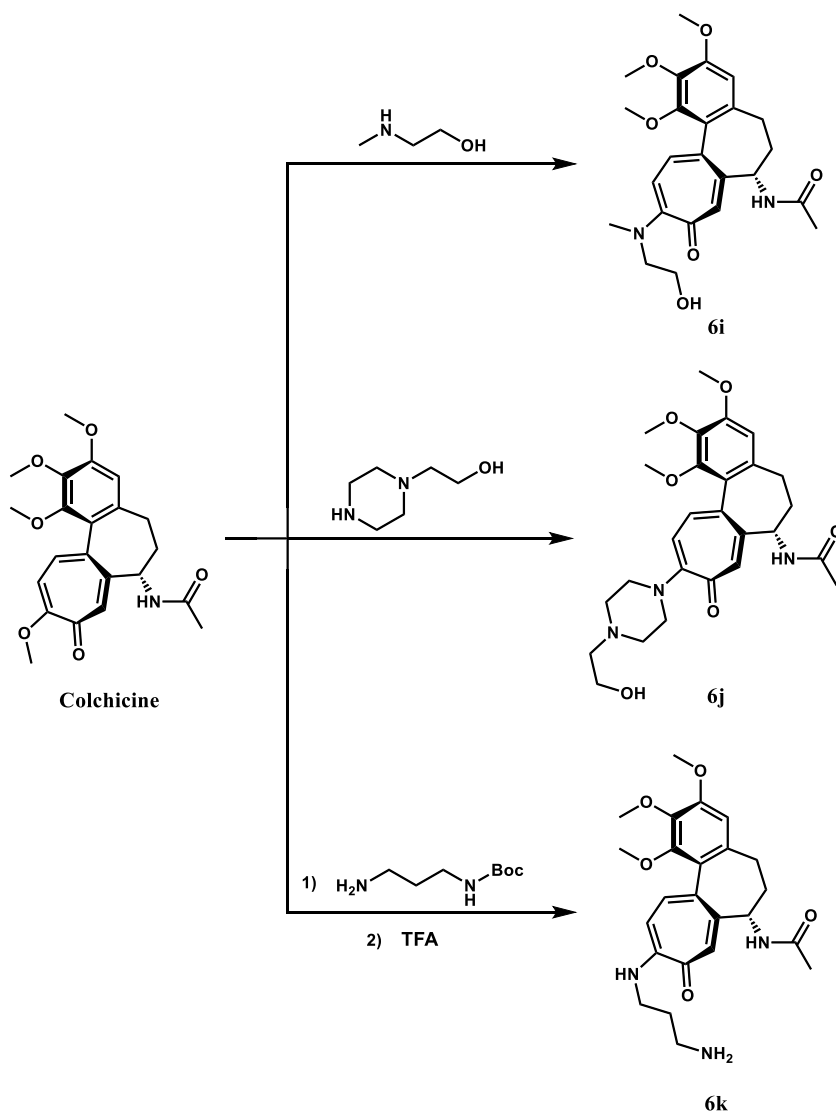


Figure 6-11: Displacement of methoxy group in colchicine with a primary or secondary amines resulting in the incorporation of either a primary amine (**6k**) or a primary hydroxyl (**6i** and **6j**)

The hydroxy groups on **6i** and **6j** were then treated with CDI resulting in the corresponding *O*-alkyl carbamoylimidazole **6l-m**. These were then reacted with primary amines resulting in the formation of carbamates **6n-p** (Figure 6-12). *O*-alkyl carbamoylimidazole **6l** was reacted with propanediamine resulting in the incorporation of a primary amine in **6n**. **6m** was treated with propanediamine and N,N-

dimethylpropanediamine resulting in the incorporation of a primary amine (**6o**) and a tertiary amine (**6p**) respectively.

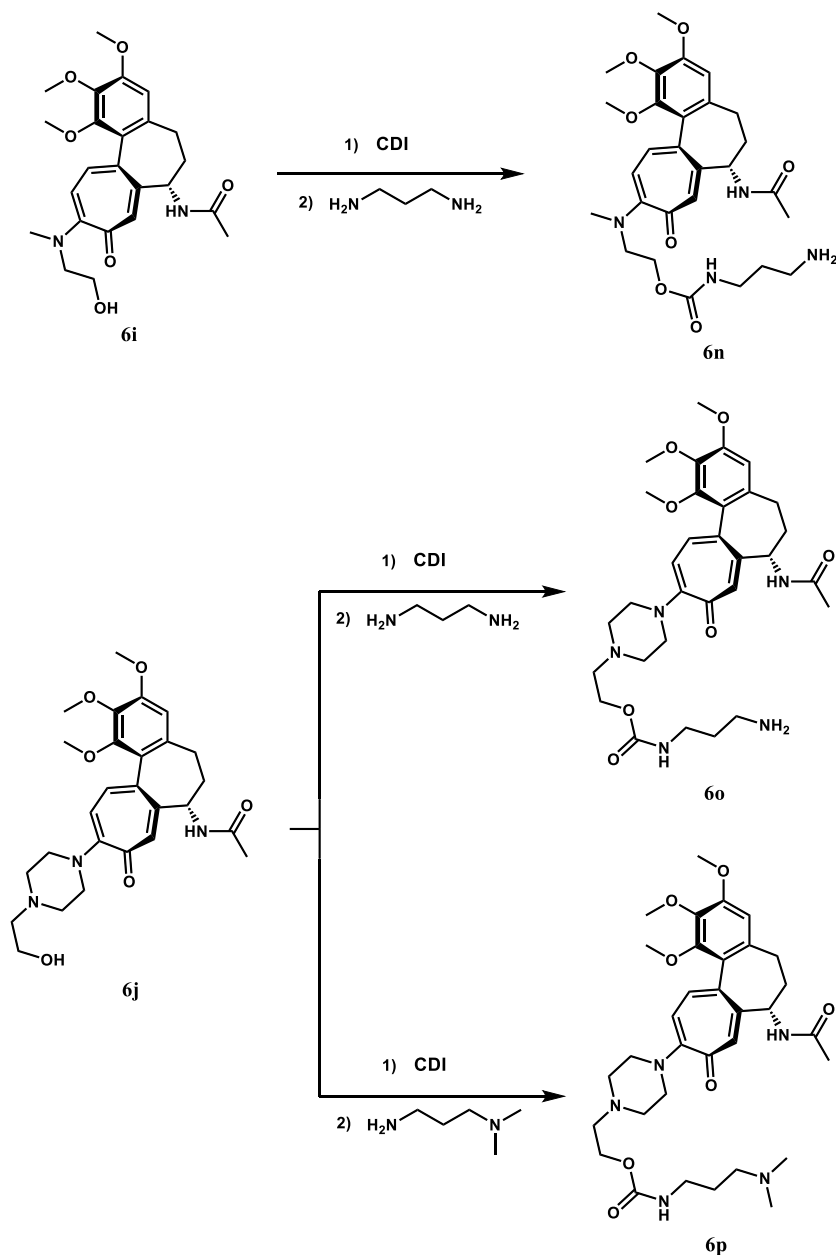


Figure 6-12: Incorporation of a primary amine (**6n** and **6o**) or a tertiary amine (**6p**) into colchicine by first activating reagents **6j** and **6k** with CDI followed by reaction with a primary amine.

Three colchicine prodrugs with primary amines incorporated into them have been produced, which can be easily reacted with the anhydride in our platform (Figure 6-13). These three prodrugs were reacted with 1 equivalent of **30** to incorporate an alkyne functional group into them.

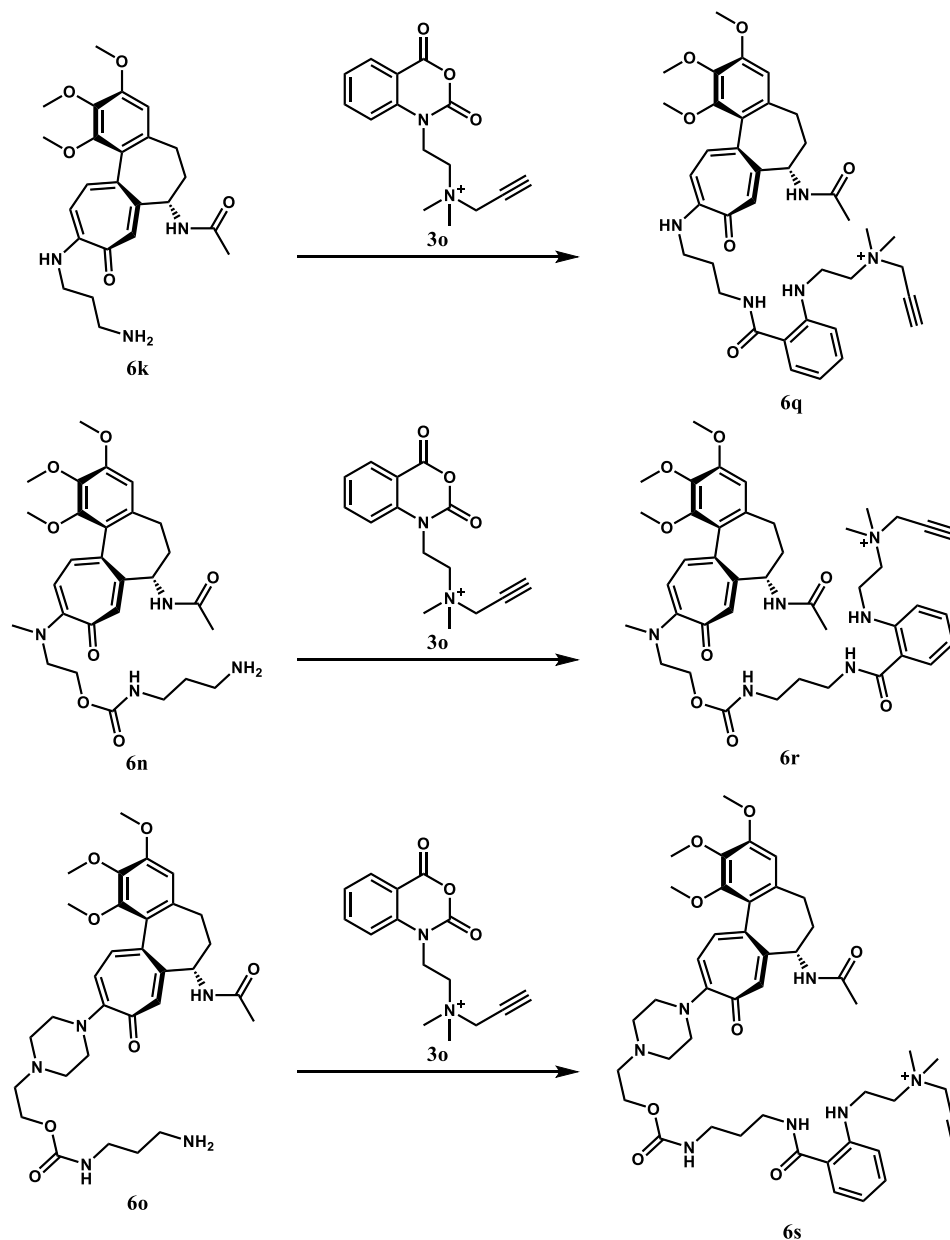


Figure 6-13: Incorporation of alkyne into colchicine by the reaction of **30** with colchicine derivatives containing primary amines



One additional colchicine prodrug was synthesized that incorporated an activated isatoic anhydride derivative. This was made by quaternizing colchicine derivative **6p** with **3p**.

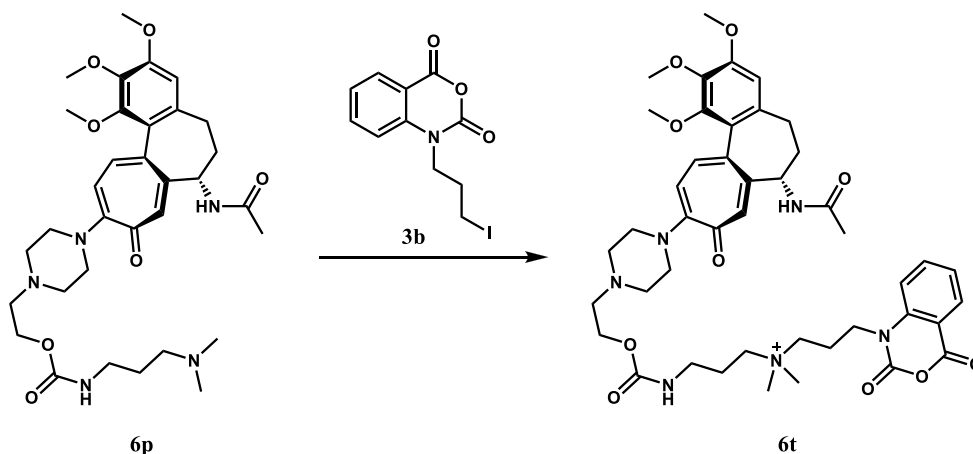


Figure 6-14: Quaternization of colchicine prodrug **6p** with reagent **3b**

Four colchicine prodrugs have been synthesized that are ready to be conjugated to an Ab. Prodrugs, **6q-s** have been functionalized with an alkyne group. These can undergo the azide-alkyne cycloaddition reaction with an Ab that has been functionalized with azide groups. Prodrug **6t** contains an activated isatoic anhydride moiety that can be conjugated directly to a native Ab through its lysine residues.

The most questionable of these derivatives is **6q** as it contains no obvious cleavage point, meaning it is likely to remain inactive once internalized into the cell. The other 3 drugs contain a carbamate linker that can potentially be enzymatically cleaved in the cell. Cleavage of this linker would result in the release of colchicine derivatives **6i**

and **6j**. Therefore the biological testing (chapter 6-4) of these two derivatives are the most important, as they will be the active components released.

### 6.2.3 Computational Analysis of Colchicine Derivatives

Once internalized in the cell, ADC linkages are designed to be cleaved. Cleavage of the carbamate linkages in colchicine prodrugs **6s** and **6t** results in the release of derivative **6j**. Similarly, cleavage of the linker in **6r** results in the release of **6i**. Ideally these derivatives would bind to tubulin and have the same effect as native colchicine. Computational models can give estimations as to how these derivatives will interact with the binding site on tubulin and their binding affinity for the binding site. AutoDock Vina, which is used here, is one such tool that allows for these estimations to be made. AutoDock Vina uses an empirical free energy force field in combination with a Lamarckian Genetic Algorithm to give predictions of bound conformations and free energies of association.<sup>56</sup>

The estimated binding affinities of the colchicine derivatives **6i** and **6j** with tubulin are shown in table 6-1. Although lower than that of native colchicine, both derivatives are estimated to have decent binding affinities.

Table 6-1: Estimated binding affinities of colchicine derivatives **6i** and **6j** calculated from AutoDock Vina

Derivative	Estimated Binding Affinity (kcal/mol)
Colchicine	8.7
<b>6i</b>	8.2
<b>6j</b>	7.6

The predicted binding conformations of derivatives **6i** and **6j** were compared to the crystal structure of colchicine bound to tubulin (Figure 6-15). One thing that stands out right away is that both derivatives are flipped upside-down relative to colchicine. One interaction that appears to be driving this is hydrogen bonding to adjacent residues on tubulin. The model for **6i** shows the hydroxy group in a hydrogen bonding interaction, represented by the dashed line, with a lysine residue (Figure 6-15B). Similarly, **6j** is shown to be participating in hydrogen bonding with a tyrosine residue (Figure 6-15C).

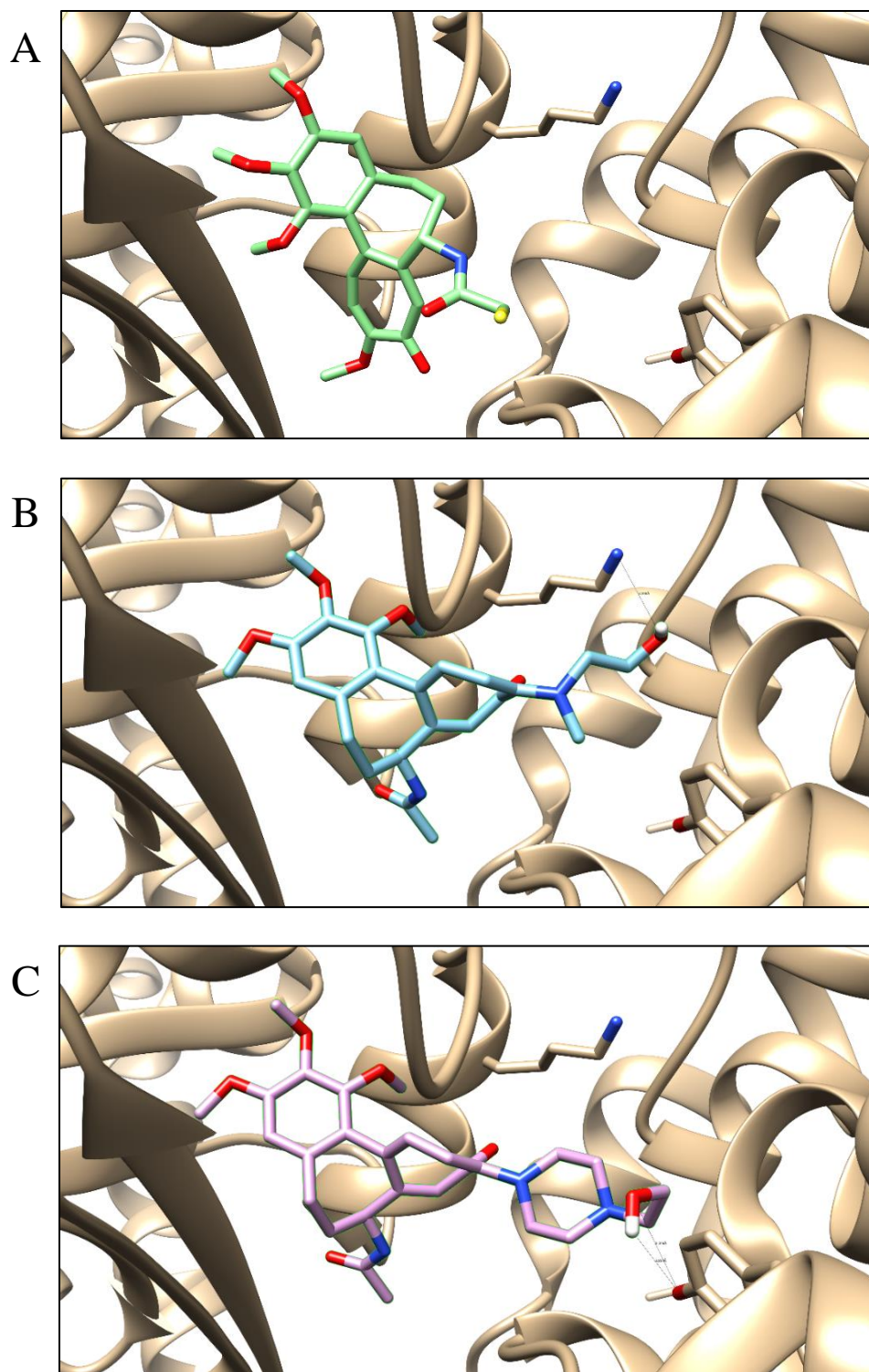


Figure 6-15: Models of colchicine and colchicine derivatives in tubulin binding site with hydrogen bonding represented by dashed lines. The tubulin is represented by ribbons, with residues that participate in hydrogen bonding with the derivatives shown. A) Colchicine bound to tubulin based off an X-ray crystallography structure. B) Predicted binding of derivative **6i**. C) Predicted binding of derivative **6j**

It is also possible that steric effects are driving the derivatives to become flipped in the binding site. When looking closely at the methoxy group on the seven-membered ring of colchicine it can be seen that it is tucked into a pocket and very close to a peptide chain (Figure 6-16). This is methoxy group that is being substituted for the linkage in the derivatives. The substitution of these bulkier substituents could prevent the derivatives from binding in the same way as colchicine, causing them to flip in the binding site.

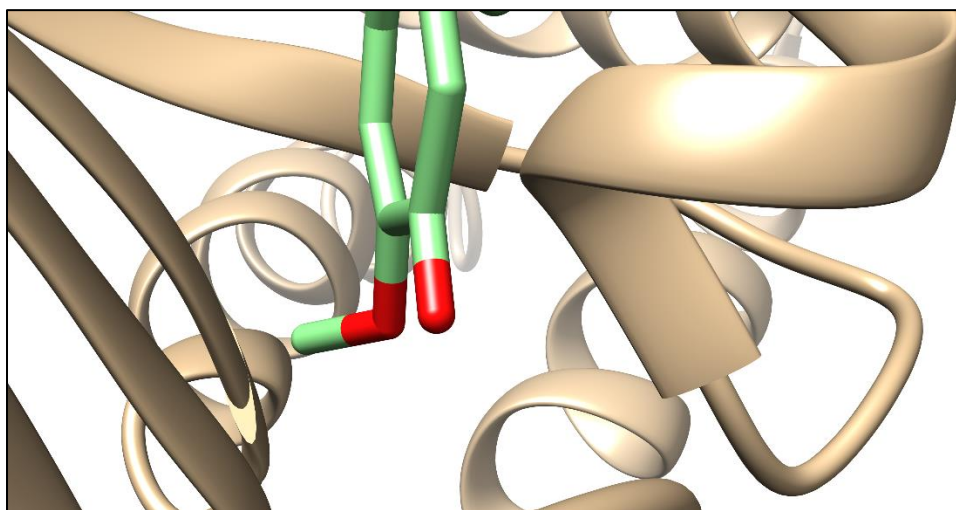


Figure 6-16: Close-up of the methoxy on the seven-membered ring of colchicine, showing its distance to a peptide chain

Based on computational models, both derivatives **6i** and **6j** bind to tubulin at the same site as colchicine with decent affinity. However, they bind to this site upside-down relative to tubulin. Two main interactions seem to be responsible for this. The first is hydrogen bonding interactions between the hydroxy groups introduced into the derivatives and adjacent residues in tubulin. The second is steric interactions caused by the substitution of the linkage in place of the methoxy group. While these models do

predict that the derivatives will bind to tubulin, cell studies will have to be carried out to determine if they are cytotoxic.

### 6.3 Antibody-Drug Conjugate Synthesis

TAB004 was labeled using the same procedure used to label BSA. However derivative **3p** was used to incorporate azides in the Ab. Various equivalents of **3p** were reacted with TAB004 for one hour in 25 mM bicarbonate buffer at pH 8.4 to give ADC **6u** a range of DOLs from 0.8 to 3.8 (Table 6-2). These will be tested *in vitro* for activity. It is expected that the activity will decrease as the DOL increases.

Table 6-2: Measured DOLs of ADC **6u** after labeling TAB004 with varying equivalents of reagent **3p**

<b>3p</b> equivalents	DOL
5	0.8
10	1.1
25	1.5
50	2.2
100	3.8

ADCs with a variable amount of drug loading were produced via the CuAAC reaction between prodrug **6s** and azide functionalized TAB004 reagents **6u**. An additional ADC will be produced between TAB004 and **6t**. To be able to determine the DOL by absorbance of these ADCs, the molar extinction coefficients and correction factors of the two linkages produced must be determined. The first linkage, **6v**, was made by the CuAAC reaction of **5b** with **6s** (Figure 6-17A). The second linkage, **6w**, was made through the ring-opening of **6t** with butylamine (Figure 6-17B). **6v** was found to have a molar extinction coefficient of  $9720\text{M}^{-1}\text{cm}^{-1}$  at 330nm, with a correction

factor of 1.1. **6w** was found to have a molar extinction coefficient of  $5633 \text{ M}^{-1}\text{cm}^{-1}$  at 330 nm, with a correction factor of 1.9.

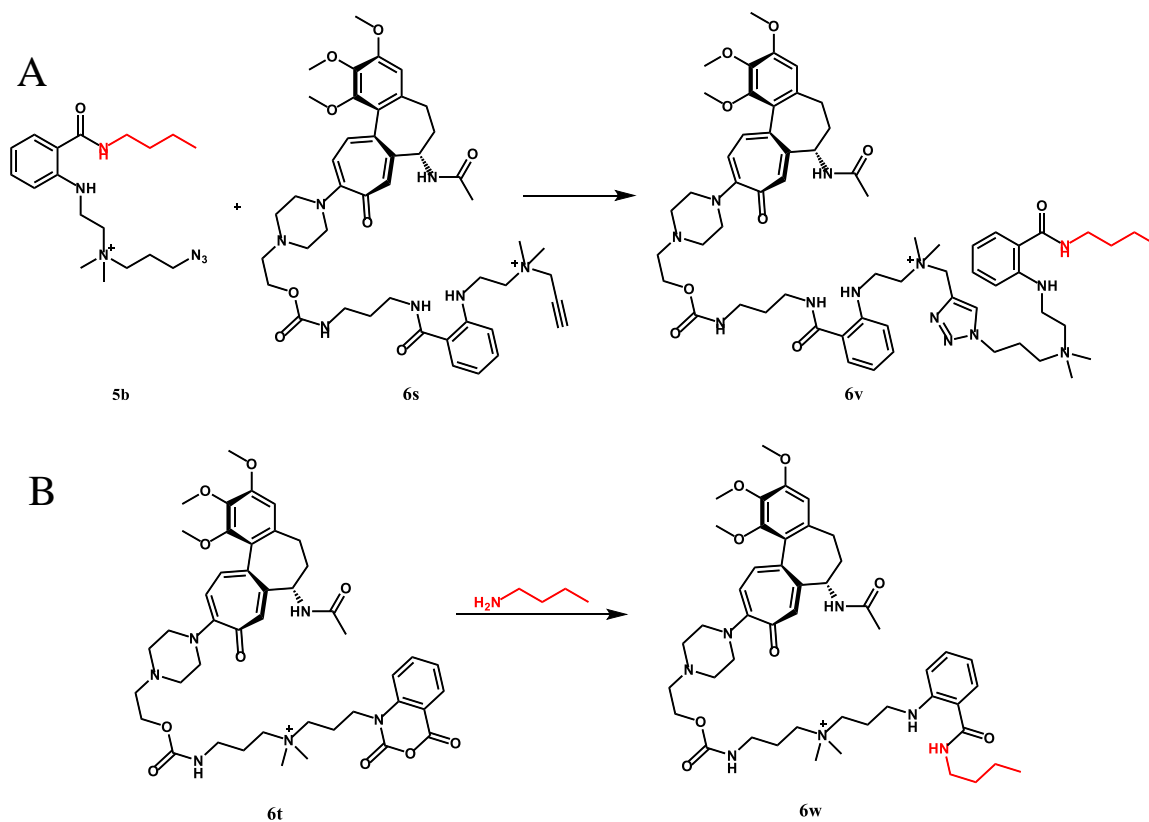


Figure 6-17: Synthesis of linkages that will be in the ADCs produced here, where butylamine (in red) is used as a model for lysine residues in the Ab

The activated isatoic anhydride moiety present in prodrug **6t** was utilized to form an ADC with TAB004 (Figure 6-18). This reaction was carried out using 50 molar equivalents of **6t** in 25 mM bicarbonate buffer at pH 8.4. The reaction was allowed to sit at room temperature for one hour, at which point the ADC was purified by passing the reaction through a GPC column. This gave ADC **6x** containing a DOL of 2.3.

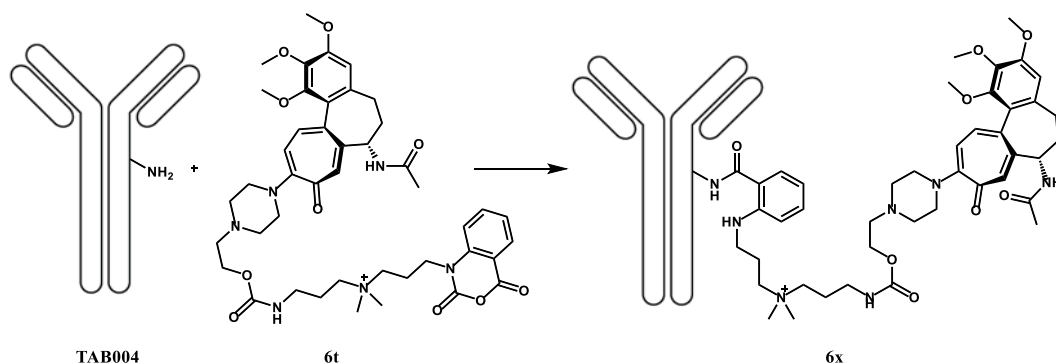


Figure 6-18: Treatment of TAB004 with 50 equivalents of reagent **6t** to give ADC **6x** with a DOL of 2.3

Prodrug **6s** was conjugated to azide functionalized TAB004 through the CuAAC reaction (Figure 6-19). Ab **6u** with DOLs of 1.1, 2.2, and 3.8 were used to give ADCs with a range of drug-loading. These reactions were carried using the same procedure described for BSA in chapter 5.4. The only exception being that three equivalents of the small molecule were used instead of two. These reactions were carried out at 35 °C over the course of 27 hours, at which point they were passed through a GPC to give ADCs **6y**. **6u** containing a DOL of 1.1 gave an ADC with a drug-loading of 1.1, showing that the reaction went to completion.



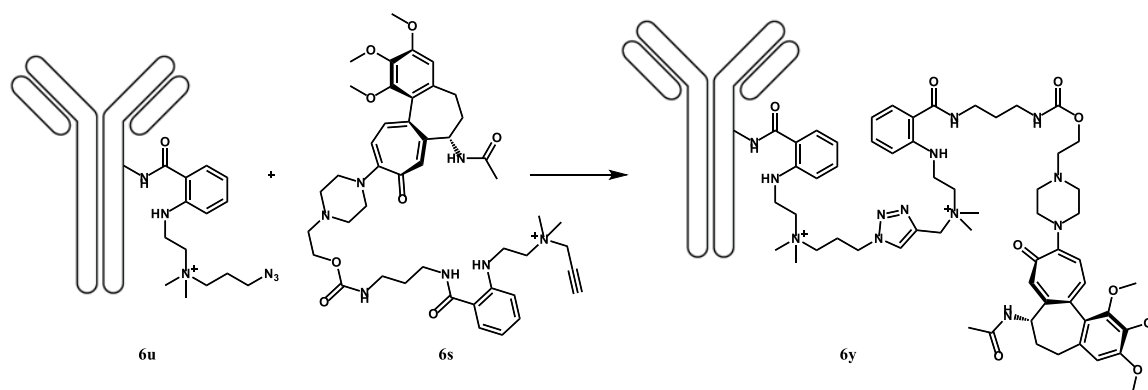


Figure 6-19: CuAAC reaction between **6s** and azide functionalized TAB004 to give ADC **6y**

ADC **6y** was prepared with a drug-loading of 1.1, 1.9, and 2.9 from **6u** with DOLs of 1.1, 2.2, and 3.8 respectively. Additionally, ADC **6x** was prepared with a drug-loading of 2.3. Each of these ADCs contain TAB004 and colchicine and have been produced utilizing the isatoic anhydride platform. Each of these utilize carbamate linkages, which are putative targets of CES2.<sup>44</sup> Cleavage of the linkage in each of these ADCs results in the liberation of colchicine derivative **6j**.

#### 6.4 Biological Evaluation

Both hypoglycosylated MUC1 and CES2 has been shown to be overexpressed in pancreatic cancer,<sup>40,57</sup> making the ADCs produced here particularly suitable for use in the treatment of this type of cancer. Additionally, gemcitabine is commonly used in the treatment of pancreatic cancer.<sup>47</sup> The Mukherjee group carried out *in vitro* cell viability studies on the pancreatic cancer cell lines using colchicine derivatives **6i** and **6j** and with gemcitabine prodrugs **6d** and **6e**. The cell lines used were BxPC-3 and HPAF-II. BxPC-3 is an established pancreatic cell line, resembling the primary tumor in which it was

harvested from, that has been shown to produce mucin.<sup>58</sup> HPAF-II is a pancreatic cancer cell line that has proven to be drug-resistant.<sup>59</sup>

The toxicities of the colchicine derivatives were first analyzed in triplicate and compared to colchicine as a standard (Figure 6-20). In both cell lines, derivative **6j** shows a lower toxicity than colchicine, with this difference being more pronounced in the BxPC-3 cell line. However, **6i** shows toxicities comparable to that of colchicine in both cell lines. In BxPC-3, **6i** proves to be almost or just as toxic as colchicine from a concentration of 0.125-2  $\mu$ M. Interestingly, **6i** appears to be more toxic than colchicine in the drug-resistant cell at concentrations of 0.25-2  $\mu$ M. This may indicate that **6i** exhibits an additional mechanism of action that becomes effective at higher concentrations. Additional biological studies would have to be carried out to determine if this is the case.

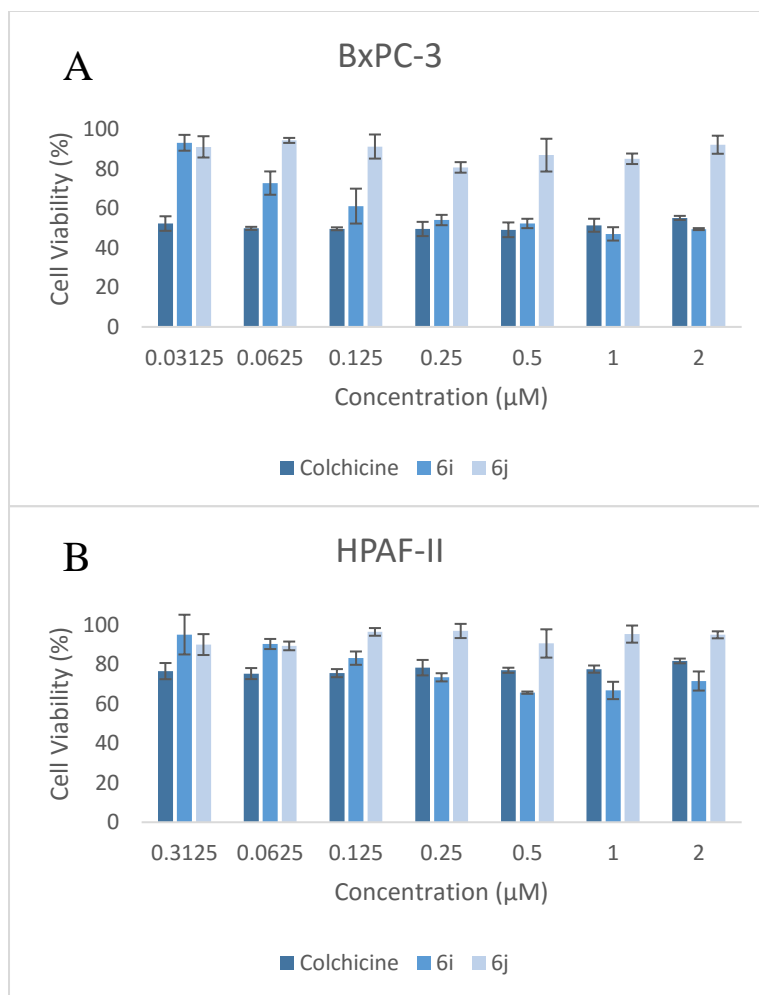


Figure 6-20: Cell viability studies carried out with colchicine derivatives **6i** and **6j** on the pancreatic cancer cell lines BxPC-3 (A) and HPAF-II (B)

The toxicities of gemcitabine prodrugs **6d** and **6e** were analyzed the same way (Figure 6-21). These prodrugs exhibit toxicities comparable to gemcitabine in both cell lines. This indicates that both of these are active and that their respective linkages, the carbamate or carbonate, are able to be cleaved once internalized in the cell.

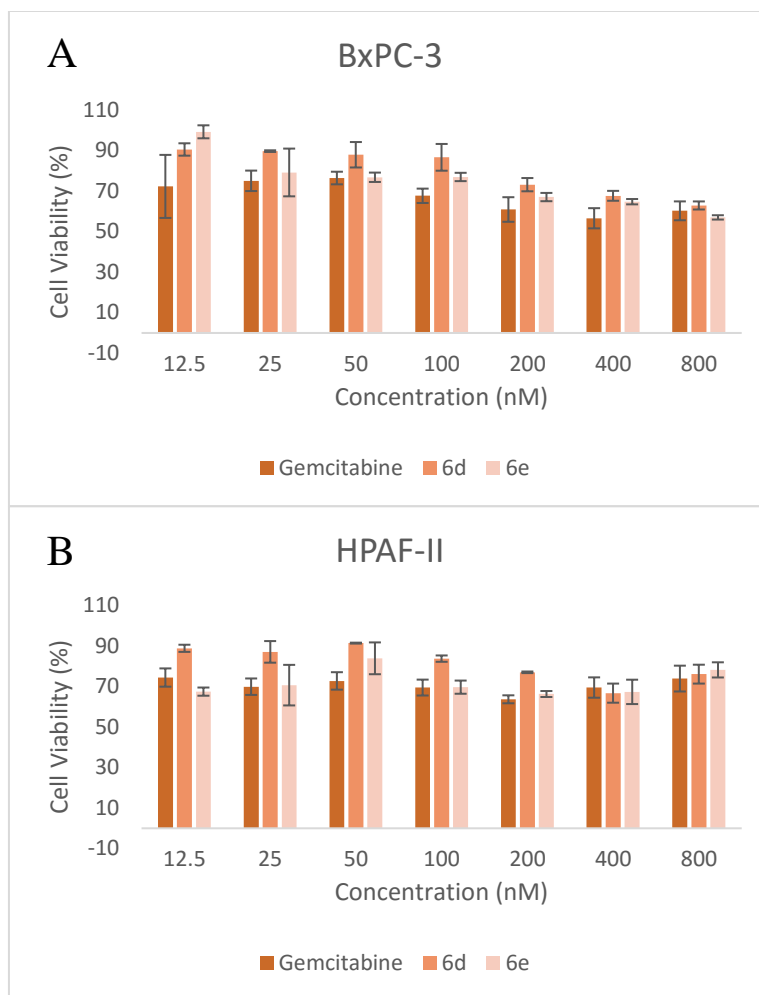


Figure 6-21: Cell viability studies carried out with gemcitabine prodrugs **6d** and **6e** on the pancreatic cancer cell lines BxPC-3 (A) and HPAF-II (B)

## CHAPTER 7: CONCLUSIONS

Synthetic methods have been developed for producing both neutral and water-soluble derivatives of isatoic anhydride. Two unique reagents, **3o** and **3p**, have been developed that can easily be rendered water-soluble through the formation of a quaternary ammonium salt. **3o**, however, has shown limitations in the substrates that it can react with to form ammonium salts. **3o** has been shown to be sluggish with primary chlorides, primary bromides, and activated chlorides. However **3p** has been shown to react with tertiary amines at accelerated rates due to anchimeric assistance. The use of these two reagents, which utilize complementary chemistries, allows for incorporation of a wide variety of functional groups into the water-soluble platform.

It has been shown that the anhydride functional group present in isatoic anhydride has remarkable hydrolytic stability. They exhibit reasonably long half-lives in bicarbonate buffers at pH 8.4 over range of concentrations typically used for bioconjugation. Additionally they have a half-life of 16 hours at 25 °C in DI water and longer than two days when stored at 4 °C. Despite the anhydride being fairly hydrolytically stable, it has also been shown to be activated towards reactions with primary amines under the same conditions. At variety of concentrations and primary amine equivalents the acylation reaction is complete in under five seconds. The hydrolytic stability of these derivatives paired with their significant activation towards

primary amines makes this an excellent new platform for the conjugation of lysine residues in proteins.

This platform has been shown to have a unique spectroscopic profile upon ring-opening of the anhydride. This gives a species that now absorbs at 330 nm and fluoresces at 420 nm, both of which can be utilized to determine the DOL of a protein. This was demonstrated using BSA as a model protein. A number of parameters for the bioconjugation reaction have been explored in order to understand how to control the DOL. It was first shown that conjugation with this platform gives highly reproducible results. The parameters explored were the reaction time, the pH of the buffer, the buffer concentration, and the reagent concentration. The bioconjugation reaction was shown to proceed rapidly at first and to be essentially complete in an hour. In the first 5 minutes of the reaction the DOL reaches at least 70% of its final DOL, depending on the reagent concentrations. A pH of about 8.4 in a 25 mM buffer proved to give the highest DOL. As the molar equivalents of the bioconjugation reagent is increased the DOL increases, as expected. Increasing the concentration of the protein while holding the concentration of the bioconjugation results in reduced DOL, however this also greatly increases the reaction efficiency of the bioconjugation reagent. All of these parameters can be manipulated to give control over the DOL achieved, a desirable characteristic for any bioconjugation reagent.

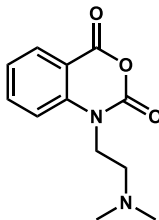
Utilizing this new platform, four ADCs have been produced. The antibody used in these ADCs was TAB004 which is specific for the peptide backbone of the glycoprotein MUC1. MUC1 is overexpressed in a variety of cancers. Additionally, on cancerous cells, MUC1 is hypoglycosylated which exposes its peptide core, allowing TAB004 to bind it

more effectively. Colchicine is the cytotoxin that was incorporated into these ADCs. Colchicine, a substoichiometric cytotoxin, is highly toxic at small doses, making it an ideal drug for use in ADCs. All of the ADCs produced incorporate a carbamate linkage between the antibody and the drug. These linkages are putative targets of the CES2 enzyme. CES2 has been shown to be upregulated in a multiple types of cancer. Hopefully, this combined with TAB004, makes these highly selective ADCs in that TAB004 selectively binds to cancerous cells and the cytotoxin is only released in the presence of CES2. Other prodrugs of colchicine, gemcitabine, and 5-fluorouracil, that are ready to be incorporated into an ADC, have also been synthesized.

## CHAPTER 8: EXPERIMENTAL

**General Procedure 1.** To a Schlenk flask under dry N<sub>2</sub> was added 60% wt/wt NaH suspended in oil (1.5 g, 36 mmol). To this was added 15 ml of dry hexanes, the suspension briefly stirred then allowed to settle, and the hexanes removed via cannula. This process was repeated 3 x. To the freshly rinsed NaH was added anhydrous DMF (30 ml) at room temperature, resulting in a cloudy suspension. To this suspension was added isatoic anhydride (5.1 g, 30 mmol) in one portion. Following this addition, an additional 20 ml of anhydrous DMF was added and the resulting suspension was stirred for 60 min, upon which time the alkyl halide was added (36 mmol) in one portion. The resulting suspension was stirred 12 hrs yielding a clear and colored solution containing the desired product. The resulting solution is concentrated under vacuum at 100 °C resulting in a darkly colored viscous residue. This residue is then dissolved into DCM (150 ml) and extracted 3 x with 100 ml of saturated NaHCO<sub>3</sub> (aq). Finally the organic layer is rinsed 1 x wash with 100 ml of brine solution. The organic layer is then collected and stirred with activated carbon (0.5 g) for 30 min. The resulting organic solution is then filtered through a plug of MgSO<sub>4</sub> to both remove the activated carbon and dry the solution of residual water. The resulting solution is then concentrated under vacuum to remove the DCM resulting in a lightly colored solid that is then recrystallized from isopropanol.





**3a.** General procedure 1 was followed as above using 2-chloro-N,N-dimethylethylamine HCl (5.19 g, 36 mmol) salt with the following exceptions. To account for the HCl salt, 2.6 equivalents of NaH (3.25 g, 78 mmol) was used. The final product was recrystallized from tert-butanol. The product (1.98g, 28%) was isolated as a colorless solid.  $C_{12}H_{14}N_2O_3$  (234.25),  $^1H$  NMR (500 MHz, acetone- $d_6$ ):  $\delta$  2.27 (s, 6H), 2.62 (t, 2H,  $J = 7.1$  Hz), 4.21 (t, 2H,  $J = 7.1$  Hz), 7.35 (m, 1H), 7.50 (d, 1H,  $J = 8.4$  Hz), 7.87 (m, 1H), 8.07 (dd, 1H,  $J = 7.9, 1.6$  Hz) ppm,  $^{13}C$  NMR (500 MHz, acetone- $d_6$ ):  $\delta$  43.6, 46.0, 56.5, 112.8, 115.5, 124.4, 130.8, 138.0, 142.8, 148.6, 159.7 ppm, MS (EI): Calc. 234.10; Found 234.1 ( $M^+$ , < 1%), 58.1 (100%)  $m/z$ .

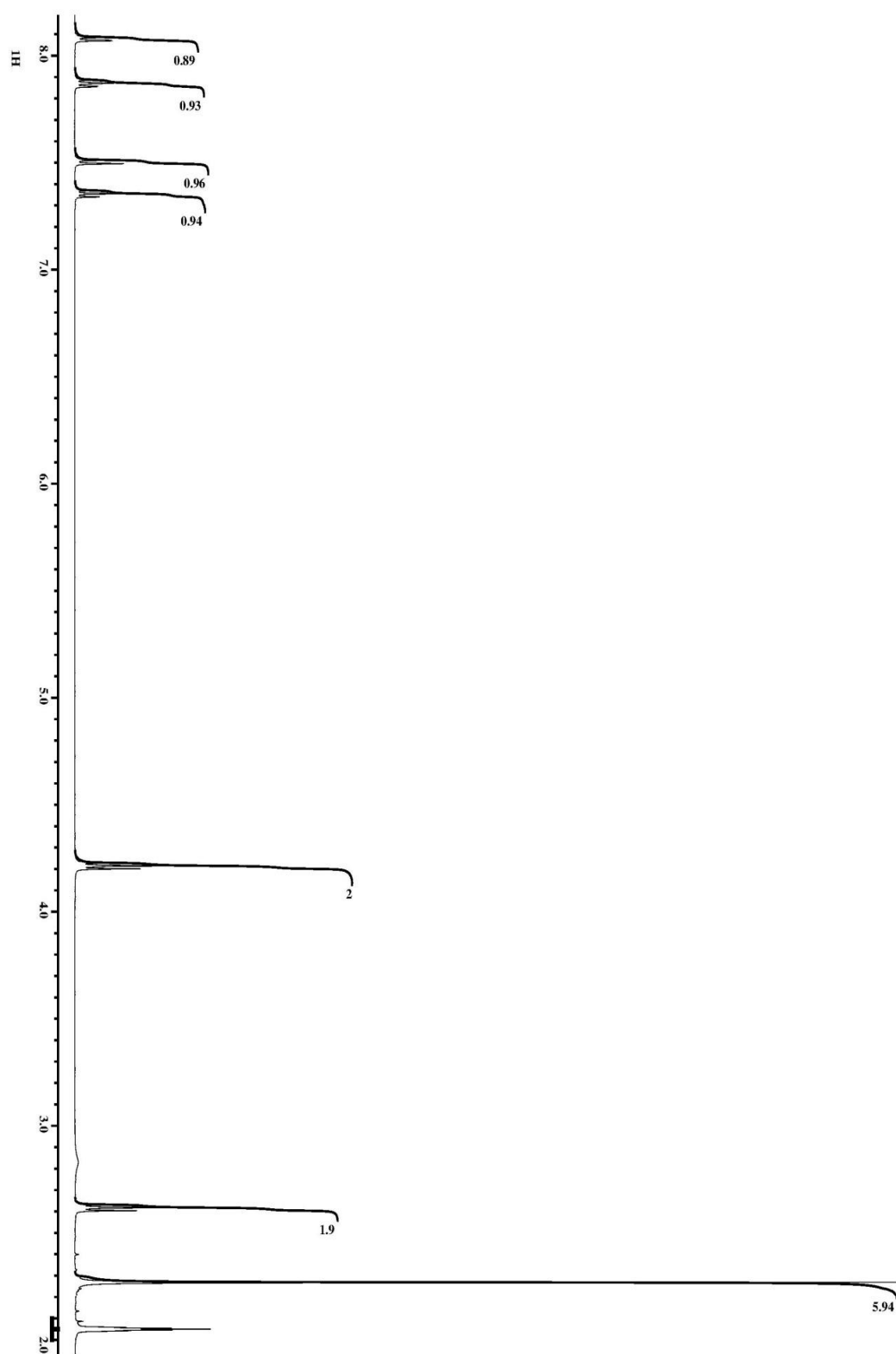
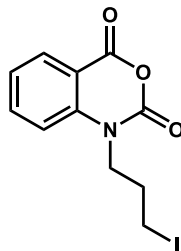


Figure 8-1:  $^1\text{H}$  NMR spectrum of **3a** in acetone- $\text{d}_6$



**3b.** General procedure 1 was followed as above using 1-Chloro-3-iodopropane (3.9 mL, 36 mmol) as the halide. The final product (6.19 g, 62%) was isolated as an off white solid.  $C_{11}H_{10}N_2O_3I$  (331.11),  $^1H$  NMR (500 MHz, acetone- $d_6$ ):  $\delta$  2.34 (m, 2H,), 3.44 (t, 2H,  $J = 7.1$  Hz), 4.23 (t, 2H,  $J = 7.3$  Hz), 7.36 (m, 1H), 7.55 (d, 1H,  $J = 8.7$  Hz), 7.87 (m, 1H), 8.08 (dd, 1H,  $J = 8.0, 1.5$  Hz) ppm,  $^{13}C$  NMR (500 MHz, acetone- $d_6$ ):  $\delta$  2.4, 31.9, 45.9, 112.9, 115.2, 124.4, 130.8, 137.9, 142.6, 148.7, 159.6 ppm, MS (EI): Calc. 330.97; Found 331.0 ( $M^+$ , 11%), 132.1 (100%)  $m/z$ .

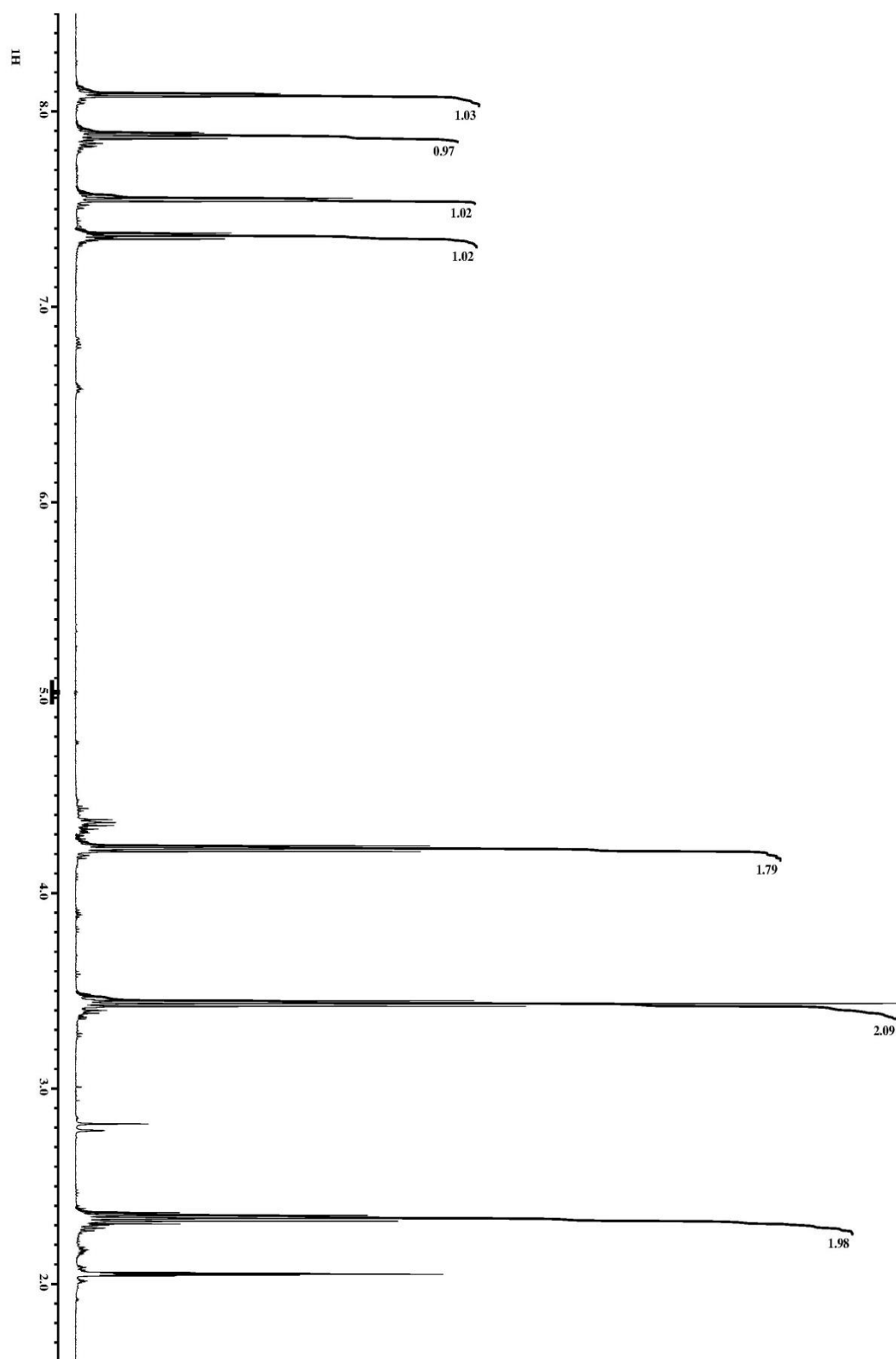
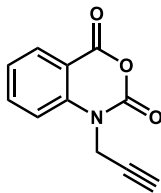
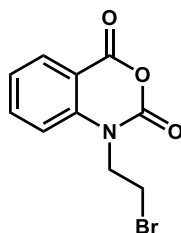


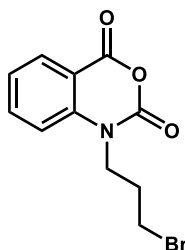
Figure 8-2:  $^1\text{H}$  NMR spectrum of **3b** in acetone- $\text{d}_6$



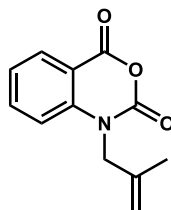
**3c.** General procedure 1 was followed as above using an 80% solution of propargyl bromide (3.9 mL, 36 mmol) as the halide. The final product (3.19 g, 53%) was isolated as a crystalline, colorless solid.  $C_{11}H_7NO_3$  (201.18),  $^1H$  NMR (500 MHz, acetone- $d_6$ ):  $\delta$  2.97 (t, 1H,  $J$  = 2.5 Hz), 4.97 (d, 2H,  $J$  = 2.8 Hz), 7.42 (m, 1H), 7.57 (d, 1H,  $J$  = 8.2 Hz), 7.93 (m, 1H), 8.11 (dd, 1H,  $J$  = 7.8, 1.6 Hz) ppm,  $^{13}C$  NMR (500 MHz, acetone- $d_6$ ):  $\delta$  35.2, 75.1, 77.9, 113.0, 115.8, 124.9, 130.8, 138.0, 141.8, 148.3, 159.3 ppm, MS (EI): Calc. 201.04; Found 201.0 ( $M^+$ , 37%), 129.1 (100%)  $m/z$ .



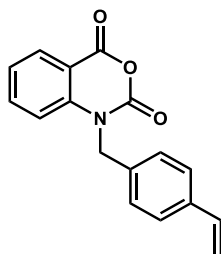
**3d.** General procedure 1 was followed as above using 1,2-dibromoethane (3.4 mL, 39 mmol) as the halide. The final product (2.51 g, 31%) was isolated as an off white solid.  $C_{10}H_8NO_3Br$  (270.08),  $^1H$  NMR (500 MHz, acetone- $d_6$ ):  $\delta$  3.76 (t, 2H,  $J$  = 7.3 Hz), 4.54 (t, 2H,  $J$  = 7.3 Hz), 7.39 (m, 1H), 7.60 (d, 1H,  $J$  = 8.7 Hz), 7.89 (m, 1H), 8.10 (dd, 1H,  $J$  = 7.8, 1.5 Hz) ppm,  $^{13}C$  NMR (500 MHz, acetone- $d_6$ ):  $\delta$  27.5, 46.4, 112.8, 115.4, 124.7, 131.0, 138.1, 142.4, 148.6, 159.4 ppm, MS (EI): Calc. 268.97; Found 269.0 ( $M^+$ , 9%), 146.1 (100%)  $m/z$ .



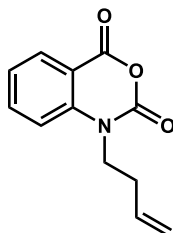
**3e.** General procedure 1 was followed as above using 1,3-dibromopropane (4.0 mL, 39 mmol) as the halide. The final product (1.64 g, 19%) was isolated as a light yellow solid.  $C_{11}H_{10}NO_3Br$  (284.11),  $^1H$  NMR (500 MHz, acetone- $d_6$ ):  $\delta$  2.35 (m, 2H), 3.68 (t, 2H,  $J = 6.9$  Hz), 4.28 (t, 2H,  $J = 7.3$  Hz), 7.36 (m, 1H), 7.54 (d, 1H,  $J = 8.2$  Hz), 7.88 (m, 1H), 8.08, (dd, 1H,  $J = 7.8, 1.5$  Hz) ppm,  $^{13}C$  NMR (500 MHz, acetone- $d_6$ ):  $\delta$  31.0, 31.3, 44.2, 113.0, 115.1, 124.4, 130.9, 138.0, 142.6, 148.7, 159.7 ppm, MS (EI): Calc. 282.98; Found 283.0 ( $M^+$ , 11%), 132.1 (100%)  $m/z$ .



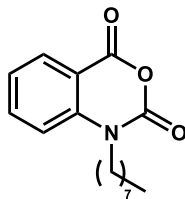
**3f.** General procedure 1 was followed as above using a 90% solution of 3-chloro-2-methylpropene (4.0 mL, 36 mmol) as the halide. The final product (3.06 g, 47%) was isolated as a colorless solid.  $C_{12}H_{11}NO_3$  (217.22),  $^1H$  NMR (500 MHz, acetone- $d_6$ ):  $\delta$  1.85 (s, 3H), 4.68 (s, 2H), 4.89 (m, 1H), 4.94 (m, 1H), 7.31 (d, 1H,  $J = 8.5$  Hz), 7.35 (m, 1H), 7.81 (m, 1H), 8.08 (dd, 1H,  $J = 7.8, 1.5$  Hz) ppm,  $^{13}C$  NMR (500 MHz, acetone- $d_6$ ):  $\delta$  20.0, 50.6, 111.7, 112.8, 116.1, 124.5, 130.6, 137.8, 139.4, 142.9, 148.8, 159.6 ppm, MS (EI): Calc. 217.07; Found 217.1 ( $M^+$ , 30%), 144.1 (100%)  $m/z$ .



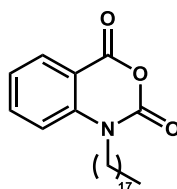
**3g.** General procedure 1 was followed as above using NaH (1.32 g, 33 mmol) and a 90% solution of 4-vinylbenzyl chloride (5.7 mL, 36 mmol) as the halide. The final product (4.86 g, 58%) was isolated as a crystalline, colorless solid.  $C_{17}H_{13}NO_3$  (279.29),  $^1H$  NMR (500 MHz, acetone- $d_6$ ):  $\delta$  5.22 (dd, 1H,  $J = 11.0$  Hz), 5.39 (s, 2H), 5.79 (dd, 1H,  $J = 17.7$  Hz), 6.73 (dd, 1H,  $J = 17.6$  Hz), 7.32 (m, 2H), 7.44 (m, 4H), 7.74 (m, 1H), 8.13 (dd, 1H,  $J = 8.1, 1.6$  Hz) ppm,  $^{13}C$  NMR (500 MHz, acetone- $d_6$ ):  $\delta$  48.6, 113.1, 114.4, 116.0, 124.6, 127.5, 127.9, 136.0, 137.2, 137.8, 137.9, 142.7, 149.4, 159.6 ppm, MS (EI): Calc. 279.09; Found 279.1 ( $M^+$ , 16%), 117.1 (100%)  $m/z$ .



**3h.** General procedure 1 was followed as above using NaH (1.32 g, 33 mmol) and 4-bromobut-1-ene (3.73 mL, 36 mmol) as the halide. The final product (2.34 g, 36%) was isolated as a colorless solid.  $C_{12}H_{11}NO_3$  (217.22),  $^1H$  NMR (500 MHz, acetone- $d_6$ ):  $\delta$  2.53 (m, 2H), 4.19 (m, 2H), 5.06 (m, 1H), 5.13 (m, 1H), 5.94 (m, 1H), 7.36 (m, 1H), 7.52 (d, 1H,  $J = 8.6$  Hz), 7.87 (m, 1H), 8.08 (dd, 1H,  $J = 7.8, 1.5$  Hz) ppm,  $^{13}C$  NMR (500 MHz, acetone- $d_6$ ):  $\delta$  31.9, 44.6, 112.9, 115.5, 117.8, 124.4, 130.9, 135.2, 138.0, 142.6, 148.6, 159.7 ppm, MS (EI): Calc. 217.07; Found 217.1 ( $M^+$ , 12%), 132.1 (100%)  $m/z$ .



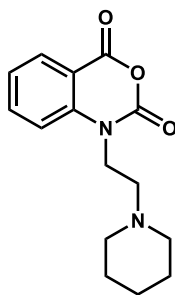
**3i.** General procedure 1 was followed as above using NaH (1.32 g, 33 mmol) and 1-bromooctane (5.8 mL, 33 mmol) as the halide. The final product (3.03 g, 37%) was isolated as a colorless solid.  $C_{15}H_{19}NO_3$  (261.32),  $^1H$  NMR (500 MHz, acetone- $d_6$ ):  $\delta$  0.87 (t, 3H,  $J = 6.9$  Hz), 1.37 (m, 10H), 1.76 (quin, 2H,  $J = 7.7$  Hz), 4.10 (t, 2H,  $J = 7.7$  Hz), 7.33 (m, 1H), 7.48 (d, 1H,  $J = 8.5$  Hz), 7.85 (m, 1H), 8.05 (dd, 1H,  $J = 7.8, 1.5$  Hz) ppm,  $^{13}C$  NMR (500 MHz, acetone- $d_6$ ):  $\delta$  14.3, 23.2, 27.2, 27.6, 29.9, 30.0, 45.4, 112.8, 115.4, 124.3, 130.8, 138.0, 142.6, 148.5, 159.7 ppm, MS (EI): Calc. 275.15; Found 275.1 ( $M^+$ , 25%), 132.1 (100%)  $m/z$ .



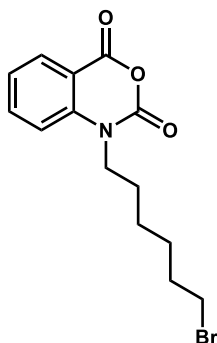
**3j.** General procedure 1 was followed as above with the following exceptions. The reaction was carried out on a reduced scale using isatoic anhydride (0.90 g, 5.5 mmol), NaH (0.24 g, 6.0 mmol), and 1-iodooctadecane (1.90, 5.0 mmol) as the halide. The final product (1.03 g, 50%) was recrystallized from isooctane and was isolated as a colorless solid.  $C_{26}H_{41}NO_3$  (415.61),  $^1H$  NMR (500 MHz, acetone- $d_6$ ):  $\delta$  0.88 (t, 3H,  $J = 6.9$  Hz), 1.28 (m, 26H), 1.38 (m, 2H), 1.47 (quin, 2H,  $J = 7.6$  Hz), 1.77 (quin, 2H,  $J = 7.7$  Hz), 4.11 (t, 2H,  $J = 7.7$  Hz), 7.35 (m, 1H), 7.50 (d, 1H,  $J = 8.5$  Hz), 7.86 (m, 1H), 8.08 (dd, 1H,  $J = 7.8, 1.5$  Hz) ppm,  $^{13}C$  NMR (500 MHz, acetone- $d_6$ ):  $\delta$  14.4, 23.3, 27.3, 27.6,



30.1, 30.1, 30.3, 30.4, 30.4, 32.6, 45.4, 113.0, 115.4, 124.3, 130.8, 138.0, 142.8, 148.6, 159.8 ppm, MS (EI): Calc. 415.31; Found 415.3 ( $M^+$ , 1%), 164.0 (100%) m/z.

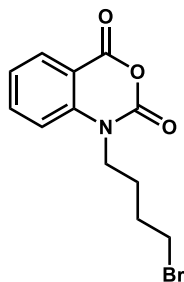


**3k.** General procedure 1 was followed as above with the following exceptions. The reaction was carried out on a reduced scale using isatoic anhydride (1.63 g, 10 mmol) and 1-(2-chloroethyl)piperidine HCl salt (2.21 g, 12 mmol). To account for the HCl salt, 2.4 equivalents of NaH (0.97 g, 24 mmol) was used. The product (3.75 g, 46%) was isolated as a colorless solid.  $C_{15}H_{18}N_2O_3$  (274.32),  $^1H$  NMR (500 MHz, acetone- $d_6$ ):  $\delta$  1.40 (m, 2H), 1.51 (quin, 4H,  $J = 5.6$  Hz), 2.47 (bs, 4H), 2.64 (t, 2H,  $J = 6.9$  Hz), 4.22 (t, 2H,  $J = 6.9$  Hz), 7.35 (m, 1H), 7.53 (d, 1H,  $J = 8.6$  Hz), 7.87 (m, 1H), 8.07 (dd, 1H,  $J = 7.8, 1.6$  Hz) ppm,  $^{13}C$  NMR (500 MHz, acetone- $d_6$ ):  $\delta$  25.0, 26.9, 43.4, 55.6, 56.1, 112.8, 115.7, 124.3, 130.8, 137.9, 142.9, 148.7, 159.8 ppm, MS (EI): Calc. 274.13; Found 274.1 ( $M^+$ , < 1%), 98.1 (100%) m/z.

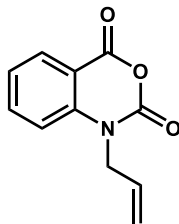


**3l.** General procedure 1 was followed as above with the following exceptions. The reaction was carried out on a reduced scale using isatoic anhydride (1.63 g, 10 mmol),

NaH (0.44 g, 11 mmol), and 1,6-dibromohexane (3.08 mL, 20 mmol) as the halide. After extraction, removal of DCM gave a thick brown liquid. Product was purified by column chromatography over silica gel with 25:75 ethyl acetate:hexanes. Solvent was removed under vacuum to give the final product (1.87 g, 57%) as a colorless solid.  $C_{14}H_{16}NO_3Br$  (326.19),  $^1H$  NMR (500 MHz, acetone- $d_6$ ):  $\delta$  1.51 (m, 4H), 1.78 (quin, 2H,  $J = 7.3$  Hz), 1.87(quin, 2H,  $J = 6.9$  Hz), 3.48 (t, 2H,  $J = 6.8$  Hz), 4.11 (t, 2H,  $J = 7.7$  Hz), 7.33 (m, 1H), 7.49 (d, 1H,  $J = 8.8$  Hz), 7.85 (m, 1H), 8.05 (dd, 1H,  $J = 7.8, 1.5$  Hz) ppm,  $^{13}C$  NMR (500 MHz, acetone- $d_6$ ):  $\delta$  26.3, 27.4, 28.4, 33.4, 34.6, 45.2, 112.7, 115.3, 124.2, 130.7, 137.9, 142.5, 148.5, 159.6 ppm, MS (EI): Calc. 325.03; Found 325.0 ( $M^+$ , 11%), 132.0 (100%)  $m/z$ .

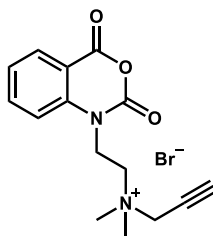


**3m.** General procedure 1 was followed as above with the following exceptions. The reaction was carried out on a reduced scale using isatoic anhydride (3.37 g, 20 mmol), NaH (0.89 g, 22 mmol), and 1,4-dibromobutane (7.3 mL, 60 mmol) as the halide. The final product (1.67 g, 28%) was isolated as a light yellow solid.  $C_{12}H_{12}NO_3Br$  (298.13),  $^1H$  NMR (500 MHz, dichloromethane- $d_2$ ):  $\delta$  1.92 (m, 2H), 2.01 (m, 2H), 3.50 (t, 2H,  $J = 6.4$  Hz), 4.10 (t, 2H,  $J = 7.4$ ), 7.24 (d, 1H,  $J = 8.8$  Hz), 7.31 (m, 1H), 7.80 (m, 1H), 8.12 (dd, 1H,  $J = 7.8, 1.5$  Hz) ppm,  $^{13}C$  NMR (500 MHz, acetone- $d_6$ ):  $\delta$  26.4, 30.5, 34.2, 44.5, 113.0, 115.4, 124.4, 130.8, 138.0, 142.6, 148.7, 159.7 ppm, MS (EI): Calc. 297.00; Found 297.0 ( $M^+$ , 11%), 132.1 (100%)  $m/z$ .



**3n.** General procedure 1 was followed as above using allyl bromide (3.2 mL, 36 mmol) as the halide. The final product (4.65 g, 76%) was isolated as a crystalline, colorless solid.  $C_{11}H_9NO_3$  (203.19),  $^1H$  NMR (500 MHz, acetone- $d_6$ ):  $\delta$  4.77 (m, 2H), 5.25 (m, 1H), 5.36 (m, 1H), 6.00 (m, 1H), 7.35 (m, 1H), 7.40 (d, 1H,  $J = 8.5$ ), 7.83 (m, 1H), 8.08 (dd, 1H,  $J = 7.8, 1.5$  Hz) ppm,  $^{13}C$  NMR (500 MHz, acetone- $d_6$ ):  $\delta$  47.5, 112.9, 115.9, 117.8, 124.5, 130.7, 132.1, 137.8, 142.7, 148.6, 159.7 ppm, MS (EI): Calc. 203.06; Found 203.1 ( $M^+$ , 26%), 130.1 (100%)  $m/z$ .

**General Procedure 2.** To a 3 ml screw capped vial containing compound **3a** (100 mg, 0.43 mmol) was added 1 ml of reagent grade acetone (unless otherwise noted) and the solution heated to completely dissolve the reagent. To this solution was added the corresponding alkyl halide electrophile (0.47 mmol) and the solution let sit over 18 hrs at 40 °C (unless otherwise noted). The solution was then stored at -20 °C overnight followed by filtration of the product. When no solid formed ESI mass spectrometry of the reaction mix was used to confirm product formation.



**30.** General procedure 2 was followed as above using an 80% solution of propargyl bromide (54  $\mu$ L, 0.5 mmol) as the electrophile with the following exceptions. Product formation was complete within 20 min at room temperature. The resulting product (157 mg, 89%) was isolated as a colorless solid which formed readily upon addition of the halide and precipitated from acetone.  $C_{15}H_{17}N_2O_3Br$  (353.21),  $^1H$  NMR (500 MHz, dimethyl sulfoxide- $d_6$ ):  $\delta$  3.27 (s, 6H), 3.68 (t, 2H,  $J = 7.8$  Hz), 4.16 (t, 1H,  $J = 2.4$  Hz), 4.52 (t, 2H,  $J = 7.8$  Hz), 4.58 (d, 2H,  $J = 2.3$  Hz), 7.39 (t, 1H,  $J = 7.5$  Hz), 7.55 (d, 1H,  $J = 8.5$  Hz), 7.90 (m, 1H), 8.06 (dd, 1H,  $J = 7.7, 1.6$  Hz) ppm,  $^{13}C$  NMR (500 MHz, dimethyl sulfoxide- $d_6$ ):  $\delta$  37.8, 50.2, 54.4, 58.3, 72.2, 83.6, 112.1, 114.4, 124.1, 129.8, 137.3, 140.8, 147.7, 158.7 ppm, MS (ESI): Calc. 273.12; Found 273.18 ( $M^+$ ) m/z.

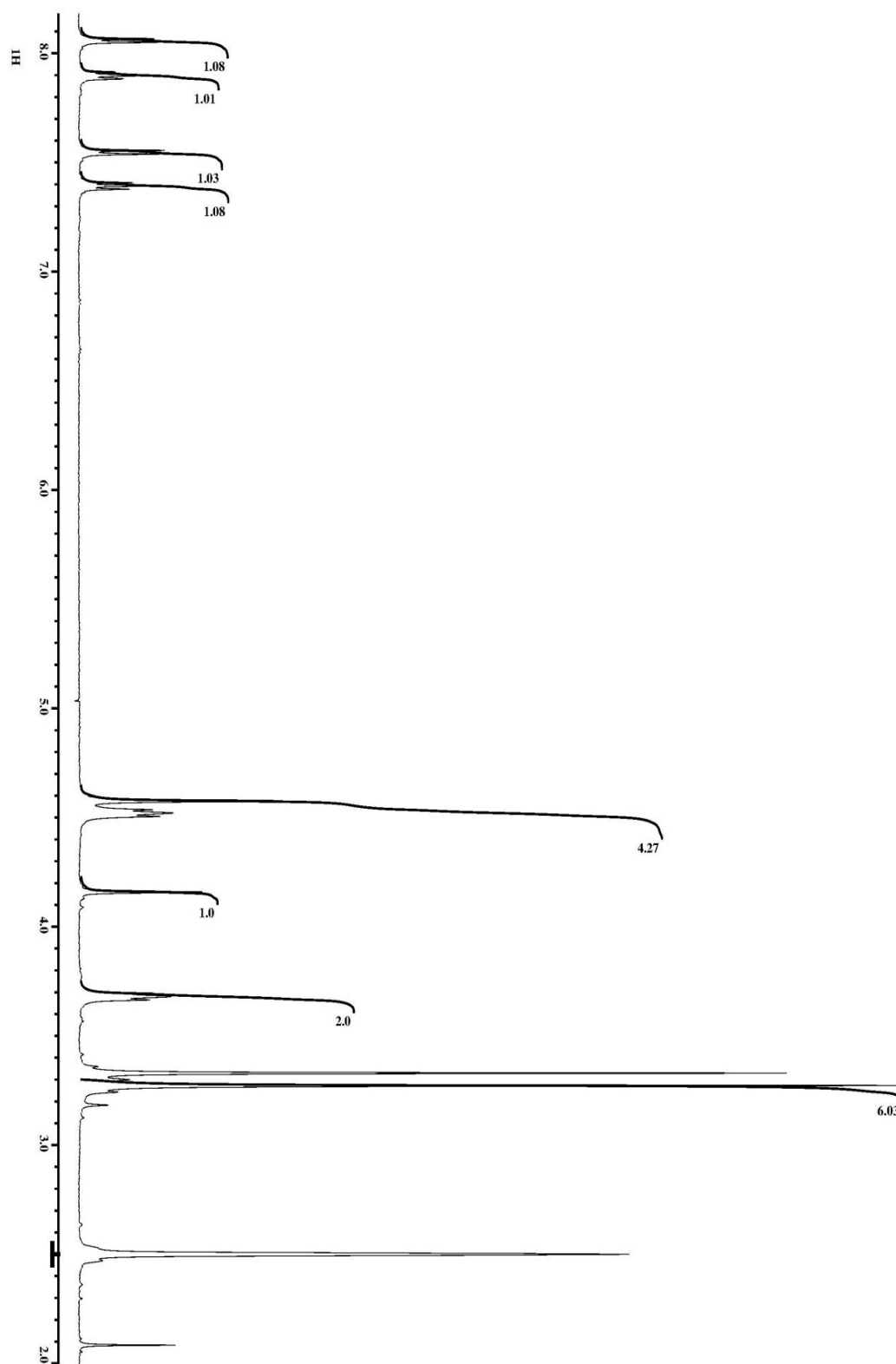
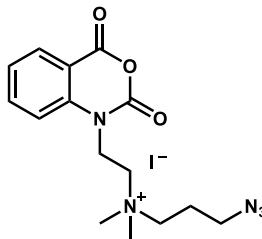


Figure 8-3:  $^1\text{H}$  NMR spectrum of **3o** in dimethyl sulfoxide- $\text{d}_6$



**3p.** General procedure 2 was followed as above using 1-azido-3-iodopropane (0.24 g, 1.1 mmol) as the electrophile. The final product (123 mg, 64%) was isolated as a light brown solid which precipitated readily from the acetone at -20 °C.  $C_{15}H_{20}N_5O_3I$  (445.26),  $^1H$  NMR (500 MHz, dimethyl sulfoxide- $d_6$ ):  $\delta$  2.02 (m, 2H), 3.21 (s, 6H), 3.51 (m, 4H), 3.62 (t, 2H,  $J = 7.7$  Hz), 4.49 (t, 2H,  $J = 7.7$  Hz), 7.40 (m, 1H), 7.55 (d, 1H,  $J = 8.5$  Hz), 7.91 (m, 1H), 8.06 (dd, 1H,  $J = 7.8, 1.5$  Hz) ppm,  $^{13}C$  NMR (500 MHz, dimethyl sulfoxide- $d_6$ ):  $\delta$  21.9, 37.7, 47.8, 50.6, 58.4, 61.4, 112.0, 114.5, 124.1, 129.7, 137.3, 140.8, 147.6, 158.6 ppm, MS (ESI): Calc. 318.16; Found 318.30 ( $M^+$ ) m/z.

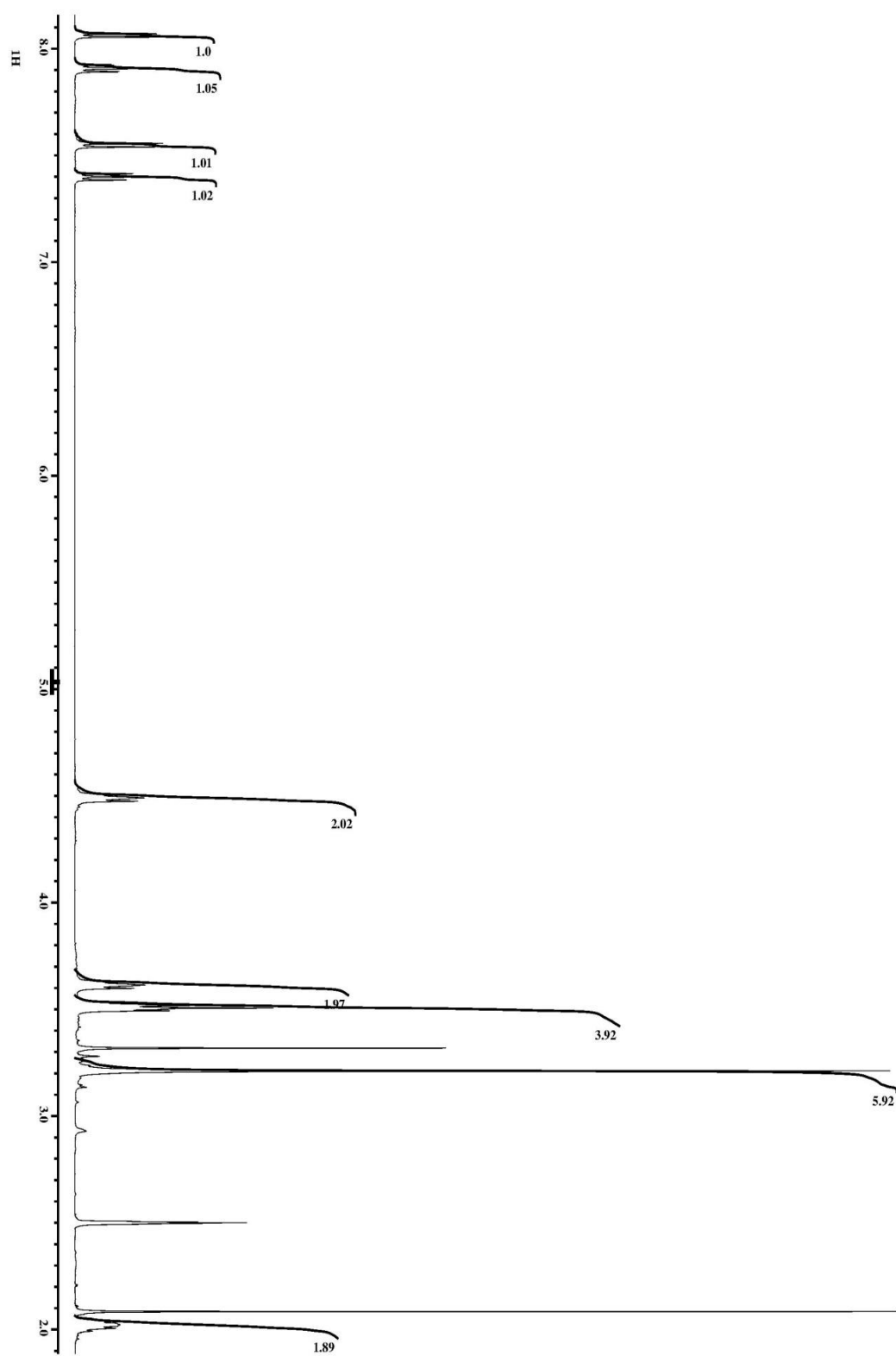
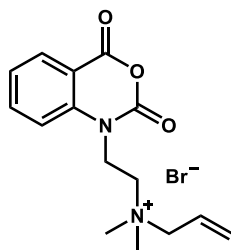
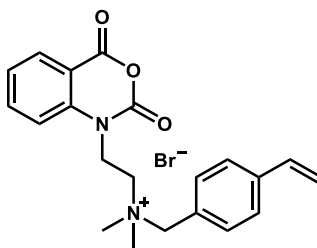


Figure 8-4:  $^1\text{H}$  NMR spectrum of **3p** in dimethyl sulfoxide- $\text{d}_6$



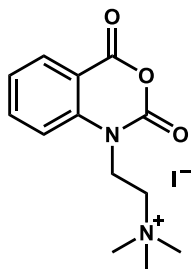
**3q.** General procedure 2 was followed as above using anhydrous THF as the solvent (1 mL) and allyl bromide (41  $\mu$ L, 0.47 mmol) as the electrophile. The final product (128 mg, 84%) was isolated as a colorless solid which precipitated readily from the acetone.  $C_{15}H_{19}N_2O_3Br$  (355.23),  $^1H$  NMR (500 MHz, dimethyl sulfoxide- $d_6$ ):  $\delta$  3.20 (s, 6H), 3.60 (t, 2H,  $J = 7.8$  Hz), 4.18 (d, 2H,  $J = 7.3$  Hz), 4.53 (t, 2H,  $J = 7.8$  Hz), 5.70 (m, 2H), 6.10 (m, 1H), 7.39 (m, 1H), 7.59 (d, 1H,  $J = 8.5$  Hz), 7.9 (m, 1H), 8.05 (dd, 1H,  $J = 7.8, 1.6$  Hz) ppm,  $^{13}C$  NMR (500 MHz, dimethyl sulfoxide- $d_6$ ):  $\delta$  37.7, 49.9, 58.3, 66.0, 112.0, 114.5, 124.0, 125.6, 128.2, 129.7, 137.3, 140.8, 147.6, 158.6 ppm.



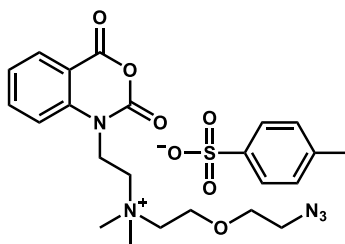
**3r.** General procedure 2 was followed as above using compound **3a** (117 mg, 0.50 mmol) and 1-(Bromomethyl)-vinylbenzene (0.10 mg, 0.51 mmol) as the electrophile with the following exceptions. A small amount of butylated hydroxytoluene was added to the solution. The product (115 mg, 53%) was isolated as a colorless solid which formed readily upon addition of the halide.  $C_{21}H_{23}N_2O_3Br$  (431.32),  $^1H$  NMR (500 MHz, dimethyl sulfoxide- $d_6$ ):  $\delta$  3.19 (s, 6H), 3.69 (t, 2H,  $J = 7.7$  Hz), 4.62 (t, 2H,  $J = 7.7$  Hz), 4.78 (s, 2H), 5.37 (d, 1H,  $J = 11.0$  Hz), 5.94 (d, 1H,  $J = 17.6$  Hz), 6.79 (dd, 1H,  $J = 17.6, 11.0$  Hz), 7.39 (m, 1H), 7.62 (m, 5H), 7.89 (m, 1H), 8.04 (dd, 1H,  $J = 7.8, 1.2$  Hz) ppm,



$^{13}\text{C}$  NMR (500 MHz, dimethyl sulfoxide- $d_6$ ):  $\delta$  38.1, 49.4, 58.9, 66.9, 112.0, 114.7, 116.3, 124.1, 126.5, 127.1, 129.7, 133.5, 135.8, 137.5, 139.0, 140.8, 147.7, 158.7 ppm, MS (ESI): Calc. 351.17; Found 351.04 ( $\text{M}^+$ )  $m/z$ .



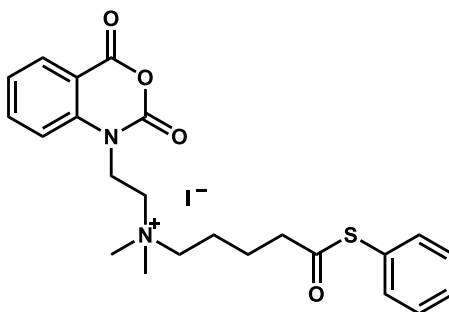
**3s.** General procedure 2 was followed as above using compound **3a** (117 mg, 0.50 mmol) and iodomethane (35  $\mu\text{L}$ , 0.56 mmol) as the electrophile with the following exceptions. Solids started precipitating after 20 mins and the reaction was filtered. The product (130 mg, 69%) was isolated as a colorless solid that formed readily upon addition of the halide.  $\text{C}_{13}\text{H}_{17}\text{N}_2\text{O}_3\text{I}$  (376.19),  $^1\text{H}$  NMR (500 MHz, dimethyl sulfoxide- $d_6$ ):  $\delta$  3.23 (s, 9H), 3.62 (t, 2H,  $J = 7.8$  Hz), 4.49 (t, 2H,  $J = 7.8$  Hz), 7.40 (m, 1H), 7.53 (d, 1H,  $J = 8.5$  Hz), 7.91 (m, 1H), 8.06 (dd, 1H,  $J = 7.8, 1.6$  Hz) ppm,  $^{13}\text{C}$  NMR (500 MHz, dimethyl sulfoxide- $d_6$ ):  $\delta$  38.0, 52.7, 60.4, 112.1, 114.4, 124.0, 129.8, 137.3, 140.8, 147.6, 158.6 ppm, MS (ESI): Calc. 249.12; Found 249.24 ( $\text{M}^+$ )  $m/z$ .



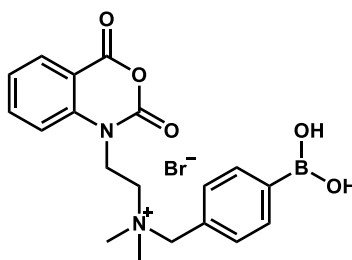
**3t.** General procedure 2 was followed as above using compound **3a** (117 mg, 0.50 mmol) and a 70% solution of 5-Azido-3-oxapentyl-1-p-toluenesulfonate (0.21 g, 0.52 mmol) as

the electrophile. The reaction mixture was analyzed by ESI to confirm product formation.

$C_{23}H_{29}N_5O_7S$  (519.57), MS (ESI): Calc. 348.17; Found 322.18 ( $M^+ - N_2 + H_2$ ) m/z.



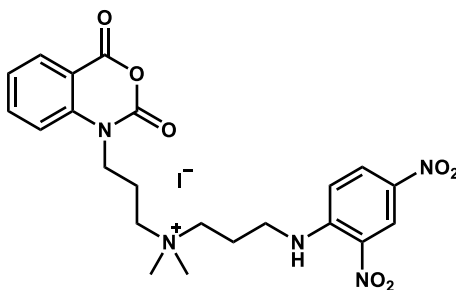
**3u.** General procedure 2 was followed as above using S-phenyl 5-iodopentanethioate (137 mg, 0.43mmol) as the electrophile. The product (62 mg, 26%) was isolated as a colorless solid that formed readily upon addition of the halide.  $C_{23}H_{27}N_2O_4I$  (554.44),  $^1H$  NMR (500 MHz, dimethyl sulfoxide- $d_6$ ):  $\delta$  1.66 (quin, 2H,  $J = 7.3$  Hz), 1.80 (m, 2H), 2.83 (t, 2H,  $J = 7.3$  Hz), 3.19 (s, 6H), 3.48 (t, 2H,  $J = 8.4$  Hz), 3.59 (t, 2H,  $J = 7.7$  Hz), 4.49 (t, 2H,  $J = 7.7$  Hz), 7.39 (m, 1H), 7.45 (m, 5H), 7.55 (d, 1H,  $J = 8.4$  Hz), 7.89 (m, 1H), 8.06 (dd, 1H,  $J = 7.8, 1.4$  Hz) ppm,  $^{13}C$  NMR (500 MHz, dimethyl sulfoxide- $d_6$ ):  $\delta$  21.0, 21.6, 37.6, 42.2, 50.4, 58.4, 63.2, 112.0, 114.5, 124.0, 127.2, 129.3, 129.6, 129.7, 134.4, 137.3, 140.8, 147.6, 158.6, 196.3 ppm.



**3v.** General procedure 2 was followed as above using compound **3a** (50 mg, 0.21 mmol) and 4-(bromomethyl)phenylboronic acid (46 mg, 0.21 mmol) as the electrophile. The final product (73 mg, 76%) was isolated as a light brown solid which precipitated readily from the acetone at  $-20$  °C.  $C_{19}H_{22}BN_2O_5Br$  (449.10),  $^1H$  NMR (500 MHz, dimethyl

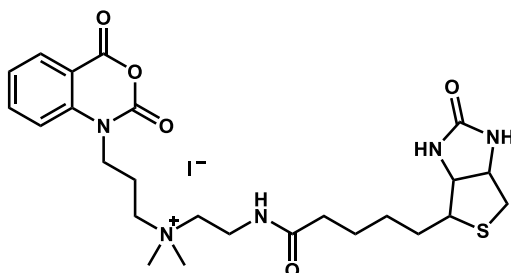
sulfoxide-d6):  $\delta$  3.16 (s, 6H), 3.65 (t, 2H,  $J = 7.7$  Hz), 4.60 (t, 2H,  $J = 7.7$  Hz), 4.73 (s, 2H), 7.40 (m, 1H), 7.59 (m, 3H), 7.90 (m, 3H), 8.06 (dd, 1H,  $J = 7.8, 1.4$  Hz), 8.21 (s, 2H) ppm,  $^{13}\text{C}$  NMR (500 MHz, dimethyl sulfoxide-d6):  $\delta$  37.9, 49.3, 58.9, 67.2, 112.1, 114.5, 124.0, 129.2, 129.7, 132.1, 134.5, 137.3, 140.9, 147.7, 158.7 ppm.

**General procedure 3.** To a 3 ml screw capped vial containing compound **3b** (100 mg, 0.3 mmol) was added 1 ml of reagent grade acetone and the solution heated to completely dissolve the reagent then filtered through a 0.4  $\mu\text{m}$  syringe filter. To this solution was added the corresponding nucleophile (0.3 mmol) and the solution was allowed to sit for 18 hrs at 40  $^{\circ}\text{C}$ . The solution was then stored at -20  $^{\circ}\text{C}$  overnight followed by filtration of the product. When no solid formed, ESI mass spectrometry of the reaction mix was used to confirm product formation.

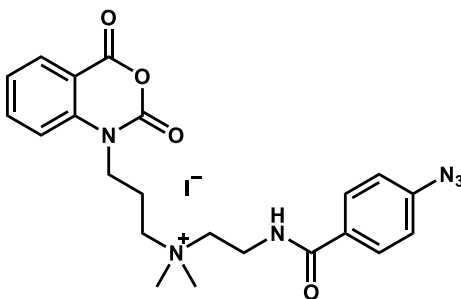


**3w.** General procedure 3 was followed as above using N-2,4-Dinitrophenyl-N',N'-dimethylpropylenediamine (81 mg, 0.3 mmol) as the nucleophile. The final product (116 mg, 64%) was isolated as a yellow solid.  $\text{C}_{22}\text{H}_{26}\text{N}_5\text{O}_7\text{I}$  (599.38),  $^1\text{H}$  NMR (500 MHz, dimethyl sulfoxide-d6):  $\delta$  2.07 (m, 4H), 3.00 (s, 6H), 3.35 (m, 2H), 3.46 (m, 2H), 3.57 (q, 2H,  $J = 6.6$  Hz), 4.11 (t, 2H,  $J = 6.7$  Hz), 7.28 (d, 1H,  $J = 9.6$  Hz), 7.36 (m, 1H), 7.54 (d, 1H,  $J = 8.5$  Hz), 7.86 (m, 1H), 8.05 (dd, 1H,  $J = 7.8$  Hz), 8.27 (dd, 1H,  $J = 9.6, 2.6$  Hz), 8.88 (d, 1H,  $J = 2.8$  Hz), 8.90 (t, 1H,  $J = 6.1$  Hz) ppm,  $^{13}\text{C}$  NMR (500 MHz, dimethyl

sulfoxide-d6):  $\delta$  20.3, 21.5, 41.4, 50.1, 60.6, 61.1, 111.8, 114.6, 115.2, 123.6, 123.8, 129.7, 130.0, 135.0, 137.3, 141.1, 147.8, 147.9, 158.9 ppm, MS (ESI): Calc. 472.18; Found 471.90 ( $M^+$ )  $m/z$ .

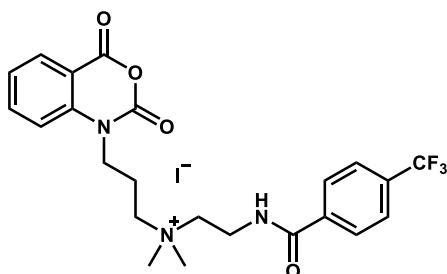


**3x.** General procedure 3 was followed as above with the following exceptions. The reaction was carried out on a reduced scale using anhydrous DMF as the solvent, compound **3b** (1.1 mg, 3.4  $\mu$ mol), and N-Biotin-N',N'-ethanediamine (1.3 mg, 4.2  $\mu$ mol) as the nucleophile. The reaction was carried out using DMF as the solvent. The final product did not form a solid and product formation was confirmed using ESI MS.  $C_{25}H_{36}N_5O_5SI$  (645.55), MS (ESI): Calc. 518.24; Found 517.98 ( $M^+$ )  $m/z$ .

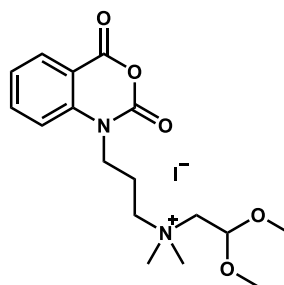


**3y.** General procedure 3 was followed as above using 4-azido-N-(2-(dimethylamino)ethyl)benzamide (70 mg, 0.3 mmol) as the nucleophile. The final product (116 mg, 66%) was isolated as a light brown solid.  $C_{22}H_{25}N_6O_4I$  (564.38),  $^1H$  NMR (500 MHz, dimethyl sulfoxide-d6):  $\delta$  2.16 (m, 2H), 3.10 (s, 6H), 3.45 (t, 2H,  $J$  = 6.8 Hz), 3.58 (m, 2H), 3.66 (q, 2H,  $J$  = 6.3 Hz), 4.13 (t, 2H,  $J$  = 6.7 Hz), 7.23 (d, 2H,  $J$  =

8.8 Hz), 7.37 (m, 1H), 7.57 (d, 1H,  $J = 8.4$  Hz), 7.87 (m, 3H), 8.05 (dd, 1H,  $J = 7.8, 1.5$  Hz), 8.78 (t, 1H,  $J = 5.6$  Hz) ppm,  $^{13}\text{C}$  NMR (500 MHz, dimethyl sulfoxide- $d_6$ ):  $\delta$  20.4, 33.4, 41.4, 50.5, 60.8, 61.4, 111.8, 114.7, 119.1, 123.8, 129.1, 129.7, 130.0, 137.3, 141.1, 142.7, 147.8, 158.9, 165.7 ppm, MS (ESI): Calc. 437.19; Found 437.15 ( $\text{M}^+$ )  $m/z$ .

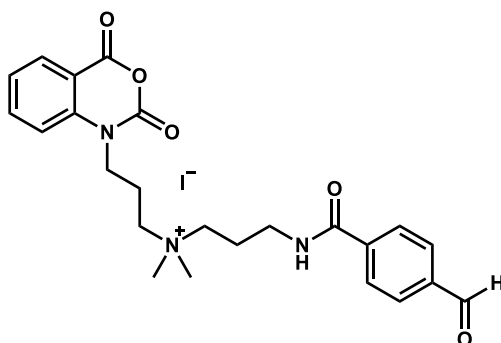


**3z.** General procedure 3 was followed as above using compound **3b** (180 mg, 0.54 mmol) and N-(2-(dimethylamino)ethyl)-4-(trifluoromethyl)benzamide (170 mg, 0.65 mmol) as the nucleophile. The final product (105 mg, 33%) was isolated as a light yellow solid.  $\text{C}_{23}\text{H}_{25}\text{N}_3\text{O}_4\text{F}_3\text{I}$  (591.36),  $^1\text{H}$  NMR (500 MHz, dimethyl sulfoxide- $d_6$ ):  $\delta$  2.16 (m, 2H), 3.11 (s, 6H), 3.47 (t, 2H,  $J = 6.7$  Hz), 3.58 (m, 2H), 3.70 (q, 2H,  $J = 6.2$  Hz), 4.14 (t, 2H,  $J = 6.7$  Hz), 7.37 (m, 1H), 7.57 (d, 1H,  $J = 8.5$  Hz), 7.88 (m, 3H), 8.04 (m, 3H), 9.01 (t, 1H,  $J = 5.5$  Hz) ppm,  $^{13}\text{C}$  NMR (500 MHz, dimethyl sulfoxide- $d_6$ ):  $\delta$  20.4, 33.5, 41.4, 50.5, 60.9, 61.4, 111.8, 114.7, 123.8, 125.5, 128.1, 129.7, 137.3, 137.3, 141.1, 147.8, 158.9, 165.5 ppm, MS (ESI): Calc. 464.18; Found 464.01 ( $\text{M}^+$ )  $m/z$ .

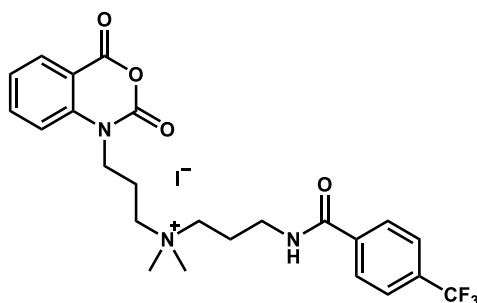


**3a'.** General procedure 3 was followed as above with the following exceptions. The reaction was carried out on a larger scale using compound **3b** (200 mg, 0.60 mmol) and

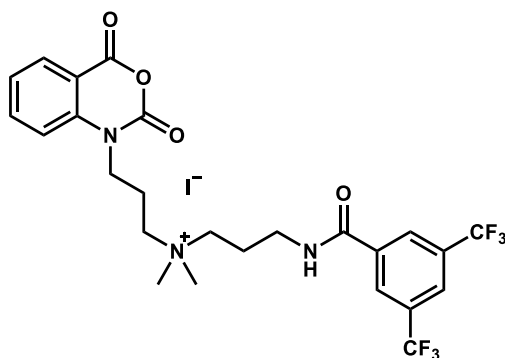
2,2-Dimethoxy-N,N-dimethyl-ethanamine (98  $\mu$ L, 0.65 mmol) as the nucleophile. The final product (139 mg, 69%) was isolated as a colorless solid.  $C_{17}H_{25}N_2O_5I$  (464.30),  $^1H$  NMR (500 MHz, dimethyl sulfoxide- $d_6$ ):  $\delta$  2.13 (m, 2H), 3.09 (s, 6H), 3.32 (s, 6H), 3.46 (d, 2H,  $J = 4.8$  Hz), 3.53 (m, 2H), 4.12 (t, 2H,  $J = 6.8$  Hz), 4.90 (t, 2H,  $J = 4.8$  Hz), 7.38 (m, 1H), 7.55 (d, 1H,  $J = 8.5$  Hz), 7.90 (m, 1H), 8.06 (dd, 1H,  $J = 7.8, 1.5$  Hz) ppm,  $^{13}C$  NMR (500 MHz, dimethyl sulfoxide- $d_6$ ):  $\delta$  20.4, 41.4, 51.4, 53.9, 61.7, 63.2, 98.1, 111.8, 114.7, 123.8, 129.7, 137.3, 141.1, 147.8, 158.9 ppm, MS (ESI): Calc. 337.18; Found 337.17 ( $M^+$ )  $m/z$ .



**3b'.** General procedure 3 was followed as above using N-(3-(dimethylamino)propyl)-4-formylbenzamide (71 mg, 0.3 mmol) as the nucleophile. The final product (127 mg, 74%) was isolated as a light yellow solid.  $C_{24}H_{28}N_3O_5I$  (565.40),  $^1H$  NMR (500 MHz, dimethyl sulfoxide- $d_6$ ):  $\delta$  1.97 (m, 2H), 2.10 (m, 2H), 3.02 (s, 6H), 3.35 (m, 4H), 3.49 (m, 2H), 4.12 (t, 2H,  $J = 6.8$  Hz), 7.36 (m, 1H), 7.55 (d, 1H,  $J = 8.5$  Hz), 7.86 (m, 1H), 8.02 (m, 5H), 8.80 (t, 1H,  $J = 5.7$  Hz), 10.09 (s, 1H) ppm,  $^{13}C$  NMR (500 MHz, dimethyl sulfoxide- $d_6$ ):  $\delta$  20.3, 22.5, 36.4, 41.4, 50.0, 60.4, 61.9, 111.8, 114.7, 123.8, 127.9, 129.4, 129.7, 137.3, 137.8, 139.2, 141.1, 147.8, 158.9, 165.6, 192.9 ppm.

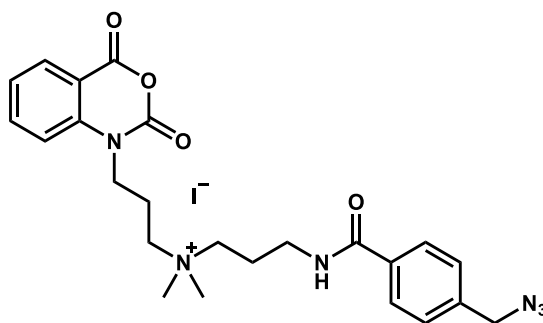


**3c'.** General procedure 3 was followed as above using N-(3-(dimethylamino)propyl)-4-(trifluoromethyl)benzamide (83 mg, 0.3 mmol) as the nucleophile. The final product (126 mg, 69%) was isolated as a colorless solid.  $C_{24}H_{27}N_3O_4F_3I$  (605.39),  $^1H$  NMR (500 MHz, dimethyl sulfoxide- $d_6$ ):  $\delta$  1.96 (m, 2H), 2.09 (m, 2H), 3.01 (s, 6H), 3.34 (m, 4H), 3.47 (m, 2H), 4.11 (t, 2H,  $J = 6.8$  Hz), 7.36 (m, 1H), 7.54 (d, 1H,  $J = 8.5$  Hz), 7.86 (m, 3H), 8.04 (m, 3H), 8.82 (t, 1H,  $J = 5.6$  Hz) ppm,  $^{13}C$  NMR (500 MHz, dimethyl sulfoxide- $d_6$ ):  $\delta$  20.3, 22.5, 36.4, 41.4, 50.0, 60.4, 61.8, 111.8, 114.6, 123.8, 125.3, 128.1, 129.7, 137.3, 138.0, 141.1, 147.8, 158.9, 165.3 ppm.



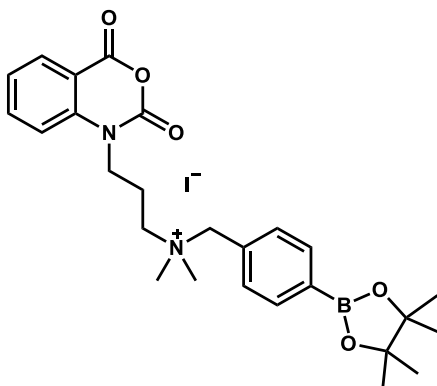
**3d'.** General procedure 3 was followed as above using anhydrous THF as the solvent and N-(3-(dimethylamino)propyl)-3,5-bis(trifluoromethyl)benzamide (103 mg, 0.3 mmol) as the nucleophile. The final product (106 mg, 52%) was isolated as a colorless solid.  $C_{25}H_{26}N_3O_4F_6I$  (673.39),  $^1H$  NMR (500 MHz, dimethyl sulfoxide- $d_6$ ):  $\delta$  1.98 (m, 2H), 2.10 (m, 2H), 3.01 (s, 6H), 3.37 (m, 4H), 3.47 (m, 2H), 4.11 (t, 2H,  $J = 6.8$  Hz), 7.35 (m,

1H), 7.54 (d, 1H, J = 8.5 Hz), 7.85 (m, 1H), 8.04 (dd, 1H, J = 7.8, 1.5 Hz), 8.34 (s, 1H), 8.48 (s, 2H), 9.10 (t, 1H, J = 5.7 Hz) ppm,  $^{13}\text{C}$  NMR (500 MHz, dimethyl sulfoxide-d<sub>6</sub>):  $\delta$  20.3, 22.5, 36.5, 41.4, 50.1, 60.4, 61.8, 111.8, 114.6, 123.8, 128.0, 129.7, 130.3, 130.6, 136.4, 137.3, 141.1, 147.8, 158.9, 163.5 ppm.

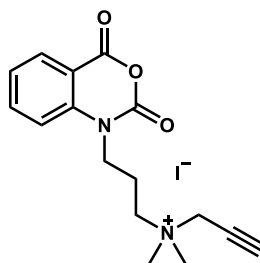


**3e'.** General procedure 3 was followed as above using 4-(azidomethyl)-N-(3-(dimethylamino)propyl)benzamide (79 mg, 0.3 mmol) as the nucleophile. The final product (106 mg, 59%) was isolated as a light yellow solid.  $\text{C}_{24}\text{H}_{29}\text{N}_6\text{O}_4\text{I}$  (592.43),  $^1\text{H}$  NMR (500 MHz, dimethyl sulfoxide-d<sub>6</sub>):  $\delta$  1.96 (m, 2H), 2.10 (m, 2H), 3.01 (s, 6H), 3.33 (m, 4H), 3.47 (m, 2H), 4.12 (t, 2H, J = 6.7 Hz), 4.53 (s, 2H), 7.36 (m, 1H), 7.46 (d, 2H, J = 8.1 Hz), 7.54 (d, 1H, J = 8.5 Hz), 7.86 (m, 3H), 8.05 (dd, 1H, J = 7.8, 1.3 Hz), 8.59 (t, 1H, J = 5.6 Hz) ppm,  $^{13}\text{C}$  NMR (500 MHz, dimethyl sulfoxide-d<sub>6</sub>):  $\delta$  20.3, 22.6, 36.3, 41.4, 50.0, 53.1, 60.4, 61.9, 111.8, 114.7, 123.8, 127.6, 128.2, 129.7, 134.0, 137.3, 138.8, 141.1, 147.8, 158.9, 166.1 ppm.



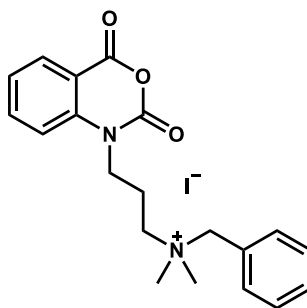


**3f'.** General procedure 3 was followed as above using anhydrous THF as the solvent. N,N-dimethyl-1-(4-(4,4,5,5-tetramethyl-1,3,2-dioxaborolan-2-yl)phenyl)methanamine hydrochloride salt (48 mg, 0.16 mmol) and sodium carbonate (24 mg, 0.23 mmol) were dissolved in anhydrous THF (5 mL) and stirred overnight. The N,N-dimethyl-1-(4-(4,4,5,5-tetramethyl-1,3,2-dioxaborolan-2-yl)phenyl)methanamine product (0.20 mg, 77  $\mu$ mol) was filtered and used as the nucleophile with compound **5** (25 mg, 77  $\mu$ mol). The final product (76 mg, 43%) was isolated as a brown solid.  $C_{26}H_{34}N_2O_5BI$  (592.27),  $^1H$  NMR (500 MHz, dimethyl sulfoxide- $d_6$ ):  $\delta$  1.31 (s, 12H), 2.19 (m, 2H), 2.96 (s, 6H), 3.42 (m, 2H), 4.11 (t, 2H,  $J = 6.7$  Hz), 4.35 (s, 2H), 7.39 (m, 1H), 7.53 (m, 3H), 7.76 (d, 2H,  $J = 8.0$  Hz), 7.89 (m, 1H), 8.06 (dd, 1H,  $J = 7.8, 1.5$  Hz) ppm,  $^{13}C$  NMR (500 MHz, dimethyl sulfoxide- $d_6$ ):  $\delta$  20.4, 24.6, 41.4, 49.3, 60.7, 67.0, 84.0, 111.8, 114.7, 123.8, 129.7, 130.9, 132.4, 134.7, 137.3, 141.2, 147.8, 158.9 ppm.

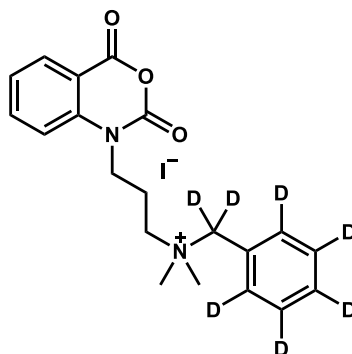


**3g'.** General procedure 3 was followed as above using N,N-dimethylprop-2-yn-1-amine (36  $\mu$ L, 0.33 mmol) as the nucleophile. The final product (98 mg, 78%) was isolated as a

light yellow solid.  $C_{16}H_{19}N_2O_3I$  (414.24),  $^1H$  NMR (500 MHz, dimethyl sulfoxide- $d_6$ ):  $\delta$  2.14 (m, 2H), 3.07 (s, 6H), 3.56 (m, 2H), 4.08 (t, 1H,  $J = 2.5$  Hz), 4.13 (t, 2H,  $J = 6.8$  Hz), 4.37 (d, 2H,  $J = 2.4$  Hz), 7.38 (m, 1H), 7.57 (d, 1H,  $J = 8.5$  Hz), 7.89 (m, 1H), 8.05 (dd, 1H,  $J = 7.8, 1.5$  Hz) ppm,  $^{13}C$  NMR (500 MHz, dimethyl sulfoxide- $d_6$ ):  $\delta$  20.5, 41.3, 49.9, 53.9, 60.7, 72.2, 83.1, 111.8, 114.7, 123.8, 129.7, 137.3, 141.1, 147.8, 158.8 ppm.



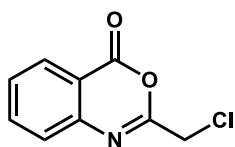
**3h'.** General procedure 3 was followed as above using N,N-dimethyl-1-phenylmethanamine (55  $\mu$ L, 0.37 mmol) as the nucleophile. The final product (96 mg, 68%) was isolated as a light yellow solid.  $C_{20}H_{23}N_2O_3I$  (466.31),  $^1H$  NMR (500 MHz, dimethyl sulfoxide- $d_6$ ):  $\delta$  2.20 (m, 2H), 2.95 (s, 6H), 3.43 (m, 2H), 4.13 (t, 2H,  $J = 6.75$  Hz), 4.50 (s, 2H), 7.39 (m, 1H), 7.49 (m, 4H), 7.54 (m, 2H) 7.90 (m, 1H), 8.07 (dd, 1H,  $J = 7.8, 1.4$  Hz) ppm,  $^{13}C$  NMR (500 MHz, dimethyl sulfoxide- $d_6$ ):  $\delta$  20.5, 41.4, 49.2, 60.5, 67.0, 111.8, 114.8, 123.8, 127.9, 128.9, 129.7, 130.3, 132.9, 137.4, 141.2, 147.7, 158.9 ppm.



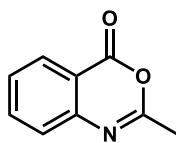
**3i'.** General procedure 3 was followed as above using 1,1-dideutero-*N,N*-dimethyl-1-(perdeuterophenyl)methanamine (57  $\mu$ L, 0.37 mmol) as the nucleophile. The final product (58 mg, 41%) was isolated as a colorless solid.  $C_{20}H_{16}D_7N_2O_3I$  (473.36),  $^1H$  NMR (500 MHz, dimethyl sulfoxide- $d_6$ ):  $\delta$  2.19 (m, 2H), 2.94 (s, 6H), 3.42 (m, 2H), 4.13 (t, 2H,  $J = 6.5$  Hz), 7.39 (m, 1H), 7.55 (d, 1H,  $J = 8.5$  Hz), 7.90 (m, 1H), 8.07 (dd, 1H,  $J = 7.8, 0.9$  Hz) ppm,  $^{13}C$  NMR (500 MHz, dimethyl sulfoxide- $d_6$ ):  $\delta$  20.4, 30.7, 41.4, 49.1, 60.5, 111.8, 114.7, 123.8, 127.6, 129.7, 137.3, 141.2, 147.8, 158.9 ppm.

**General procedure 4.** To a Schlenk flask under dry  $N_2$  was added 60% wt/wt NaH suspended in oil (1.5 g, 36 mmol). To this was added 15 ml of dry hexanes, the suspension briefly stirred then allowed to settle, and the hexanes removed via cannula. This process was repeated 3 x. To the freshly rinsed NaH was added anhydrous DMF (30 ml) at room temperature resulting in a cloudy suspension. To this suspension was added isatoic anhydride (5.1 g, 30 mmol) in one portion. Following this addition, an additional 20 ml of anhydrous DMF was added and the resulting suspension was stirred for 60 min. The flask in then moved to an ice bath where it is cooled to 0  $^{\circ}C$  over 15 min. Following this, the corresponding acid chloride (36 mmol) was added dropwise over approximately 10 min. The resulting suspension was stirred 12 hrs yielding a clear and colored solution

containing the desired product. The resulting solution is concentrated under vacuum at 100 °C resulting in a darkly colored viscous residue. This residue is then dissolved into DCM (150 ml) and extracted 3 x with 100 ml of saturated NaHCO<sub>3</sub> (aq). Finally the organic layer is rinsed 1 x wash with 100 ml of brine solution. The organic layer is then collected and stirred with activated carbon (0.5 g) for 30 min. The resulting organic solution is then filtered through a plug of MgSO<sub>4</sub> to both remove the activated carbon and dry the solution of residual water. The resulting solution is then concentrated under vacuum to remove the DCM resulting in a lightly colored solid that is then recrystallized from isopropanol.



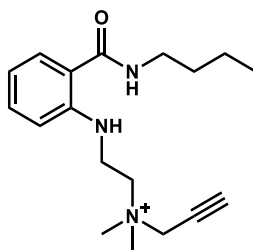
**3j'.** General procedure 4 was followed as above using chloroacetyl chloride (2.9 mL, 36 mmol) as the acid chloride. The final product (2.45 g, 42%) was isolated as a light brown solid. C<sub>9</sub>H<sub>6</sub>NO<sub>2</sub>Cl (195.60), <sup>1</sup>H NMR (500 MHz, acetone-d<sub>6</sub>): δ 4.61 (s, 2H), 7.67 (m, 2H), 7.96 (m, 1H), 8.17 (dd, 1H, J = 7.8, 1.1 Hz) ppm, <sup>13</sup>C NMR (500 MHz, acetone-d<sub>6</sub>): δ 42.9, 118.1, 128.0, 129.1, 130.2, 137.7, 146.7, 158.1, 159.2 ppm, MS (EI): Calc. 195.01; Found 195.0 (M<sup>+</sup>, 14%), 146.0 (100%) m/z.



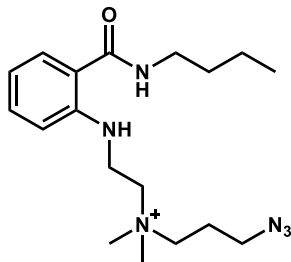
**3k'.** General procedure 4 was followed as above using acetyl chloride (2.6 mL, 36 mmol) as the acid chloride. The final product (1.11 g, 23%) was isolated as a colorless solid. C<sub>9</sub>H<sub>7</sub>NO<sub>2</sub> (161.16), <sup>1</sup>H NMR (500 MHz, acetone-d<sub>6</sub>): δ 2.41 (s, 3H), 7.54 (d, 1H, J = 7.8 Hz), 7.57 (m, 1H), 7.88 (m, 1H), 8.11 (dd, 1H, J = 7.8, 1.2 Hz) ppm, <sup>13</sup>C NMR (500

MHz, acetone-d<sub>6</sub>):  $\delta$  21.3, 117.7, 127.2, 128.8, 128.9, 137.3, 147.6, 160.0, 161.2 ppm,  
 MS (EI): Calc. 161.05; Found 161.1 ( $M^+$ , 98%), 146.1 (100%)  $m/z$ .

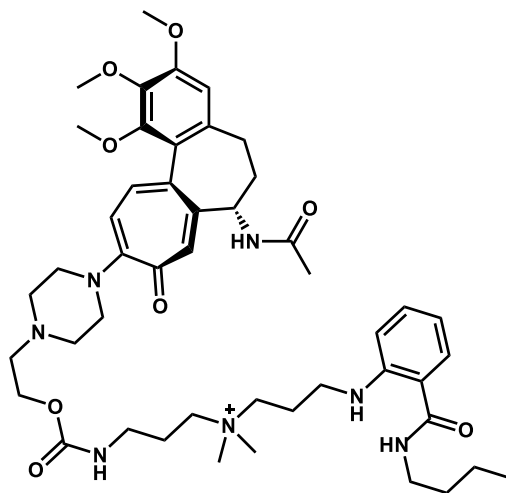
**General procedure 5.** To an Eppendorf tube was weighed the derivative. To the solid was added 10 equivalents of butylamine followed by an equal volume of anhydrous DMSO. The reaction was sonicated until all solids had dissolved. The reaction was diluted to the desired concentration with 25 mM bicarbonate buffer at pH 8.4. To confirm complete conversion to product the reaction was analyzed by HPLC on a Thermo Scientific Vanquish system with a RS diode array detector (330 nm) on a reverse-phase column (Thermo Scientific Accucore C18, 150 x 2.1 mm, 2.6  $\mu$ m) and Thermo Scientific Velos Pro mass spectrometer. The absorption spectrum was measured from 250 to 450 nm on a Shimadzu UV-1800 UV-VIS spectrophotometer.



**5a.** General procedure 5 was followed as above using **3o** (0.53 mg, 1.5  $\mu$ mol). To this was added butylamine (1.48  $\mu$ L, 14.8  $\mu$ mol, 10 eqs) followed by anhydrous DMSO (14.8  $\mu$ L). Once the solids had completely dissolved, the reaction was diluted to a concentration of 5 mM by the addition of 25mM bicarbonate at pH 8.4 (297  $\mu$ L). 50  $\mu$ L of the reaction was diluted to a concentration of 125  $\mu$ M by the addition of 1.95 mL of 25mM bicarbonate at pH 8.4. The absorbance spectrum was then measured. 280 nm = 0.072 Abs,  $\epsilon$  = 576  $M^{-1}cm^{-1}$ ; 330 nm = 0.368 Abs,  $\epsilon$  = 2942  $M^{-1}cm^{-1}$ ; correction factor = 0.2.

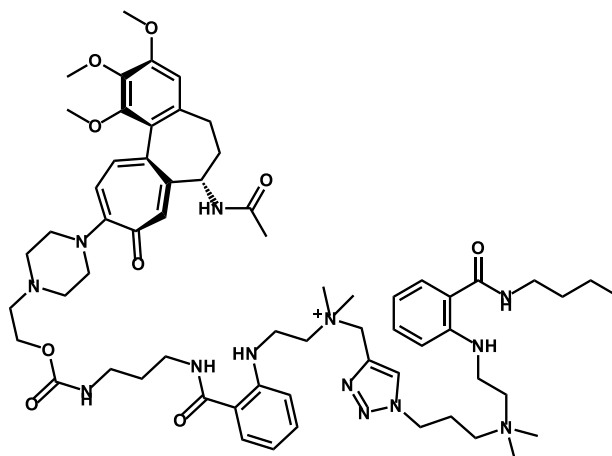


**5b.** General procedure 5 was followed as above using **3p** (1.03 mg, 2.3  $\mu\text{mol}$ ). To this was added butylamine (2.34  $\mu\text{L}$ , 23.4  $\mu\text{mol}$ , 10 eqs) followed by anhydrous DMSO (2.34  $\mu\text{L}$ ). Once the solids had completely dissolved, the reaction was diluted to a concentration of 5 mM by the addition of 25mM bicarbonate at pH 8.4 (466  $\mu\text{L}$ ). 50  $\mu\text{L}$  of the reaction was diluted to a concentration of 125  $\mu\text{M}$  by the addition of 1.95 mL of 25mM bicarbonate at pH 8.4. The absorbance spectrum was then measured. 280 nm = 0.067 Abs,  $\epsilon = 535 \text{ M}^{-1}\text{cm}^{-1}$ ; 330 nm = 0.380 Abs,  $\epsilon = 3009 \text{ M}^{-1}\text{cm}^{-1}$ ; correction factor = 0.2.



**6w.** General procedure 5 was followed as above using **6t** (1.00 mg, 1.0  $\mu\text{mol}$ ) which was dissolved in anhydrous DMSO (15.95  $\mu\text{L}$ ). To this was added butylamine (5  $\mu\text{L}$ , 51  $\mu\text{mol}$ , 51 eqs). Once the solids had completely dissolved, 14  $\mu\text{L}$  of the reaction was diluted to a concentration of 0.33 mM by the addition of DI water (1982  $\mu\text{L}$ ). 1 mL of

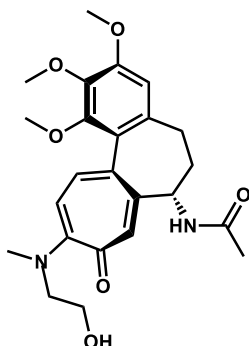
this was diluted to a concentration of 0.13 mM by the addition of 1 mL of DI water. The absorbance spectrum was then measured. 280 nm = 1.260 Abs,  $\epsilon = 10082 \text{ M}^{-1}\text{cm}^{-1}$ ; 330 nm = 0.676 Abs,  $\epsilon = 5633 \text{ M}^{-1}\text{cm}^{-1}$ ; correction factor = 1.9.



**6v.** Ascorbate was made fresh by mixing equal amounts of sodium bicarbonate (200mM) with ascorbic acid (200mM). **6s** (2.51 mg, 2.77  $\mu\text{mol}$ ) was dissolved in methanol (50 $\mu\text{L}$ ). To this was added 100 mM bicarbonate buffer at pH 7.9 (783.3  $\mu\text{L}$ ) followed by **5b** (27.7  $\mu\text{L}$ , 2.73  $\mu\text{mol}$ ). To this was added copper sulfate (6.93  $\mu\text{L}$ , 20 mM) premixed with THPTA (13.85  $\mu\text{L}$ , 50 mM). To this was added ascorbate (69.25  $\mu\text{L}$ , 0.1 M). Let sit at RT for three hours at which point the reaction was complete by LC-MS. 70  $\mu\text{L}$  of the reaction was diluted to a concentration of 102  $\mu\text{M}$  by the addition of 1.93 mL of DI water. The absorbance spectrum was then measured. 280 nm = 1.168 Abs,  $\epsilon = 11467 \text{ M}^{-1}\text{cm}^{-1}$ ; 330 nm = 1.012 Abs,  $\epsilon = 9720 \text{ M}^{-1}\text{cm}^{-1}$ ; correction factor = 1.1.

**General procedure 6.** Colchicine was weighed out in an Eppendorf tube. To this was added 100 equivalents of amine reagent. The suspension was stirred until all solids had dissolved. The reaction was allowed to sit at 40 °C for three hours. DCM was added to the solution and extracted 2 x with DI water and 1 x with brine. The organic layer was

dried over  $\text{Na}_2\text{SO}_4$  for 30 minutes. The solution was filtered and the DCM was removed under vacuum to give the final product.



**6i.** General procedure 6 was followed as above. N-Methylethanolamine (10 mL, 124 mmol) was added to colchicine (501 mg, 1.25 mmol). Solution was vortexed until colchicine completely dissolved, giving a bright yellow solution. The final product was isolated as a bright yellow solid (568 mg, quant.).  $\text{C}_{24}\text{H}_{30}\text{N}_2\text{O}_6$  (442.50),  $^1\text{H}$  NMR (500 MHz,  $\text{CDCl}_3$ ):  $\delta$  1.84 (m, 1H), 1.95 (s, 3H), 2.20 (m, 1H), 2.29 (m, 1H), 2.41 (m, 1H), 3.03 (s, 3H), 3.29 (dt, 1H,  $J = 14.7, 3.7$  Hz), 3.59 (s, 3H), 3.86 (m, 9H), 4.04 (m, 1H), 4.53 (m, 1H), 6.47 (s, 1H), 6.73 (d, 1H,  $J = 11.7$  Hz), 7.31 (m, 2H), 8.24 (d, 1H,  $J = 6.4$  Hz) ppm,  $^{13}\text{C}$  NMR (500 MHz,  $\text{CDCl}_3$ ):  $\delta$  22.8, 30.0, 36.8, 38.9, 52.2, 53.5, 54.8, 56.1, 59.1, 61.4, 107.4, 115.8, 125.9, 126.4, 132.7, 134.5, 137.5, 141.5, 151.1, 151.4, 153.1, 158.3, 170.1, 179.4 ppm, MS (ESI): Calc. 442.21; Found 443.34 ( $\text{M}^+ + \text{H}$ )  $m/z$ .



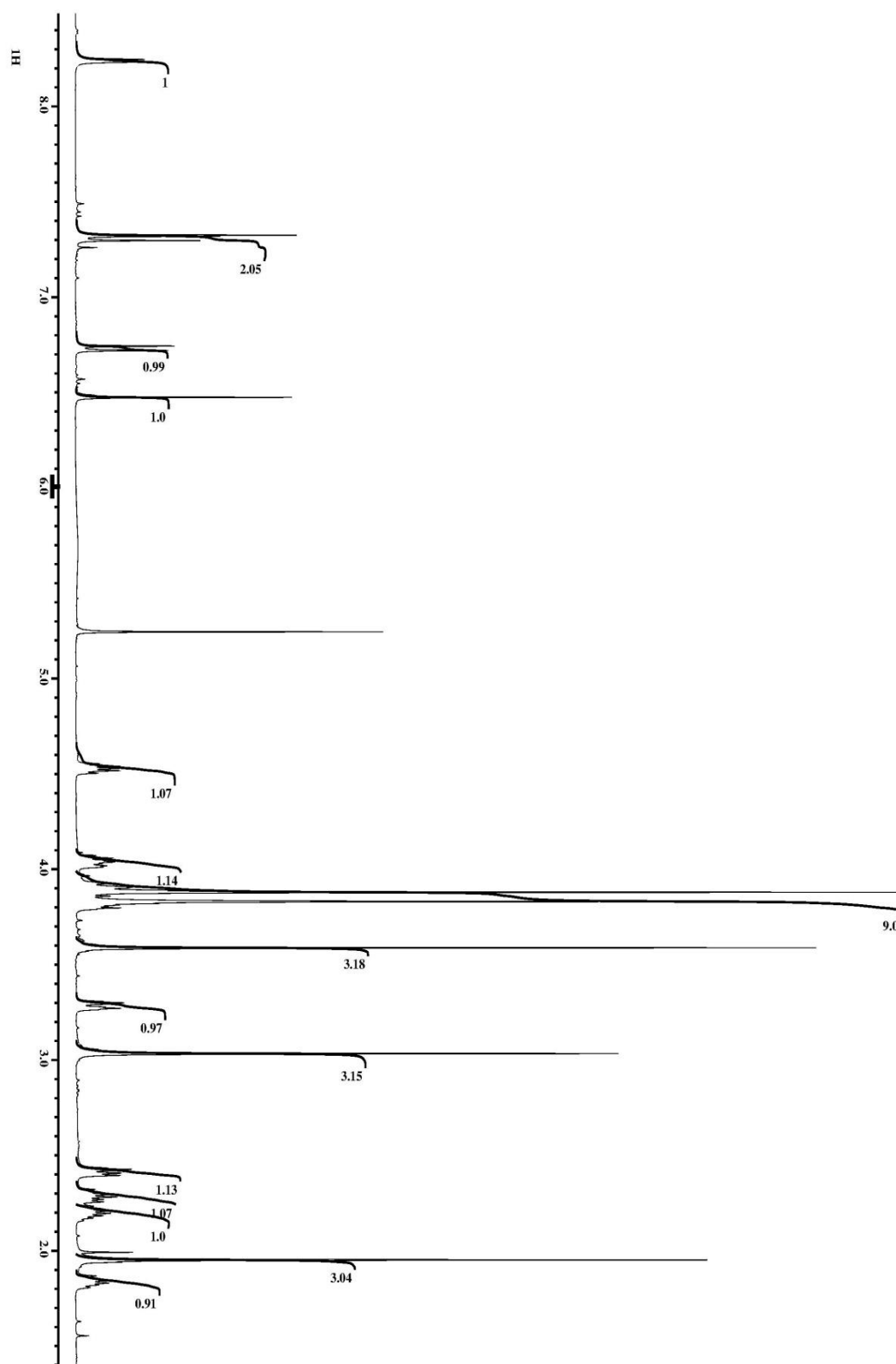
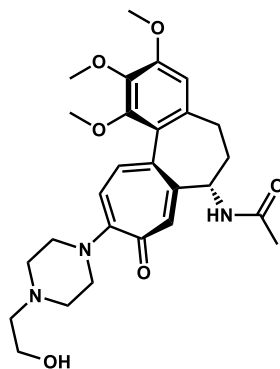


Figure 8-5:  $^1\text{H}$  NMR spectrum of **6i** in  $\text{CDCl}_3$



**6j.** General procedure 6 was followed as above with the following exceptions. Colchicine (459.6 mg, 1.15 mmol) was dissolved in methanol (1.4 mL). To this was added 2-piperazinoethanol (14 mL, 114 mmol). The reaction was allowed to sit at 40 °C for seven hours. The final product was isolated as a bright yellow solid (474 mg, 83%).  $C_{27}H_{35}N_3O_6$  (497.58),  $^1H$  NMR (500 MHz,  $CDCl_3$ ):  $\delta$  1.85 (m, 1H), 2.03 (s, 3H), 2.24 (m, 1H), 2.43 (m, 1H), 2.52 (m, 1H), 2.72 (t, 1H,  $J = 5.3$  Hz), 2.83 (m, 4H), 3.45 (m, 2H), 3.63 (m, 5H), 3.75 (t, 2H,  $J = 5.0$  Hz), 3.91 (s, 3H), 3.96 (s, 3H), 4.64 (m, 1H), 6.54 (s, 1H), 6.79 (d, 1H,  $J = 11.0$  Hz), 6.94 (d, 1H,  $J = 7.1$  Hz), 7.25 (s, 1H), 7.29 (m, 1H) ppm,  $^{13}C$  NMR (500 MHz,  $CDCl_3$ ):  $\delta$  23.2, 30.2, 37.2, 48.4, 52.0, 53.0, 56.2, 57.7, 59.6, 61.5, 107.5, 118.6, 126.1, 129.6, 134.4, 134.7, 136.1, 141.8, 149.6, 151.5, 153.3, 158.0, 169.8, 181.4 ppm, MS (ESI): Calc. 497.25; Found 498.42 ( $M^+ + H$ ) m/z.

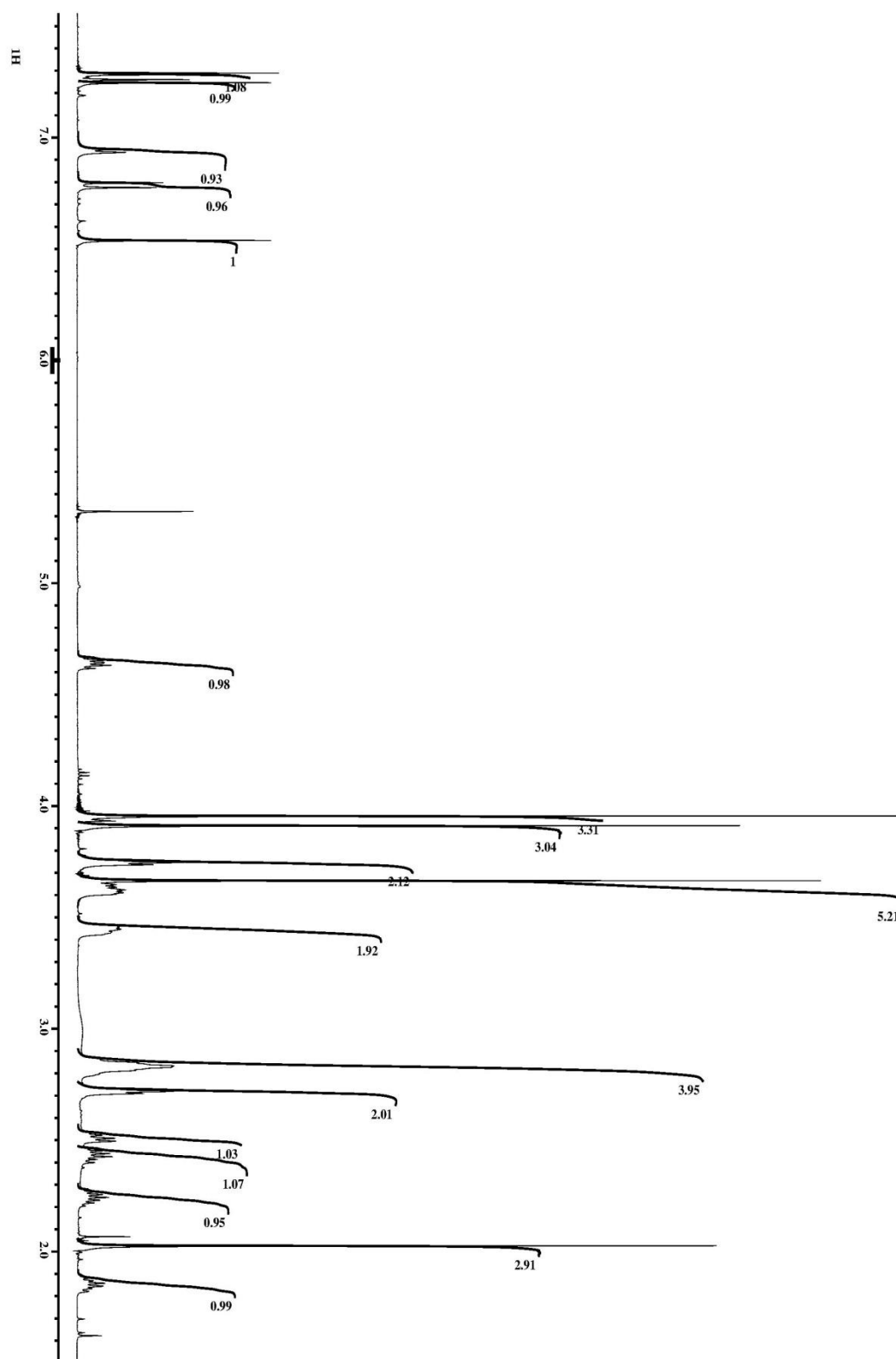
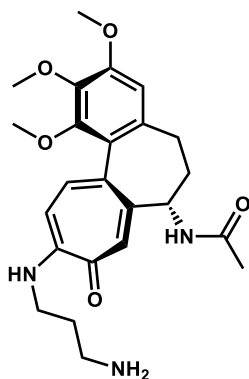
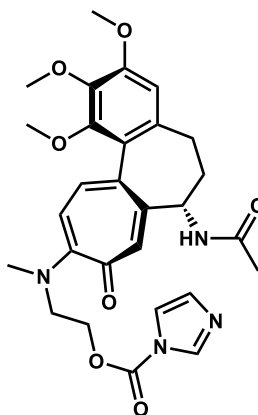


Figure 8-6:  $^1\text{H}$  NMR spectrum of **6j** in  $\text{CDCl}_3$

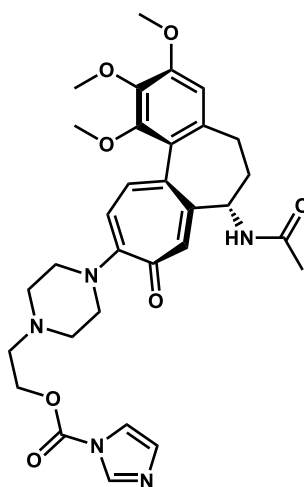
**General procedure 7.** Colchicine derivatized with a hydroxy was dissolved in anhydrous DCM (0.5 mL). To this was added 1.2 equivalents of CDI dissolved in anhydrous DCM (0.5 mL). The reaction was stirred for 30 minutes. The reaction was allowed to sit at 40 °C for three hours. This was extracted 3 x with DI water. The organic layer was dried over Na<sub>2</sub>SO<sub>4</sub> for 30 minutes. The solution was filtered and the DCM was removed under vacuum to give the final product.



**6k.** General procedure 6 was followed as above with the following exceptions. Colchicine (31.4 mg, 78.6 μmol) was dissolved in methanol (1.0 mL). To this was added N-boc-1,3-propanediamine (27.5 μL, 157 μmol). The reaction was allowed to sit at RT overnight. Reaction was then heated to 50 °C for three hours. DCM was added to the solution and extracted 3 x with DI water. The organic layer was dried over Na<sub>2</sub>SO<sub>4</sub> for 30 minutes. The solution was filtered and the DCM was removed under vacuum to a yellow solid. This was dissolved in anhydrous DCM (1 mL). The solution was put under N<sub>2</sub> and cooled in an ice bath. To this was added TFA (1 mL) drop-wise while stirring. Let reaction warm to RT and stir for 4 hours. The solvent and TFA were removed under vacuum to give the final product as yellow solid (28.4 mg, 82%). C<sub>24</sub>H<sub>31</sub>N<sub>3</sub>O<sub>5</sub> (441.52), MS (ESI): Calc. 441.23; Found 442.34 (M<sup>+</sup> + H) m/z.



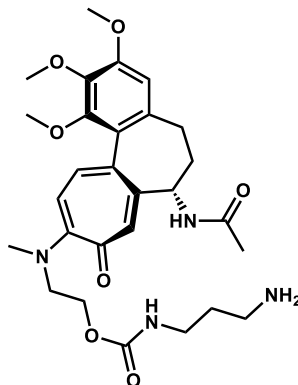
**6l.** General procedure 7 was followed as above using **6i** (413.2 mg, 934  $\mu$ mol) and CDI (168.6 mg, 1.04 mmol). The final product was isolated as a yellow solid (401.3 mg, 80%), which was immediately used in the next step.  $C_{28}H_{32}N_4O_7$  (536.58).



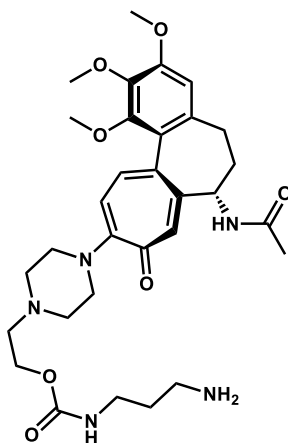
**6m.** General procedure 7 was followed as above using **6j** (50 mg, 121  $\mu$ mol) and CDI (54.7 mg, 337  $\mu$ mol). The final product was isolated as a yellow liquid (64 mg, quant.), which was immediately used in the next step.  $C_{31}H_{37}N_5O_7$  (591.65).

**General procedure 8.** The colchicine derivative activated with CDI was dissolved in 2 mL of anhydrous DCM. This was added drop-wise to 20 equivalents of the diamine reagent dissolved in 1 mL of anhydrous DCM with stirring. The reaction was allowed to

stir for 1 hour. The volume was reduced under vacuum to give the crude product. Product was purified by column chromatography over silica gel. Impurities were removed with 90:10 ethyl DCM/MeOH. The product was removed from the column by the addition of 0.1% TEA to the mobile phase. Solvent was removed under vacuum to give the final product.

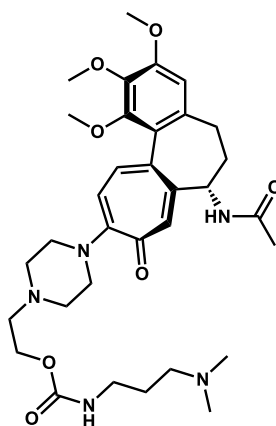


**6n.** General procedure 8 was followed as above using **6l** (50 mg, 93  $\mu\text{mol}$ ) and propane diamine (156.6  $\mu\text{L}$ , 1.86 mmol). The final product was isolated as a yellow liquid (10.8 mg, 21%).  $\text{C}_{28}\text{H}_{38}\text{N}_4\text{O}_7$  (542.62), MS (ESI): Calc. 542.27; Found 543.42 ( $\text{M}^+ + \text{H}$ )  $m/z$ .



**6o.** General procedure 8 was followed as above using **6m** (42.8 mg, 72.3  $\mu\text{mol}$ ) and propane diamine (121.8  $\mu\text{L}$ , 1.45 mmol). The final product was isolated as a yellow liquid (16 mg, 26%).  $\text{C}_{31}\text{H}_{43}\text{N}_5\text{O}_7$  (597.70),  $^1\text{H}$  NMR (500 MHz,  $\text{CDCl}_3$ ):  $\delta$  1.65 (quin,

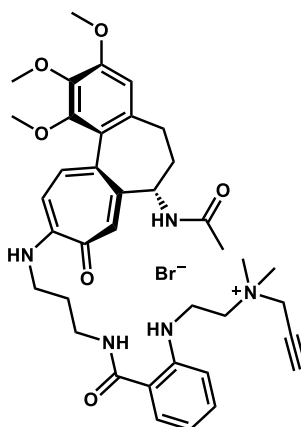
2H,  $J = 6.6$  Hz), 1.99 (s, 3H), 2.21 (m, 1H), 2.40 (m, 1H), 2.48 (m, 1H), 2.70 (m, 6H), 2.79 (t, 2H,  $J = 6.6$  Hz), 3.28 (q, 2H,  $J = 6.2$  Hz), 3.34 (m, 2H), 3.57 (m, 2H), 3.63 (s, 3H), 3.88 (s, 3H), 3.92 (s, 3H), 4.22 (t, 1H,  $J = 5.3$  Hz), 4.61 (m, 1H), 6.51 (s, 1H), 6.74 (d, 1H,  $J = 11.0$  Hz), 6.93 (s, 1H), 7.19 (s, 1H), 7.23 (d, 1H,  $J = 11.0$  Hz) ppm,  $^{13}\text{C}$  NMR (500 MHz,  $\text{CDCl}_3$ ):  $\delta$  23.2, 30.2, 33.1, 37.2, 39.2, 39.8, 48.6, 52.0, 53.3, 56.2, 57.3, 61.5, 61.9, 107.5, 118.2, 126.1, 129.3, 134.2, 134.5, 136.2, 141.8, 149.5, 151.4, 153.3, 156.8, 158.2, 169.8, 181.4 ppm, MS (ESI): Calc. 597.32; Found 598.51 ( $\text{M}^+ + \text{H}$ )  $m/z$ .



**6p.** General procedure 8 was followed as above using **6m** (42.8 mg, 72.3  $\mu\text{mol}$ ) and N,N-Dimethyl-1,3-propanediamine (10.9  $\mu\text{L}$ , 81  $\mu\text{mol}$ ). The reaction was allowed to stir overnight. The final product was isolated as a yellow liquid (21.6 mg, 40%).  $\text{C}_{33}\text{H}_{47}\text{N}_5\text{O}_7$  (625.76),  $^1\text{H}$  NMR (500 MHz, acetone- $d_6$ ):  $\delta$  1.64 (quin, 2H,  $J = 6.8$  Hz), 1.88 (m, 4H), 2.15 (s, 6H), 2.36 (m, 1H), 2.63 (m, 7H), 3.17 (q, 2H,  $J = 6.0$  Hz), 3.35 (m, 2H), 3.49 (m, 2H), 3.59 (s, 3H), 3.84 (s, 3H), 3.87 (s, 3H), 4.15 (t, 1H,  $J = 5.7$  Hz), 4.51 (m, 1H), 6.35 (bs, 1H), 6.72 (s, 1H), 6.80 (d, 1H,  $J = 10.8$  Hz), 7.08 (s, 1H), 7.11 (d, 1H,  $J = 10.8$  Hz), 7.78 (d, 1H,  $J = 7.3$  Hz) ppm,  $^{13}\text{C}$  NMR (500 MHz, acetone- $d_6$ ):  $\delta$  22.8, 28.5, 30.6, 37.5, 40.2, 45.7, 49.1, 52.3, 54.2, 55.0, 56.4, 58.0, 58.1, 61.2, 61.3, 62.3, 108.5, 117.4, 127.3,

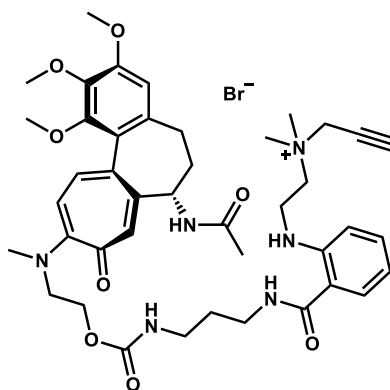
129.9, 134.2, 135.5, 136.0, 142.5, 149.9, 152.1, 154.2, 158.7, 169.2 ppm, MS (ESI): Calc. 625.35; Found 626.59 ( $M^+ + H$ , 81%), 313.84 (100%)  $m/z$ .

**General procedure 9.** **3o** was dissolved in the minimum amount of anhydrous DMSO. 1.1 equivalents of colchicine derivatized with an amine was dissolved in an equal volume of anhydrous DMSO. The solutions were mixed together and allowed to sit for five minutes at RT. The solvent was then removed under vacuum to give the final product, which was used without further purification.

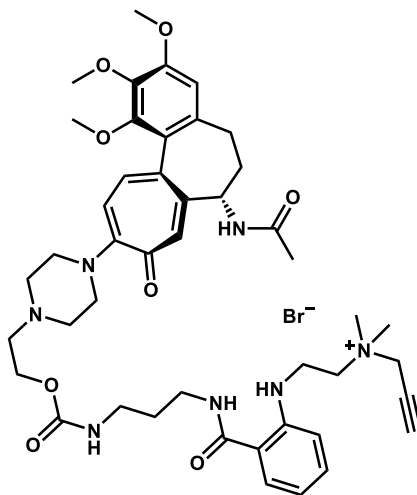


**6q.** General procedure 9 was followed as above using **6k** (7.17 mg, 16.2  $\mu\text{mol}$ ) and **3o** (5.24 mg, 14.8  $\mu\text{mol}$ ), each dissolved in 45  $\mu\text{L}$  of A-DMSO. The final product was a yellow solid (12.5 mg, quant.).  $\text{C}_{38}\text{H}_{48}\text{N}_5\text{O}_6\text{Br}$  (750.72), MS (ESI): Calc. 670.36; Found 670.51 ( $M^+$ , 74%), 335.75 (100%)  $m/z$ .

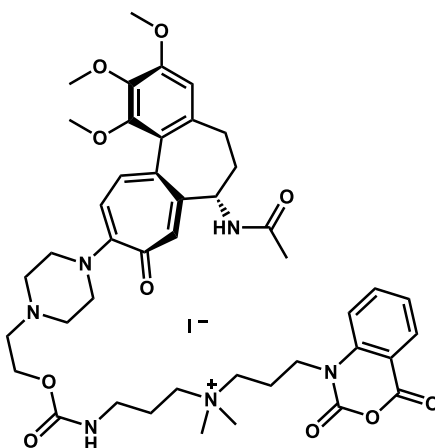




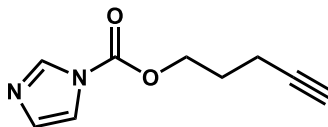
**6r.** General procedure 9 was followed as above using **6n** (9.29 mg, 17.1  $\mu\text{mol}$ ) and **3o** (5.15 mg, 14.6  $\mu\text{mol}$ ), each dissolved in 42  $\mu\text{L}$  of A-DMSO. The final product was a yellow solid (11.7 mg, 80%).  $\text{C}_{42}\text{H}_{55}\text{N}_6\text{O}_8\text{Br}$  (851.83), MS (ESI): Calc. 771.41; Found 771.68 ( $\text{M}^+$ , 40%), 386.34 (100%)  $m/z$ .



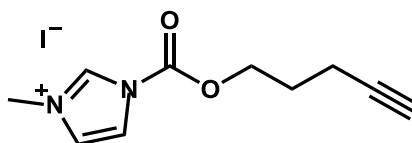
**6s.** General procedure 9 was followed as above using **6o** (13.17 mg, 22.0  $\mu\text{mol}$ ) and **3o** (6.98 mg, 19.8  $\mu\text{mol}$ ), each dissolved in 55  $\mu\text{L}$  of A-DMSO. The final product was a yellow solid (22.2 mg, quant.).  $\text{C}_{45}\text{H}_{60}\text{N}_7\text{O}_8\text{Br}$  (906.90), MS (ESI): Calc. 826.45; Found 826.68 ( $\text{M}^+ + \text{H}$ , 23%), 413.92 (100%)  $m/z$ .



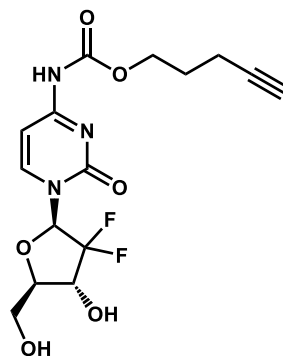
**6t.** In a vial, **6p** (20.24 mg, 32.3  $\mu\text{mol}$ ) was dissolved in anhydrous acetone (200  $\mu\text{L}$ ). **3p** (10.8 mg, 32.7  $\mu\text{mol}$ ) was dissolved in anhydrous acetone (200  $\mu\text{L}$ ) and filtered through a 2 micron syringe filter. The solutions were mixed together and allowed to sit on the oven overnight. The next day an oily substance had formed on the sides. The acetone was decanted off and the oil was washed with fresh acetone. This was repeated 2 x more. The residual solvent was removed under vacuum to give the product as a yellow solid (8.3 mg, 27%).  $\text{C}_{44}\text{H}_{57}\text{N}_6\text{O}_{10}\text{I}$  (956.86),  $^1\text{H}$  NMR (500 MHz, dimethyl sulfoxide- $d_6$ ):  $\delta$  1.83 (s, 6H), 2.01 (m, 1H), 2.09 (m, 1H), 2.19 (m, 1H), 2.56 (m, 7H), 3.03 (m, 7H), 3.28 (m, 8H), 3.44 (m, 3H), 3.51 (s, 3H), 3.77 (s, 3H), 3.82 (s, 3H), 4.10 (m, 3H), 4.30 (m, 1H), 6.75 (s, 1H), 6.84 (d, 1H,  $J = 11.2$  Hz), 6.94 (s, 1H), 7.05 (d, 1H,  $J = 11.0$  Hz), 7.33 (m, 1H), 7.37 (t, 1H,  $J = 7.6$  Hz), 7.54 (d, 1H,  $J = 8.7$  Hz), 7.88 (m, 1H), 8.06 (d, 1H,  $J = 7.8$  Hz), 8.51 (d, 1H,  $J = 7.6$ ) ppm,  $^{13}\text{C}$  NMR (500 MHz, dimethyl sulfoxide- $d_6$ ):  $\delta$  20.3, 22.5, 22.7, 29.4, 36.1, 37.4, 41.4, 47.7, 50.0, 50.9, 52.8, 55.8, 60.6, 60.7, 60.7, 61.2, 61.7, 107.7, 111.8, 114.7, 116.7, 123.8, 125.7, 128.5, 129.7, 132.7, 134.3, 135.1, 137.3, 140.7, 141.2, 147.8, 149.0, 150.5, 152.6, 157.2, 158.9, 168.4, 179.9, 206.8 ppm, MS (ESI): Calc. 829.41; Found 829.59 ( $\text{M}^+ + \text{H}$ , 62%), 415.34 (100%)  $m/z$ .



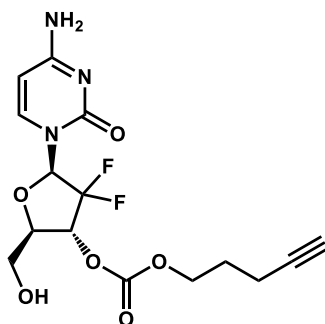
**6b.** 4-Pentyn-1-ol (1.21 g, 14.4 mmol) was dissolved in anhydrous DCM (11.7 mL) under N<sub>2</sub>. To this was added a suspension of CDI (4.66 g, 28.7 mmol) in anhydrous DCM (36.6 mL). The reaction was allowed to stir overnight. The reaction was cooled in an ice bath and then washed 3 x with ice cold DI water. The organic layer was dried over Na<sub>2</sub>SO<sub>4</sub> for 30 minutes. The solution was filtered and the DCM was removed under vacuum to give the final product as a light yellow solid (2.27 g, 89%) which was used immediately in the next step. C<sub>9</sub>H<sub>10</sub>N<sub>2</sub>O<sub>2</sub> (178.19).



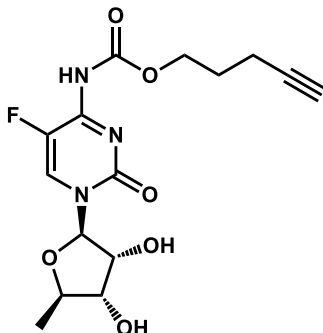
**6c.** In an Eppendorf tube, **6b** (56.1 mg, 315 μmol) was dissolved in anhydrous ACN (1.25 mL). To this was added methyl iodide (206 μL, 3.3 mmol). The reaction was covered in foil and allowed to sit overnight at RT. The solvent was removed under vacuum to give the product as an orange liquid (85.5 mg, 85%), which was used immediately in the next step. C<sub>10</sub>H<sub>13</sub>N<sub>2</sub>O<sub>2</sub>I (320.13),



**6d.** Gemcitabine (50.5 mg, 192  $\mu\text{mol}$ ) was dissolved in of anhydrous DMSO (10mL) under  $\text{N}_2$  followed by the addition of TEA (29.4  $\mu\text{L}$ , 211  $\mu\text{mol}$ ). **6c** (55.2 mg, 173  $\mu\text{mol}$ ) was dissolved in anhydrous DMSO (6.5 mL) and added drop-wise to the gemcitabine solution with stirring over the course of 30 minutes. This was then allowed to stir overnight. The DMSO was removed under vacuum to give the crude product. The product was purified by column chromatography over silica gel by using four CVs of 60:40 EtOAc:Hexanes followed by of 80:40 EtOAc:Hexanes to push off the product. The product was isolated as a clear liquid (4.66 mg, 7%).  $\text{C}_{15}\text{H}_{17}\text{N}_3\text{O}_6\text{F}_2$  (373.31),  $^1\text{H}$  NMR (500 MHz, dimethyl sulfoxide- $d_6$ ):  $\delta$  1.79 (quin, 2H,  $J = 6.6$  Hz), 2.27 (td, 2H,  $J = 7.1$ , 2.6 Hz), 2.83 (t, 1H,  $J = 2.5$  Hz), 3.17 (d, 1H,  $J = 5.3$  Hz), 3.65 (m, 1H), 3.80 (m, 1H), 3.88 (m, 1H), 5.29 (t, 1H,  $J = 5.5$  Hz), 6.16 (t, 1H,  $J = 7.3$  Hz), 6.31 (d, 1H,  $J = 6.4$  Hz), 7.09 (d, 1H,  $J = 7.6$  Hz), 8.22 (d, 1H,  $J = 7.6$  Hz), 10.85 (s, 1H) ppm.



**6e.** Gemcitabine (17.2 mg, 65.4  $\mu\text{mol}$ ) was dissolved in of anhydrous DMSO (1mL) under  $\text{N}_2$  followed by the addition of TEA (9.64  $\mu\text{L}$ , 69  $\mu\text{mol}$ ). **6c** (17.7 mg, 55.3  $\mu\text{mol}$ ) was dissolved in anhydrous DMSO (1 mL) and added drop-wise to the gemcitabine solution with stirring over the course of 30 minutes. This was then allowed to stir overnight. The DMSO was removed under vacuum to give the crude product. The product was purified by column chromatography over silica gel by using four CVs of 95:5 DCM:MeOH followed by of 90:10 DCM:MeOH to push off the product. The product was isolated as a clear liquid (1.85 mg, 8%).  $\text{C}_{15}\text{H}_{17}\text{N}_3\text{O}_6\text{F}_2$  (373.31),  $^1\text{H}$  NMR (500 MHz, dimethyl sulfoxide- $d_6$ ):  $\delta$  1.82 (quin, 2H,  $J = 6.7$  Hz), 2.26 (td, 2H,  $J = 7.1$ , 2.7 Hz), 2.83 (t, 1H,  $J = 2.7$  Hz), 3.66 (m, 1H), 3.76 (m, 1H), 4.17 (m, 1H), 4.25 (t, 2H,  $J = 6.1$  Hz), 5.24 (m, 2H), 5.81 (d, 1H,  $J = 7.6$  Hz), 6.24 (t, 1H,  $J = 8.8$  Hz), 7.43 (d, 2H,  $J = 13.6$  Hz), 7.65 (d, 1H,  $J = 7.5$  Hz) ppm.



**6g.** Capecitabine impurity A (51.4 mg, 210  $\mu\text{mol}$ ) was dissolved in of anhydrous DMSO (10mL) under  $\text{N}_2$  followed by the addition of TEA (32.2.4  $\mu\text{L}$ , 231  $\mu\text{mol}$ ). **6c** (60.4 mg, 189  $\mu\text{mol}$ ) was dissolved in anhydrous DMSO (6.5 mL) and added drop-wise to the gemcitabine solution with stirring over the course of 30 minutes. This was then allowed to stir overnight. The DMSO was removed under vacuum to give the crude product.  $\text{C}_{15}\text{H}_{18}\text{N}_3\text{O}_6\text{F}$  (355.32), MS (ESI): Calc. 355.12; Found 356.25 ( $\text{M}^+ + \text{H}$ , 41%), 711.51 (100%)  $m/z$ .

**General bioconjugation of BSA.** A stock solution of BSA (20 mg/mL) in 50 mM sodium bicarbonate buffer pH 8.4 was diluted to a final concentration of 1 mg/mL in 25 mM sodium bicarbonate buffer pH 8.4. To this was added the desired equivalents of **3o** or **3p** dissolved in DI water. The solution was vortexed and allowed to sit at RT for the course of the reaction. The reaction was stopped by the addition of ammonium hydroxide (5  $\mu\text{L}$ ) or by passing the reaction through a Princeton Separations CS-800 Pro Spin GPC column. The DOL of the conjugate was determined by HPLC on a Thermo Scientific Dionex Ultimate 3000 system with a RS diode array detector (280 and 330 nm) on a reverse-phase column (Thermo Scientific Accucore C4, 150 x 2.1 mm, 2.6  $\mu\text{m}$ ). The HPLC conditions are as follows conditions: column temperature = 40  $^\circ\text{C}$ , flow rate = 0.4

mL min<sup>-1</sup>, A = 0.1% aqueous formic acid, B = 0.1% formic acid in ACN, with a multistep gradient of 30 to 50% B from 0-8 min, 50 to 95% B from 8-10 min, 95% B from 10-11 min, 95 to 30% B from 11-12 min, and 30% B from 12-16 min.

**General bioconjugation of TAB004.** A stock solution of TAB004 (6.14 mg/mL) in DI water was diluted to a final concentration of 1 mg/mL in 25 mM sodium bicarbonate buffer pH 8.4. To this was added the desired equivalents of **3p** dissolved in DI water. The solution was vortexed and allowed to sit at RT for the course of the reaction. The reaction was stopped by passing the reaction through a Princeton Separations CS-800 Pro Spin GPC column. The DOL of the conjugate was determined by HPLC on a Thermo Scientific Vanquish system with a RS diode array detector (280 and 330 nm) on a reverse-phase column (Thermo Scientific Accucore C4, 150 x 2.1 mm, 2.6  $\mu$ m). The conjugate showed an elution time of 10.2 min under the following conditions: column temperature = 40 °C, flow rate = 0.25 mL min<sup>-1</sup>, A = 0.1% aqueous formic acid, B = ACN, with a multistep gradient of 5% B from 0-1 min, 5 to 95% B from 1-11 min, 95%B from 11-16 min, 95 to 5% B from 16-17 min, and 5% B from 17-22 min.

**General CuAAC reaction for biomolecules.** The bioconjugate was diluted in 100 mM sodium bicarbonate buffer pH 7.9 to a final volume of 500  $\mu$ L and a final concentration of 1 mg/mL. Two equivalents, with respect to the alkyne/azide present on the bioconjugate, of alkyne/azide small molecule was added to the solution. THPTA ligand (50 mM, 5  $\mu$ L) was premixed with CuSO<sub>4</sub> (20 mM, 2.5  $\mu$ L) and added to the solution. Aminoguanidine hydrochloride (100 mM, 25  $\mu$ L) was added to the solution followed by

freshly made sodium ascorbate (100 mM, 25  $\mu$ L). The solution was vortexed and allowed to sit at 35  $^{\circ}$ C for the course of the reaction. The reaction was stopped by the addition of ammonium hydroxide (5  $\mu$ L) or by passing the reaction through a Princeton Separations CS-800 Pro Spin GPC column. The DOL of the conjugate was determined by HPLC on a Thermo Scientific Dionex Ultimate 3000 system with a RS diode array detector (280 and 330 nm) on a reverse-phase column (Thermo Scientific Accucore C4, 150 x 2.1 mm, 2.6  $\mu$ m). The general HPLC conditions are as follows conditions: column temperature = 40  $^{\circ}$ C, flow rate = 0.25 mL min<sup>-1</sup>, A = 0.1% aqueous formic acid, B = ACN, with a multistep gradient of 5% B from 0-1 min, 5 to 95% B from 1-11 min, 95%B from 11-16 min, 95 to 5% B from 16-17 min, and 5% B from 17-22 min.

**3o Hydrolysis.** In an NMR tube containing compound **3o** (2.6 mg, 7.4  $\mu$ mol) was dissolved in sodium bicarbonate D<sub>2</sub>O buffer (500  $\mu$ L) pD 8.4 at the desired concentration (0, 5, 10, 15, 25, 50, 100 mM). The hydrolysis reaction was monitored at 25  $^{\circ}$ C by <sup>1</sup>H NMR on an Oxford 500 MHz NMR. The reaction was tracked by the disappearance of the reagent peak at 8.1 ppm and by the growth of the product peak at 6.7 ppm. Scans were taken every 20 min with the initial scan being taken at 7 min.

**3o Amidation, 1 and 10 butylamine eqs.** A stock solution of compound **3o** dissolved in D<sub>2</sub>O (45.8 mM, 60  $\mu$ L) was injected into an NMR tube already present in the NMR containing a solution (410  $\mu$ L) of butylamine (0.25, 1, 10 eqs) in sodium bicarbonate D<sub>2</sub>O buffer (0, 10, 100 mM) pD 8.4. The amidation reaction was monitored at 25  $^{\circ}$ C by <sup>1</sup>H NMR on an Oxford 500 MHz NMR. The reaction was tracked by the disappearance of



the reagent peak at 8.1 ppm and by the growth of the product peak at 7.2 ppm. Scans were taken every five seconds.

**3o Amidation, 0.25 butylamine eqs.** A stock solution of compound **3o** dissolved in D<sub>2</sub>O (88.5 mM, 60  $\mu$ L) was injected into an NMR tube already present in the NMR containing a solution (410  $\mu$ L) of butylamine (0.25eqs) in sodium bicarbonate D<sub>2</sub>O buffer (0, 10, 100 mM) pD 8.4. The amidation reaction was monitored at 25 °C by <sup>1</sup>H NMR on an Oxford 500 MHz NMR. The reaction was tracked by the disappearance of the reagent peak at 8.1 ppm and by the growth of the product peak at 7.2 ppm. Scans were taken every five seconds.

## REFERENCES

1. Overview of ELISA. <https://www.thermofisher.com/us/en/home/life-science/protein-biology/protein-biology-learning-center/protein-biology-resource-library/pierce-protein-methods/overview-elisa.html> (accessed August 23 2015).
2. Mahmood, T.; Yang, P.-C., Western Blot: Technique, Theory, and Trouble Shooting. *North American Journal of Medical Sciences* 2012, 4 (9), 429-434.
3. Hermanson, G. T., Chapter 1 - Introduction to Bioconjugation. In *Bioconjugate Techniques* (Third edition), Hermanson, G. T., Ed. Academic Press: Boston, 2013; pp 1-125.
4. Kalia, J.; Raines, R. T., Hydrolytic Stability of Hydrazones and Oximes. *Angewandte Chemie* (International ed. in English) 2008, 47 (39), 7523-7526.
5. Boeneman Gemmill, K.; Deschamps, J. R.; Delehanty, J. B.; Susumu, K.; Stewart, M. H.; Glaven, R. H.; Anderson, G. P.; Goldman, E. R.; Huston, A. L.; Medintz, I. L., Optimizing Protein Coordination to Quantum Dots with Designer Peptidyl Linkers. *Bioconjugate Chemistry* 2013, 24 (2), 269-281.
6. Roberts, M. J.; Bentley, M. D.; Harris, J. M., Chemistry for peptide and protein PEGylation. *Advanced Drug Delivery Reviews* 2002, 54 (4), 459-476.
7. Kolb, H. C.; Finn, M. G.; Sharpless, K. B., Click Chemistry: Diverse Chemical Function from a Few Good Reactions. *Angewandte Chemie International Edition* 2001, 40 (11), 2004-2021.
8. Himo, F.; Lovell, T.; Hilgraf, R.; Rostovtsev, V. V.; Noodleman, L.; Sharpless, K. B.; Fokin, V. V., Copper(I)-Catalyzed Synthesis of Azoles. DFT Study Predicts Unprecedented Reactivity and Intermediates. *Journal of the American Chemical Society* 2005, 127 (1), 210-216.
9. Sletten, E. M.; Bertozzi, C. R., Bioorthogonal Chemistry: Fishing for Selectivity in a Sea of Functionality. *Angewandte Chemie* (International ed. in English) 2009, 48 (38), 6974-6998.
10. Wolbers, F.; ter Braak, P.; Le Gac, S.; Luttge, R.; Andersson, H.; Vermes, I.; van den Berg, A., Viability study of HL60 cells in contact with commonly used microchip materials. *ELECTROPHORESIS* 2006, 27 (24), 5073-5080.
11. Agard, N. J.; Prescher, J. A.; Bertozzi, C. R., A Strain-Promoted [3 + 2] Azide-Alkyne Cycloaddition for Covalent Modification of Biomolecules in Living Systems. *Journal of the American Chemical Society* 2004, 126 (46), 15046-15047.

12. Köhn, M.; Breinbauer, R., The Staudinger Ligation—A Gift to Chemical Biology. *Angewandte Chemie International Edition* 2004, 43 (24), 3106-3116.
13. Tam, A.; Raines, R. T., Protein Engineering with the Traceless Staudinger Ligation. *Methods in enzymology* 2009, 462, 25-44.
14. Stephanopoulos, N.; Francis, M. B., Choosing an effective protein bioconjugation strategy. *Nat Chem Biol* 2011, 7 (12), 876-884.
15. Brun, M.-P.; Gauzy-Lazo, L., Protocols for Lysine Conjugation. In *Antibody-Drug Conjugates*, Ducry, L., Ed. Humana Press: 2013; Vol. 1045, pp 173-187.
16. Carbodiimide Crosslinker Chemistry. <https://www.thermofisher.com/us/en/home/life-science/protein-biology/protein-biology-learning-center/protein-biology-resource-library/pierce-protein-methods/carbodiimide-crosslinker-chemistry.html> (accessed August 23 2015).
17. Kalia, J.; Raines, R. T., Advances in Bioconjugation. *Current organic chemistry* 2010, 14 (2), 138-147.
18. Amine-Reactive Crosslinker Chemistry. <https://www.thermofisher.com/us/en/home/life-science/protein-biology/protein-biology-learning-center/protein-biology-resource-library/pierce-protein-methods/amine-reactive-crosslinker-chemistry.html> (accessed August 23 2015).
19. Chalker, J. M.; Bernardes, G. J. L.; Lin, Y. A.; Davis, B. G., Chemical Modification of Proteins at Cysteine: Opportunities in Chemistry and Biology. *Chemistry – An Asian Journal* 2009, 4 (5), 630-640.
20. Sulfhydryl-Reactive Crosslinker Chemistry. <https://www.thermofisher.com/us/en/home/life-science/protein-biology/protein-biology-learning-center/protein-biology-resource-library/pierce-protein-methods/sulfhydryl-reactive-crosslinker-chemistry.html> (accessed August 23 2015).
21. Cha, T.; Guo, A.; Zhu, X.-Y., Enzymatic activity on a chip: The critical role of protein orientation. *PROTEOMICS* 2005, 5 (2), 416-419.
22. Dawson, P.; Muir, T.; Clark-Lewis, I.; Kent, S., Synthesis of proteins by native chemical ligation. *Science* 1994, 266 (5186), 776-779.
23. Alley, S. C.; Okeley, N. M.; Senter, P. D., Antibody–drug conjugates: targeted drug delivery for cancer. *Current Opinion in Chemical Biology* 2010, 14 (4), 529-537.
24. Kohler, G.; Milstein, C., Continuous cultures of fused cells secreting antibody of predefined specificity. *Nature* 1975, 256 (5517), 495-497.

25. Ducry, L.; Stump, B., Antibody–Drug Conjugates: Linking Cytotoxic Payloads to Monoclonal Antibodies. *Bioconjugate Chemistry* 2010, 21 (1), 5-13.
26. Shen, W.-C., Antibody-Drug Conjugates: A Historical Review. In *Antibody-Drug Conjugates*, Wang, J.; Shen, W.-C.; Zaro, J. L., Eds. Springer International Publishing: 2015; Vol. 17, pp 3-7.
27. Sanderson, R. J.; Hering, M. A.; James, S. F.; Sun, M. M. C.; Doronina, S. O.; Siadak, A. W.; Senter, P. D.; Wahl, A. F., In vivo Drug-Linker Stability of an Anti-CD30 Dipeptide-Linked Auristatin Immunoconjugate. *Clinical Cancer Research* 2005, 11 (2), 843-852.
28. Hamblett, K. J.; Senter, P. D.; Chace, D. F.; Sun, M. M. C.; Lenox, J.; Cervený, C. G.; Kissler, K. M.; Bernhardt, S. X.; Kopcha, A. K.; Zabinski, R. F.; Meyer, D. L.; Francisco, J. A., Effects of Drug Loading on the Antitumor Activity of a Monoclonal Antibody Drug Conjugate. *Clinical Cancer Research* 2004, 10 (20), 7063-7070.
29. Merten, H.; Brandl, F.; Plückthun, A.; Zangemeister-Wittke, U., Antibody–Drug Conjugates for Tumor Targeting—Novel Conjugation Chemistries and the Promise of non-IgG Binding Proteins. *Bioconjugate Chemistry* 2015.
30. Jovin, T. M.; Englund, P. T.; Kornberg, A., Enzymatic Synthesis of Deoxyribonucleic Acid: XXVII. CHEMICAL MODIFICATIONS OF DEOXYRIBONUCLEIC ACID POLYMERASE. *Journal of Biological Chemistry* 1969, 244 (11), 3009-3018.
31. Merino, E. J.; Wilkinson, K. A.; Coughlan, J. L.; Weeks, K. M., RNA Structure Analysis at Single Nucleotide Resolution by Selective 2'-Hydroxyl Acylation and Primer Extension (SHAPE). *Journal of the American Chemical Society* 2005, 127 (12), 4223-4231.
32. Mortimer, S. A.; Weeks, K. M., A Fast-Acting Reagent for Accurate Analysis of RNA Secondary and Tertiary Structure by SHAPE Chemistry. *Journal of the American Chemical Society* 2007, 129 (14), 4144-4145.
33. Winstein, S.; Hanson, C.; Grunwald, E., The Role of Neighboring Groups in Replacement Reactions. X.1 Kinetics of Solvolysis of trans-2-Acetoxycyclohexyl p-Toluenesulfonate. *Journal of the American Chemical Society* 1948, 70 (2), 812-816.
34. Abberior Degree of Labeling (DOL). <http://www.abberior.com/knowledge/application-notes/degree-of-labeling-doi/> (accessed July 25, 2016).
35. Hirayama, K.; Akashi, S.; Furuya, M.; Fukuhara, K.-i., Rapid confirmation and revision of the primary structure of bovine serum albumin by ESIMS and frit-FAB LC/MS. *Biochemical and Biophysical Research Communications* 1990, 173 (2), 639-646.

36. Agarwal, R.; Gupta, M. N., Copper affinity precipitation as an initial step in protein purification. *Biotechnology Techniques* 1994, 8 (9), 655-658.
37. Hong, V.; Presolski, S. I.; Ma, C.; Finn, M. G., Analysis and Optimization of Copper-Catalyzed Azide–Alkyne Cycloaddition for Bioconjugation. *Angewandte Chemie International Edition* 2009, 48 (52), 9879-9883.
38. Curry, J. M.; Thompson, K. J.; Rao, S. G.; Besmer, D. M.; Murphy, A. M.; Grdzlishvili, V. Z.; Ahrens, W. A.; McKillop, I. H.; Sindram, D.; Iannitti, D. A.; Martinie, J. B.; Mukherjee, P., The Use of a Novel MUC1 Antibody to Identify Cancer Stem Cells and Circulating MUC1 in Mice and Patients With Pancreatic Cancer. *Journal of surgical oncology* 2013, 107 (7), 10.1002/jso.23316.
39. Kufe, D. W., Mucins in cancer: function, prognosis and therapy. *Nat Rev Cancer* 2009, 9 (12), 874-85.
40. Singh, R.; Bandyopadhyay, D., MUC1: a target molecule for cancer therapy. *Cancer biology & therapy* 2007, 6 (4), 481-6.
41. Ritchie, M.; Tchistiakova, L.; Scott, N., Implications of receptor-mediated endocytosis and intracellular trafficking dynamics in the development of antibody drug conjugates. *mAbs* 2013, 5 (1), 13-21.
42. Beck, A.; Haeuw, J. F.; Wurch, T.; Goetsch, L.; Bailly, C.; Corvaia, N., The next generation of antibody-drug conjugates comes of age. *Discovery medicine* 2010, 10 (53), 329-39.
43. Doronina, S. O.; Mendelsohn, B. A.; Bovee, T. D.; Cervený, C. G.; Alley, S. C.; Meyer, D. L.; Oflazoglu, E.; Toki, B. E.; Sanderson, R. J.; Zabinski, R. F.; Wahl, A. F.; Senter, P. D., Enhanced activity of monomethylauristatin F through monoclonal antibody delivery: effects of linker technology on efficacy and toxicity. *Bioconjugate chemistry* 2006, 17 (1), 114-24.
44. Merali, Z.; Ross, S.; Pare, G., The pharmacogenetics of carboxylesterases: CES1 and CES2 genetic variants and their clinical effect. *Drug metabolism and drug interactions* 2014, 29 (3), 143-51.
45. Xu, G.; Zhang, W.; Ma, M. K.; McLeod, H. L., Human Carboxylesterase 2 Is Commonly Expressed in Tumor Tissue and Is Correlated with Activation of Irinotecan. *American Association for Cancer Research* 2002, 8 (8), 2605-2611.
46. Organization, W. H. WHO Model List of Essential Medicines. (accessed 2016).
47. de Sousa Cavalcante, L.; Monteiro, G., Gemcitabine: Metabolism and molecular mechanisms of action, sensitivity and chemoresistance in pancreatic cancer. *European Journal of Pharmacology* 2014, 741, 8-16.

48. Badger, S. A.; Brant, J. L.; Jones, C.; McClements, J.; Loughrey, M. B.; Taylor, M. A.; Diamond, T.; McKie, L. D., The role of surgery for pancreatic cancer: a 12-year review of patient outcome. *The Ulster Medical Journal* 2010, 79 (2), 70-75.
49. Longley, D. B.; Harkin, D. P.; Johnston, P. G., 5-Fluorouracil: mechanisms of action and clinical strategies. *Nat Rev Cancer* 2003, 3 (5), 330-338.
50. Chintala, L.; Vaka, S.; Baranda, J.; Williamson, S. K., Capecitabine versus 5-fluorouracil in colorectal cancer: where are we now? *Oncology Reviews* 2011, 5 (2), 129-140.
51. Nerlekar, N.; Beale, A.; Harper, R. W., Colchicine--a short history of an ancient drug. *The Medical journal of Australia* 2014, 201 (11), 687-8.
52. Finkelstein, Y.; Aks, S. E.; Hutson, J. R.; Juurlink, D. N.; Nguyen, P.; Dubnov-Raz, G.; Pollak, U.; Koren, G.; Bentur, Y., Colchicine poisoning: the dark side of an ancient drug. *Clinical toxicology (Philadelphia, Pa.)* 2010, 48 (5), 407-14.
53. Skoufias, D. A.; Wilson, L., Mechanism of inhibition of microtubule polymerization by colchicine: inhibitory potencies of unliganded colchicine and tubulin-colchicine complexes. *Biochemistry* 1992, 31 (3), 738-746.
54. Perez-Ramirez, B.; Andreu, J. M.; Gorbunoff, M. J.; Timasheff, S. N., Stoichiometric and Substoichiometric Inhibition of Tubulin Self-Assembly by Colchicine Analogues. *Biochemistry* 1996, 35 (10), 3277-3285.
55. Singh, B.; Kumar, A.; Joshi, P.; Guru, S. K.; Kumar, S.; Wani, Z. A.; Mahajan, G.; Hussain, A.; Qazi, A. K.; Kumar, A.; Bharate, S. S.; Gupta, B. D.; Sharma, P. R.; Hamid, A.; Saxena, A. K.; Mondhe, D. M.; Bhushan, S.; Bharate, S. B.; Vishwakarma, R. A., Colchicine derivatives with potent anticancer activity and reduced P-glycoprotein induction liability. *Organic & biomolecular chemistry* 2015, 13 (20), 5674-89.
56. Trott, O.; Olson, A. J., AutoDock Vina: Improving the speed and accuracy of docking with a new scoring function, efficient optimization, and multithreading. *Journal of Computational Chemistry* 2010, 31 (2), 455-461.
57. Capello, M.; Lee, M.; Wang, H.; Babel, I.; Katz, M. H.; Fleming, J. B.; Maitra, A.; Wang, H.; Tian, W.; Taguchi, A.; Hanash, S. M., Carboxylesterase 2 as a Determinant of Response to Irinotecan and Neoadjuvant FOLFIRINOX Therapy in Pancreatic Ductal Adenocarcinoma. *Journal of the National Cancer Institute* 2015, 107 (8).
58. Tan, M. H.; Nowak, N. J.; Loor, R.; Ochi, H.; Sandberg, A. A.; Lopez, C.; Pickren, J. W.; Berjian, R.; Douglass, H. O., Jr.; Chu, T. M., Characterization of a new primary human pancreatic tumor line. *Cancer investigation* 1986, 4 (1), 15-23.

59. Kamath, V.; Diedrich, P.; Hindsgaul, O., Use of diethyl squarate for the coupling of oligosaccharide amines to carrier proteins and characterization of the resulting neoglycoproteins by MALDI-TOF mass spectrometry. *Glycoconjugate J* 1996, 13 (2), 315-319.